Durable Zeolite Based Catalyst Systems for Diesel Emission Control

Hammershøi, Peter S.

Publication date:
2018

Document Version
Publisher's PDF, also known as Version of record

Durable Zeolite Based Catalyst Systems for Diesel Emission Control

Peter S. Hammershøi

PhD Thesis

2018

DTU Chemical Engineering
Department of Chemical and Biochemical Engineering

Durable Zeolite Based Catalyst Systems for Diesel Emission Control

Peter S. Hammershøi

Supervisors:
Prof. Anker D. Jensen
Dr. Ton V. W. Janssens

PhD Thesis
Submitted October 2018

Department of Chemical and Biochemical Engineering
Technical University of Denmark

Department of Chemical and Biochemical Engineering
Technical University of Denmark
Søltofts Plads B229, 2800 Kgs. Lyngby, Denmark

Umicore Denmark ApS
Nøjsomhedsvej 20, 2800 Kgs. Lyngby, Denmark

Preface

Submission of this thesis is part of the candidature for the Ph.D. degree from the Technical University of Denmark (DTU). The contents of the thesis is the outcome of the work that has been carried out for the past three years, since the project started on May 15th 2015. The project was initially a collaboration between the CHEC (Combustion and Harmful Emission Control) centre of the Department of Chemical and Biochemical Engineering at DTU, and the Automotive department of Haldor Topsøe A/S with Prof. Anker D. Jensen and Dr. Ton V. W. Janssens as supervisors, respectively. Since the acquisition of the Automotive department by the Umicore organization, the industrial partner of the project has been Umicore Denmark ApS, at which the final year of the project has been carried out without changes to the supervisor team. The Innovation Fund Denmark (grant number 5139-0023B) is gratefully acknowledged for financial support throughout the duration of the project.

First, I would like to state my gratitude to my supervisors Prof. Anker D. Jensen and Dr. Ton V. W. Janssens for their guidance, support, dedication and interest, which has made it a pleasure to be a PhD student. I highly appreciate the professionalism and meticulousness that Anker represents, and his ever good spirits. A particular thank you to Ton, for enthusiastically sharing his wide technical knowledge within chemical engineering, chemistry, physics, for teaching me "pirate experiments" (I will miss those!), and for our discussions on results and many other technical and non-technical things – I am deeply grateful. Another person, without whom this project would not have materialized, is Dr. Peter N. R. Vennestrøm, who has acted as an unofficial co-supervisor. I am profoundly thankful for his priceless contributions to the project, and his continuous care, guidance and challenging questions. Also, I would like to thank Dr. Pär L. T. Gabrielsson for supporting the project and providing a place for it in his department, and for help establishing a good professional network.

The predominant part of the project was spent in Haldor Topsøe A/S, where I have been fortunate to be surrounded by many intellectual, helpful and kind people. I would like to thank Renato, Juan, Andrea, Dani, Malthe, Logi and Pablo from the "PhD office" for the enjoyable conversations in this international and diverse crowd, who gladly shared their experiences as PhD students, and made the coffee breaks and lunches very cheerful. I will also take the opportunity to thank Gitte Marquardt for introducing me to the "TPX4", and for the relaxed chats while she aided the clean-up of most of the reactor setup after my sulfurous experiments clogged the system again (and again…). A great thanks to Dr. Pablo Beato for collaboration and insightful discussions about the NH_3-SCR mechanism, to Dr. Hanne Falsig for DFT calculations, to Dr. Søren B. Rasmussen for help with spectroscopic experiments, to Dr. Ramchandra Tiruvalarm for microscopy work, to Brian Jensen for showing me zeolite synthesis, and to the Analysis Lab for numerous S and Cu analyses.

At Umicore Denmark ApS I gratefully acknowledge Jesper S. Larsen for his invaluable help with conducting an extensive amount of SO_2-exposures, and for ensuring some great guitar solos in the test lab.

Futhermore, I have had the pleasure to take part in collaborations with other spectroscopic research groups, which has been most illuminating. For that, I want to thank Dr. Chiara Negri, Assoc. Prof. Gloria Berlier and Prof. Silvia Bordiga from the University of Turin, and Dr. Anita L. Godiksen and Assoc. Prof. Susanne Mossin from DTU Chemistry. After an intense experimental stay at the University of Houston, my warmest (like Houston in July) appreciations go to Dr. Yasser Jangjou for the great and efficient collaboration in the lab and interesting football discussions, and to Prof. William S. Epling for his valuable scientific input and for introducing me to Corn Hole at the 8th Wonder.

Finally, I would like to express my deepest gratitude to all of my family for always supporting me in my studies and taking (or faking?) interest in my work. The most loving and profound thanks to my wonderful wife Pernille for her unconditional love and support, which was ever present while also giving birth to our two dear daughters, who taught me efficiency and the value of a good night's sleep.

Abstract

Diesel vehicles are widely used for transportation of people and goods, which is responsible for a significant consumption of diesel, and the associated release of mainly CO_2, but also pollutants such as CO, hydrocarbons, soot particles and NO_x (x = 1,2). These pollutants threat the health of humans and negatively affect the environment, and therefore, abatement is enforced by legislation, which is practically handled by installation of exhaust aftertreatment systems in passenger cars as well as in heavy-duty vehicles. A crucial component of the aftertreatment systems is the catalyst for selective catalytic reduction of NO_x with NH_3 (NH_3-SCR). Current state-of-the-art SCR catalysts are zeolite-based Cu-CHA materials, which is mainly due to their unmatched low-temperature activity. Unfortunately, the presence of 0.5-2 ppmv of SO_2 in diesel exhaust significantly inhibits the low-temperature activity Cu-CHA catalysts, which diminishes the NO_x removal efficiency. In order to comply with current and future NO_x emission limits, development of more SO_2 resistant Cu-CHA catalyst systems is necessary, which requires a better fundamental understanding of the deactivation of Cu-CHA catalysts by SO_2.

In this work, Cu-CHA catalysts have been produced and exposed to SO_2 in various gas mixtures at different temperatures (200-550 °C), and exposure times, to investigate the effects of SO_2 at the various conditions of an aftertreatment system. The uptake of S, determined from elemental analysis and adsorption/desorption measurements, has been compared to the impact on the catalytic performance in the NH_3-SCR reaction after the different SO_2 exposures, and after regeneration at 550 °C in SO_2-free gas. In parallel, characterization with scanning transmission electron microscopy – energy dispersive X-ray (STEM-EDX) spectroscopy and electron paramagnetic resonance (EPR) spectroscopy have been used to assess the location of S, and density functional theory (DFT) calculations have been carried out to determine possible Cu,S species.

The deactivation is established to be the result of formation of Cu,S species, and not a consequence of ammonium sulfate precipitation, since the S/Cu ratio has not been observed to significantly exceed 1. Some Cu,S species decompose below 550 °C (reversible), while a more stable Cu sulfate species (irreversible) that decomposes around 650 °C, can form on a restricted fraction of the Cu. Formation of the different Cu,S species is dependent on several conditions such as the oxidation state of Cu, the temperature, and the presence of H_2O and SO_3. DFT calculations suggested that SO_2 adsorbs more stably on Cu^{I}, while SO_3 preferably reacts with Cu^{II}, which was consistent with experimental data. At 200 °C it was observed that the formation of Cu,S species is enhanced by co-feeding SO_3, whereas at 550 °C there is no measurable impact. In the same experiments, the presence of H_2O enhanced the formation of irreversible Cu sulfate at both 200 and 550 °C, but had no impact on the formation of reversible Cu,S species.

While there is no apparent impact of the chemical composition of the CHA framework ($H_nAl_nSi_{1-n}O_2$ vs $H_nSi_nAlP_{1-n}O_4$), the Cu^{II} sites associated with one or two framework Al centers, Z-CuOH and Z_2-Cu, respectively, have different resistance towards SO_2, as indicated by DFT calculations. The EPR characterization indirectly showed that mainly Z-CuOH reacts with SO_x to formation of the reversible Cu,S species, whereas certain Z_2-Cu sites were directly seen to participate in the

formation of irreversible Cu sulfate. Finally, other Z_2-Cu sites were inert to SO_2 exposure, which explains why a 100% deactivation has not been observed.

In terms of the impact of reversible and irreversible Cu,S species on the NH_3-SCR activity, the deactivation inferred by the reversible Cu,S species was always disproportionately larger than the S/Cu ratio, and caused a lowering of the apparent SCR activation energy with increasing S/Cu ratio. In contrast, the remaining irreversible Cu,S species after regeneration exhibited a 1:1 correlation between the deactivation and S/Cu ratio, as well as the apparent activation energies were restored to the same level as the fresh catalyst. The deactivation occurs by exposure to 1.5 ppmv SO_2, and by increasing the SO_2 concentration and simultaneously decreasing the exposure time correspondingly, similar deactivation levels are reached. Hence, it appears to depend on the product of the SO_2 concentration and exposure time. Accelerated SO_2 exposures showed that the deactivation occurs fast, reaching at least 80% before 5% of the lifetime SO_2 exposure. However, the deactivation could at all times be lowered to about 20%, which is probably dependent on the specific Cu-CHA catalyst. Thus, the application of Cu-CHA catalysts in aftertreatment systems is contingent on regeneration.

A new method to quantify the active amount of Cu in Cu-CHA catalysts by measuring the NO consumption during a temperature-programmed reduction in NO+NH_3 has been developed (NO-TPR). The method is applicable on regenerated catalysts, and potentially also on SO_2 exposed catalysts.

Dansk Resumé

Person- og godstransport har ført til stor anvendelse af dieseldrevne biler og lastbiler, som er ansvarlige for et anseeligt forbrug af diesel, og den medfølgende udledning af CO_2, CO, kulbrinter, sodpartikler og NO_x (x = 1,2), som forurener miljøet og er skadelige for menneskers helbred. For at mindske udledningen, er der indført lovgivning som definerer maksimum grænser for udledningen af disse stoffer, hvilket har medført udvikling og implementering af udstødningssystemer. For at imødekomme de nuværende, og fremtidige, emissionsgrænser for NO_x, er det nødvendigt effektivt at kunne anvende selektiv katalytisk reduktion med NH_3 (NH_3-SCR), hvilket bedst opnås over zeolit-baserede Cu-CHA katalysatorer, grundet deres særligt høje aktivitet i lav-temperaturintervallet for NH_3-SCR. Tilstedeværelsen af selv 0.5-2 ppmv SO_2 i udstødningsgassen har en negativ indvirkning på Cu-CHA katalysatorers lav-temperatur aktivitet, hvilket betydeligt forringer NO_x fjernelsen. For at kunne leve op til nuværende og fremtidige NO_x emissionsgrænser, er det nødvendigt at udvikle mere SO_2 robuste Cu-CHA katalysatorer, hvilket kræver en bedre grundlæggende forståelse af hvordan SO_2 forårsager deaktivering af disse katalysatorer.

Det eksperimentelle arbejde udført i dette projekt hat inkluderet fremstilling af pulver Cu-CHA katalysatorer, som er blevet eksponeret til SO_2 i forskellige gassammensætninger ved varierende temperaturer (200-550 °C) og eksponeringstider. Indflydelsen af svovl er blevet undersøgt ved at måle svovlindholdet med elementaranalyse og adsorption/desorption, og sammenholde dette med ændringerne i den katalytiske aktivitet efter de forskellige SO_2 eksponeringer, og efter regenerering ved 550 °C uden SO_2 i gassen. Sideløbende er prøverne blevet karakteriseret med forskellige spektroskopiske metoder såsom STEM-EDX (scanning transmission electron miscroscopy – energy dispersive X-ray) og EPR (electron paramagnetic resonance) for at bestemme hvor i Cu-CHA katakysatorerne at svovl befinder sig, og DFT (density functional theory) beregninger blevet udført for at identificere mulige Cu,S forbindelser.

Årsagen til at Cu-CHA katalysatorer deaktiverer i tilstedeværelse af SO_2, skyldes dannelse af Cu,S forbindelser, og ikke udfældning af poreblokerende ammoniumsulfat, hvilket bekræftes ved at der endnu ikke er målt S/Cu forhold, som er signifikant højere end 1. Nogle af disse Cu,S forbindelser dekomponerer ved lavere temperaturer end 550 °C (reversible), men også en mere stabil Cu sulfat (irreversibel) forbindelse dannes på en mindre fraktion af Cu, som dekomponerer ved ca. 650 °C. Dannelsen af både reversible og irreversible Cu,S forbindelser afhænger af betingelserne, hvorunder de dannes, og både Cu oxidationstrinnet, temperaturen, og tilstedeværelsen af SO_3 og H_2O en indflydelse på dette. Konsistent med eksperimentelle resultater, viser DFT beregninger at SO_2 har en større affinitet for Cu^I end Cu^{II}, hvilket er omvendt for SO_3. Temperaturen har en indirekte indflydelse på dette, idet Cu^{II} reduceres til Cu^I af NO og NH_3, som primært findes ved lavere temperaturer hvor SCR reaktionshastigheden er lavere. Ved lav temperatur (200 °C) fører SO_3-holdig gas til en markant hurtigere dannelse af Cu,S forbindelser, imens det ved 550 °C ikke har nogen målbar indflydelse grundet den højere oxidationshastighed af SO_2 ved højere temperaturer. Af samme eksperimenter med eksponering ved 200 og 550 °C, fremgik det at tilstedeværelsen af H_2O fremmer dannelsen af irreversibel Cu sulfat, men ingen betydning har for dannelsen af reversible Cu,S forbindelser.

DFT viste at indflydelsen af forskellige kemiske sammensætninger af CHA strukturen ($H_nAl_nSi_{1-n}O_2$ vs $H_nSi_nAlP_{1-n}O_4$) er minimal, men at Cu^{II} placeret i nærheden af ét (Z-CuOH) eller to (Z_2-Cu) Al centre i zeolitstrukturen, fører til store forskelligheder i affiniteten for SO_2 og SO_3. Dette blev bekræftet med EPR, som indirekte viste at primært Z-CuOH reagerer med SO_x og laver reversible Cu,S forbindelser, hvorimod det direkte kunne ses at kun nogle Z_2-Cu kunne reagere med SO_x, og lave irreversibel Cu sulfat. Den resterende del af Z_2-Cu forblev upåvirket af SO_2 eksponeringen, hvilket kunne forklare hvorfor en 100% deaktivering endnu ikke er observeret.

Effekten af de reversible og irreversible Cu,S forbindelser på NH_3-SCR aktiviteten var vidt forskellig. Således medførte de reversible Cu,S forbindelser altid en disproportional højere deaktivering end S/Cu forholdet, samt at aktiveringsenergien faldt med øgede S/Cu forhold. Modsat var der umiddelbart en 1:1 afhængighed mellem den irreversible deaktivering og S/Cu forhold, og efter regenerering var aktiveringsenergien tilbage på niveau med aktiveringsenergien for den friske katalysator.Det blev observeret at deaktiveringen steg ved eksponering til 1.5 ppmv SO_2, og at samme deaktivering kunne opnås ved at høje SO_2 koncentrationen ved samtidigt at forkorte eksponeringstiden tilsvarende. Derfor afhænger deaktiveringen tilsyneladende af produktet af SO_2 koncentrationen og eksponeringstiden. Accelererede SO_2 eksponeringer viste at allerede før man når 5%, af det der svarer til en livstidseksponeringen for en katalysator i et udstødningssystem, er deaktiveringen over 80%. Dog kunne deaktiveringen altid mindskes til ca. 20% ved regenerering, hvilket betyder at lav-temperatursaktiviteten af Cu-CHA katalysatorer kan udnyttes i udstødningssystemer, såfremt de bliver effektivt regenereret.

En ny metode til at kvantificere mængden af aktivt Cu i Cu-CHA katalysatorer er blevet introduceret, hvor forbruget af NO måles i løbet af en temperatur-programmeret reduktion (NO-TPR) i NO og NH_3. Med mindre ændringer virker denne metode også til at være anvendelig på SO_2 eksponerede og regenererede Cu-CHA katalysatorer.

Table of Contents

Chapter 1

Introduction

Motivation

During the past thirty years, there has been an increasing focus on the impact of energy consumption on the Earth's climate and the public health. The realizations that burning fossil fuels leads to global warming through accumulation of CO_2 in the atmosphere, and has a negative impact on air quality, have become focus points of environmental concerns around the world. An important part of the energy consumption lies in the transportation sector, which was responsible for 23% of the global anthropogenic CO_2 emissions in 2010 [1], and therefore a major contributor to the environmental challenges we are facing today.

Among the different sectors of transportation, i.e. aviation, marine, railway, and road, the road vehicles generate 74% of the CO_2 emissions [1]. Gasoline and diesel are the major fuels used for light-duty and heavy-duty vehicles, with CO_2 and H_2O as the major products of fuel combustion. Furthermore, exhaust gases also contain small amounts of byproducts, which are NO_x (NO and NO_2), unburned hydrocarbons (HC), CO, soot particles, and SO_2. The typical concentrations of these are listed in Table 1. The production of CO, HC, and soot particles is a consequence of incomplete combustion, while SO_2 is formed from oxidation of sulfur bound in the fuel and engine lubricants. NO_x is formed by oxidation of the nitrogen in the air at high temperatures during the combustion of fossil fuels, where air is used for supplying oxygen.

Table 1 - Typical composition of diesel vehicle exhaust based on [2].

CO_2 [vol%]	H_2O [vol%]	O_2 [vol%]	CO [ppmv]	HC [ppmv]	PM [mg/km]	NO_x [ppmv]	SO_2 [ppmv]
2-12	2-12	3-17	10-500	20-300	10-100	50-1000	0.5-2

Even though the concentrations of CO, HC, soot, SO_2 and NO_x in the exhaust from vehicles are low, their environmental impact is significant. To reduce the impact of our energy consumption on the environment, the emission of these components is regulated. In Europe, the current regulations are the EURO 6d-TEMP for light-duty vehicles and EURO VId for heavy-duty vehicles, which are listed in Table 2 [3].

Table 2 – Emission standards for CO, hydrocarbons (HC), particulate matter (PM), particulate number (PN), NO_x ($NO+NO_2$), and SO_2 for light-duty (EURO 6d-TEMP) and heavy-duty vehicles (EURO VId), which are tested for steady-state and transient emissions in the world harmonized steady-state cycle (WHSC) and the world harmonized transient cycle (WHTC).

Pollutants [Light-duty]/[Heavy-duty]	**EURO 6d (Light-duty)**		**EURO VId (Heavy-duty diesel)**	
	Gasoline	Diesel	WHSC – test	WHTC – test
CO [g/km]/[g/kWh]	1.0	0.5	1.5	4.0
HC [g/km]/[g/kWh]	0.1	-	0.13	0.16
HC+NO_x [g/km]/[g/kWh]	-	0.17	-	-
PM [g/km]/[g/kWh]	0.005	0.005	0.01	0.01
PN [#/km]/[#/kWh]	$6.0 \cdot 10^{11}$	$6.0 \cdot 10^{11}$	$8.0 \cdot 10^{11}$	$6.0 \cdot 10^{11}$
NO_x [g/km]/[g/kWh]	0.06	0.08	0.4	0.46
SO_2 [wt ppm in diesel]	-	10	10	10

For gasoline cars, the emissions of CO, HC, and NO_x are handled by a three-way catalyst, based on noble metals (Pd, Pt, Rh), sometimes assisted by a lean-NO_x trap to further reduce the emission of NO_x. Modern gasoline cars, with direct fuel injection, also produce soot [4–6], which has prompted the implementation of soot filters on gasoline cars, similar to diesel vehicles [3]. This regulation has been effective since 01.09.2018 in Europe.

The technology used for exhaust gas treatment in gasoline cars only works for combustion with fuel/air mixtures close to the stoichiometric concentrations. Diesel engines always operate under fuel-lean conditions with a larger excess of air, which means that the exhaust gas contains a substantial amount of oxygen (3-17% [2]), which prohibits the use of the three-way catalyst used in gasoline cars. Diesel engines are inherently more effective compared to gasoline engines, leading to lower emissions of CO_2 from diesel engines. They find application in passenger cars, mainly in Europe, trains, off-road machinery, and heavy-duty vehicles.

Worldwide, a significant source of NO_x emissions is from heavy-duty diesel vehicles [1]. NO_x is a major cause of air pollution, and emissions of NO_x to the atmosphere contributes to the formation of smog, acid rain and ozone [7], which threaten the health of humans as well as the local and global environment [1,7]. Therefore, it is important to minimize the emissions of NO_x, which is the motivation for this work. Aftertreatment systems are installed in heavy-duty vehicles in order to limit the emissions of the polluting compounds from the exhaust. The current technology for diesel exhaust gas treatment, to comply with the required emissions, is shown in Figure 1. The

aftertreatment system consists of a diesel oxidation catalyst (DOC), a diesel particulate filter (DPF), a catalyst for selective catalytic reduction of NO_x with ammonia (NH_3-SCR), and an ammonia slip catalyst (ASC). The DOC catalyzes the oxidation of CO and unburned hydrocarbons to CO_2 and NO to NO_2, while the DPF captures particulate matter. As the carbonaceous particulate matter accumulates on the DPF, regeneration of the DPF is necessary. This is done by burning off the particles in active or passive regeneration. In active regeneration, the temperature of the system is increased to well over 500-700 °C. This is achieved via the release of heat from the exothermic oxidation of additional diesel injected to the DOC. Passive regeneration exploits that the NO_2 formed in the DOC can burn off the soot particles in the temperature range 350-500 °C, which is in the normal operating window for a DPF. In both active and passive regeneration, the function of the DOC is important for an effective operation of the DPF.

The most efficient removal of NO_x from exhaust gas is achieved with the NH_3-SCR reaction. In this reaction, NH_3 selectively reduces NO to N_2 and H_2O in the presence of O_2, according to Eq. (1). Diesel exhaust typically contains NO in the concentration range 50-1000 ppmv and O_2 in the range 3-17 vol%, as well as 2-12 vol% of H_2O from the air [2].

$$4NO + 4NH_3 + O_2 \rightarrow 4N_2 + 6H_2O \qquad (1)$$

In an exhaust aftertreatment system, the removal of NO_x takes place over the NH_3-SCR catalyst. The NH_3 is usually supplied by injection of an aqueous solution of urea upstream to the NH_3-SCR catalyst, which thermally decomposes to NH_3 and CO_2 above 180 °C. In order to prevent emission of unreacted ammonia (ammonia slip) from the NH_3-SCR reaction, any excess NH_3 is removed by the ASC downstream to the SCR catalyst.

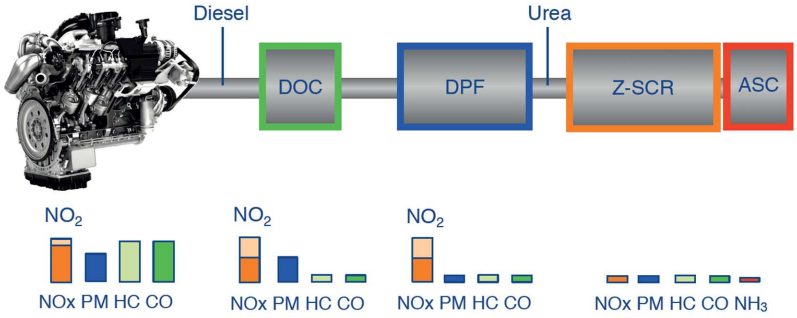

Figure 1 – Illustration of a typical heavy-duty vehicle aftertreatment system for complying with EURO VI emission standards. The amounts of NO_x, PM, HC, and CO after each component are indicated by the bars below each aftertreatment component. Adapted from [8].

The removal of NO_x in the aftertreatment system takes place in the temperature range 180-550 °C. The lower limit of 180 °C is determined by the decomposition temperature of urea to generate the NH_3. Catalysts for automotive NH_3-SCR are based on V_2O_5 and Fe- or Cu-containing zeolites. The overall performance of these catalysts is based on the catalytic activity and robustness in the

harsh conditions of an aftertreatment system. The activity of the catalysts in the 180-550 °C temperature window is of course of high importance as this determines the NO_x removal efficiency. Fe-zeolites and V_2O_5-based SCR catalysts become active in the NH_3-SCR reaction above 250 °C, as seen in Figure 2, while the Cu-zeolites are active already from 180 °C [9]. In order to comply with current and future NO_x emission limits, efficient NO_x removal in the entire temperature range is necessary. As the engine efficiency is continuously improved in order to lower the CO_2 emissions, consequently, the exhaust becomes colder. Thus, efficient NO_x removal in the low-temperature region becomes increasingly important. For example, 63% of the accumulated NO_x emissions from a EURO VI heavy-duty vehicle during a 3 h mixed drive (48% urban, 17% rural, 35% highway) occurred during the first 23 min where the aftertreatment system was still heating [10]. Therefore, the unmatched low-temperature activity of Cu-zeolites makes these catalysts the best candidates for achieving the most efficient NO_x removal for automotive aftertreatment systems.

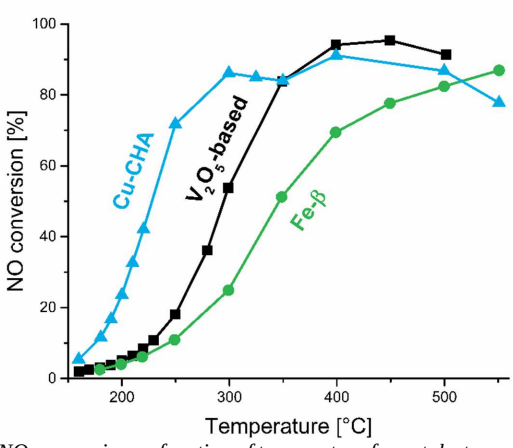

Figure 2 – Steady-state NO conversion as function of temperature for catalysts samples of Cu-zeolites (Cu-CHA), Fe-zeolites (Fe-β), and V_2O_5-based automotive NH_3-SCR catalysts, which serve to illustrate the differences between these catalyst materials as described in Chapter 8 in [9].

Current state-of-the-art Cu-zeolite catalysts for NH_3-SCR are based on the chabazite (CHA) framework (Cu-CHA) [9,11–14]. The CHA framework has a small-pore structure consisting of 4-, 6-, and 8-membered rings (see Figure 3). The best known materials with CHA structure are the SSZ-13 zeolite ($H_nAl_nSi_{1-n}O_2$) and the alumino-phosphate based SAPO-34 ($H_nSi_nAlP_{1-n}O_4$).

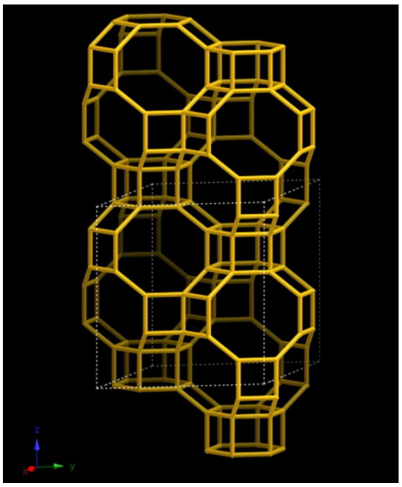

Figure 3 – Molecular structure of the CHA framework from [15]. Each corner represent a T-atom (T = Si, Al or P). Adapted from [15].

In the SSZ-13 zeolite, the microporous structure arises from a certain 3-dimensional combination of tetrahedral building units of Si^{4+} coordinated to 4 oxygen atoms. If a Si^{4+} is substituted with an Al^{3+}, a local negative charge is induced in the framework, as illustrated in Figure 4. These negative charges must be compensated by positively charged ions, which most commonly are H^+, Na^+, K^+, or NH_4^+, but other metal ions are also possible. H^+ ions in such a framework have strong acidic properties. These charge compensating ions can be easily exchanged, giving the zeolite its ion-exchange capability. In a Cu-CHA, the negative charges are compensated by Cu-ions, and these Cu ions are responsible for the activity of these materials for the NH_3-SCR reaction [13,16–25].

The most common oxidation state of Cu is Cu^{2+}, and this allows for two fundamentally different configurations for compensation of the negative framework charge. In the first configuration, the Cu^{2+} ion balances the charge induced by a single framework Al ion, by forming a Cu^{2+}-OH species at the ion-exchange site, denoted as Z-CuOH. In the second configuration, a single Cu^{2+} ion balances two negative charges simultaneously, which are induced by framework Al sites in the vicinity of each other. This state is denoted as Z_2-Cu. It is noted that the actual Cu species in the CHA zeolite is highly dependent on the conditions it is exposed to, including the combination of temperature and NH_3-, O_2- and H_2O concentration [19,26–33].

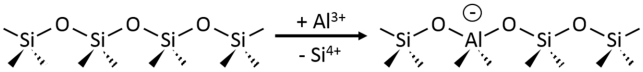

Figure 4 – Illustration of the substitution of a Si^{4+} with an Al^{3+} in a zeolite framework, thus generating an ion-exchange site.

In the NH_3-SCR reaction, the Cu in the CHA zeolite undergoes a redox cycle between Cu^{I} and Cu^{II} [16,18,20,34]. The reduction of Cu occurs in a reaction with NO and NH_3, which leads to the

formation of a mobile $[Cu(NH_3)_2]^+$ species at low temperatures [17–20,25,27,33,35] or a Cu^+ species at higher temperatures. In the oxidation part, O_2 dissociation occurs under the influence of NO, and the Cu is re-oxidized to form Cu^{II}-(N,O) species [16,18,20,36,37].

The catalytic activity of Cu-CHA catalysts in the NH_3-SCR reaction can be divided into a low-temperature region (180-300 °C) and a high-temperature region (>350 °C). These are separated by a temperature interval from 300-350 °C where the activity actually drops with increasing temperature, see Figure 5. The advantageous low-temperature activity of these materials are linked to the chemical properties of Cu in these materials. The current understanding of the low-temperature activity of Cu-CHA catalysts is that the O_2 dissociation takes place on Cu pairs. The formation of Cu pairs is facilitated by the mobility of the $[Cu(NH_3)_2]^+$ species [18,20]. Whether there is an impact of the Cu originating from a Z-CuOH or Z_2-Cu site on the stability or mobility of the $[Cu(NH_3)_2]^+$ species is not clear. At higher temperatures, the mobile $[Cu(NH_3)_2]^+$ species is not stable and Cu pair formation becomes more difficult, which can result in a lower activity with increasing temperature [20].

The expected lifetime of an NH_3-SCR catalyst in a heavy-duty vehicle is 700000 km, which corresponds to about 10000 h of operation [2]. The catalyst has to be robust enough to maintain a certain level of activity throughout this period. A reason for the great interest in Cu-CHA catalysts is their robustness, which is largely related to the small-pore structure of the CHA zeolite. Thus, the small-pore structure of Cu-CHA catalysts has a significantly better hydrothermal stability than larger pore zeolite structures [38,39], and are therefore better suited for application in exhaust gas aftertreatment systems. Additionally, diffusion of unburned hydrocarbons into the pores of the zeolite is more difficult in small-pore zeolites, resulting in a better resistance towards deactivation by hydrocarbons as well [8]. The hydrolytic stability has proved to be an issue for SAPO-34 materials, which is a consequence of its more polarized framework [40,41]. The issue with the hydrolytic stability is easily solved by the use of its structural twin, the SSZ-13. However, there are some challenges with the use of Cu-CHA catalysts that are related to their low resistance towards deactivation by SO_2.

In EU and USA, ultra-low sulfur diesel (ULSD) is used in order to limit the emissions of SO_2. SO_2 is not removed in the aftertreatment system, but instead the sulfur content in diesel fuels is regulated. In ULSD, the sulfur content is restricted to a maximum of 10 wt ppm in EU [3], and 15 wt ppm in USA [2]. The use of ULSD results in approx. 0.5-2 ppmv SO_2 in the exhaust gas leaving the engine [2]. Even at these low concentrations of SO_2, the low-temperature activity of Cu-CHA catalysts is negatively affected. This is demonstrated in Figure 5, which shows the NO conversion of a Cu-CHA catalyst before and after exposure to SO_2. Since the low-temperature activity of Cu-CHA catalysts is one of their main advantages, and this advantage is removed in the presence of exhaust levels of SO_2, the susceptibility towards deactivation by SO_2 remains an important challenge for the application of Cu-CHA catalysts in diesel exhaust aftertreatment systems.

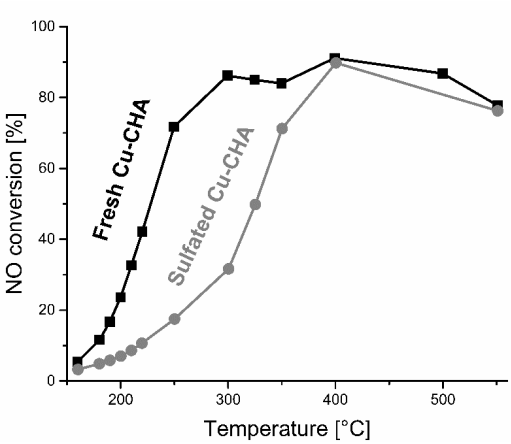

Figure 5 – Steady-state NO conversion as function of temperature for a powder Cu-CHA catalyst before (Fresh) and after (SO_2 exposed) exposure to SO_2. Adapted from [42].

At the outset of this project, the deactivation of Cu-CHA catalysts by SO_2 was suggested to be a result of ammonium sulfate and copper sulfate [43,44], which implies an oxidation of SO_2, but the deactivation mechanism was not known. In terms of the deactivation mechanism for ammonium sulfate, it could be envisioned that extensive depositions in the zeolite pores would lead to a limited accessibility of reactants and products to and from the Cu sites. Thus, a pore-blocking deactivation mechanism would be plausible for the deactivation by ammonium sulfates. For copper sulfate, it implies a more direct interaction between the sulfur species and the Cu sites. In that case, it is plausible that the deactivation occurs via a site-blocking mechanism where the redox properties, or the mobility, of the Cu sites are affected by SO_x.

An improved understanding of the deactivation mechanism(s) could enable new ways of enhancing the resistance of Cu-CHA catalysts towards SO_2-poisoning, and better assessment of the impact on the SCR performance. The approaches in this work to elucidate this includes investigations with ICP-OES (Inductively-Coupled Plasma – Optical Emission Spectroscopy), TGA (Thermo-Gravimetric Analysis), and SO_2 adsorption/desorption measurements to determine the amounts of sulfur that is captured by Cu-CHA catalysts, and the rate of the sulfur uptake. Furthermore, spectroscopic methods such as EPR (Electron Paramagnetic Spectroscopy) and STEM-EDX (Scanning Transmission Electron Microscopy – Energy Dispersive X-ray) spectroscopy have been used to detect where sulfur is located in the catalyst, and Density Functional Theory calculations have been used to evaluate possible Cu,S structures. Most extensively, kinetic measurements of Cu-CHA catalyst powders in the NH_3-SCR reaction have been carried out in parallel to all the characterization investigations in order to determine the impact of the sulfur content and the presence of SO_3 on the catalytic performance of the catalyst. Additionally, the impact of temperature and different gas compositions on the sulfation and regeneration processes has been evaluated in micro-reactor scale and monolith-reactor scale.

Objectives

If the deactivation mechanism by SO_2 can be better understood, measures to limit or prevent the deactivation of Cu-CHA catalysts may be developed, and the impact over the catalyst lifetime can be more accurately assessed. This could improve the efficiency of NO_x removal from heavy-duty diesel vehicle exhaust. The primary focus of this work is, therefore, to develop a solid fundamental understanding of the deactivation behavior of Cu-CHA catalysts by SO_2, and to assess if the presence of SO_2 in diesel exhaust is prohibitive for practical application of these catalysts in aftertreatment systems of heavy-duty diesel vehicles. These aspects of the work are presented in the different chapters of this thesis.

In Chapter 2, the effect of SO_2 concentration and exposure time on the deactivation of a Cu-SAPO-34 catalysts is established. Furthermore, the influence of $NO+NH_3$ on the sulfation process is elaborated, and particularly, the possible deactivation mechanisms by ammonium sulfate or copper sulfate are discussed. This is the only chapter where Cu-SAPO-34 has been used, but the role of the chemical composition of the CHA framework with respect to SO_2-poisoning is shown to be of limited importance.

Chapter 3 focuses on the impacts of temperature, H_2O, SO_2 and SO_3 on the deactivation of Cu-CHA catalysts. In this chapter, the terms reversible- and irreversible deactivation are introduced and defined, and the different impacts of these on the NH_3-SCR reaction mechanism are first observed and discussed.

Chapter 4 addresses the distribution of sulfur in the zeolite crystals of an SO_2 exposed Cu-CHA catalyst using scanning transmission electron microscopy with energy dispersive X-ray spectroscopy (STEM-EDX).

The impact of SO_2 over the lifetime of a Cu-CHA catalyst is studied in Chapter 5, where the deactivation after long-term SO_2 exposures at 200, 300, 400, and 500 °C, and subsequent regeneration at 550 °C, are evaluated. In this chapter, the kinetics for formation of sulfate species is touched upon by comparing mass uptakes in TGA experiments to S/Cu ratios determined by ICP-OES. Furthermore, the apparent dependence of the irreversible S/Cu ratio on the Si/Al ratio of the Cu-CHA is elucidated.

A more detailed mechanistic investigation and discussion of the deactivation by SO_2 in relation to the current understanding of the NH_3-SCR mechanism over Cu-CHA catalysts is described in Chapter 6. This is enabled by exploiting the ability of EPR to observe specific Cu sites in the Cu-CHA catalyst to monitor the development of these sites at increasingly extensive SO_2 exposures in combination with ICP-OES measurements and catalytic performance in the NH_3-SCR reaction.

A recurring challenge for the investigations of SO_2-poisoning of Cu-CHA catalysts, and Cu-CHA catalysts in general, is the measurement of active Cu sites. Chapter 7 contains a description of a newly developed method (NO-TPR) to quantify the number of active sites in Cu-CHA catalysts by measuring the consumption of NO during a temperature-programmed reduction of Cu-CHA

catalysts in NO+NH_3. The applicability of this method is explored on certain SO_2 exposed, and regenerated, Cu-CHA catalysts.

Finally, Chapter 8 summarizes the conclusions from each chapter into a combined understanding of how SO_2 deactivates Cu-CHA catalysts, and describes the implications of using these catalysts in current and future aftertreatment systems of heavy-duty diesel vehicles.

References

[1] J.D. Miller, C. Façanha, The state of clean transport policy - A 2014 synthesis of vehicle and fuel policy developments, ICCT Rep. (2014) 73. http://www.theicct.org/sites/default/files/publications/ICCT_StateOfCleanTransportPolicy_2014.pdf.

[2] DieselNet Technology Guide, (n.d.). https://dieselnet.com/tg.

[3] The International Council on Clean Transportation, A technical summary of Euro 6/VI vehicle emission standards, 2016.

[4] S.M. Platt, I. El Haddad, S.M. Pieber, A.A. Zardini, M. Clairotte, Gasoline cars produce more carbonaceous particulate matter than modern filter-equipped diesel cars, (2017) 1–9. doi:10.1038/s41598-017-03714-9.

[5] R. Suarez-bertoa, C. Astorga, Impact of cold temperature on Euro 6 passenger car emissions *, Environ. Pollut. 234 (2018) 318–329. doi:10.1016/j.envpol.2017.10.096.

[6] P. Karjalainen, L. Pirjola, J. Heikkilä, T. Lähde, T. Tzamkiozis, L. Ntziachristos, J. Keskinen, T. Rönkkö, Exhaust particles of modern gasoline vehicles: A laboratory and an on-road study, Atmos. Environ. 97 (2014) 262–270. doi:10.1016/j.atmosenv.2014.08.025.

[7] World Health Organization, WHO Air quality guidelines for particulate matter, ozone, nitrogen dioxide and sulfur dioxide: global update 2005: summary of risk assessment, 2006. doi:10.1016/0004-6981(88)90109-6.

[8] P.N.R. Vennestrøm, PhD Thesis: Selective catalytic reduction of nitrogen oxides with ammonia over microporous zeolite catalysts, Universitat Politècnica de Valencia, Instituto de Tecnología Química, Consejo Superior de Investigaciones Científicas and Haldor Topsøe A/S, 2014.

[9] I. Nova, E. Tronconi, Urea-SCR Technology for deNOx After Treatment of Diesel Exhausts, 1st ed., Springer-Verlag, New York, 2014.

[10] P. Mendoza-Villafuerte, R. Suarez-Bertoa, B. Giechaskiel, F. Riccobono, C. Bulgheroni, C. Astorga, A. Perujo, NOx, NH3, N2O and PN real driving emissions from a Euro VI heavy-duty vehicle. Impact of regulatory on-road test conditions on emissions, Sci. Total Environ. 609 (2017) 546–555. doi:10.1016/j.scitotenv.2017.07.168.

[11] F. Gao, J.H. Kwak, J. Szanyi, C.H.F. Peden, Current Understanding of Cu-Exchanged Chabazite Molecular Sieves for Use as Commercial Diesel Engine DeNOx Catalysts, Top. Catal. 56 (2013) 1441–1459.

[12] F. Gao, C.H.F. Peden, Recent Progress in Atomic-Level Understanding of Cu/SSZ-13 Selective Catalytic Reduction Catalysts, Catalysts. 8 (2018) 140. doi:10.3390/catal8040140.

[13] C. Paolucci, J.R. Di Iorio, F.H. Ribeiro, R. Gounder, W.F. Schneider, Catalysis Science of NOx Selective Catalytic Reduction With Ammonia Over Cu-SSZ-13 and Cu-SAPO-34, in: Adv. Catal., 1st ed., Elsevier Inc., 2016: pp. 1–4. doi:10.1016/bs.acat.2016.10.002.

[14] A.M. Beale, F. Gao, I. Lezcano-Gonzalez, C.H.F. Peden, J. Szanyi, Recent advances in automotive catalysis for NOx emission control by small-pore microporous materials, Chem. Soc. Rev. 44 (2015) 7371–7405. doi:10.1039/C5CS00108K.

[15] International Zeolite Association, http://www.iza-structure.org/databases/, (n.d.).

[16] T.V.W. Janssens, H. Falsig, L.F. Lundegaard, P.N.R. Vennestrøm, S.B. Rasmussen, P.G. Moses, F. Giordanino, E. Borfecchia, K.A. Lomachenko, C. Lamberti, S. Bordiga, A. Godiksen, S. Mossin, P. Beato, A Consistent Reaction Scheme for the Selective Catalytic Reduction of Nitrogen Oxides with Ammonia, ACS Catal. 5 (2015) 2832–2845. doi:10.1021/cs501673g.

[17] S. Shwan, M. Skoglundh, L.F. Lundegaard, R.R. Tiruvalam, T.V.W. Janssens, A. Carlsson, P.N.R. Vennestrøm, Solid-State Ion-Exchange of Copper into Zeolites Facilitated by Ammonia at Low Temperature, ACS Catal. 5 (2015) 16–19. doi:10.1021/cs5015139.

[18] C. Paolucci, I. Khurana, A.A. Parekh, S. Li, A.J. Shih, H. Li, J.R. Di Iorio, J.D. Albarracin-Caballero, A. Yezerets, J.T. Miller, W.N. Delgass, F.H. Ribeiro, W.F. Schneider, R. Gounder, Dynamic multinuclear sites formed by mobilized copper ions in NOx selective catalytic reduction, Science 357 (2017) 898–903. doi:10.1126/science.aan5630.

[19] C. Paolucci, A.A. Parekh, I. Khurana, J.R. Di Iorio, H. Li, J.D.A. Caballero, A.J. Shih, T. Anggara, W.N. Delgass, J.T. Miller, F.H. Ribeiro, R. Gounder, W.F. Schneider, Catalysis in a Cage: Condition-Dependent Speciation and Dynamics of Exchanged Cu Cations in SSZ-13 Zeolites, J. Am. Chem. Soc. 138 (2016) 6028–6048. doi:10.1021/jacs.6b02651.

[20] F. Gao, D. Mei, Y. Wang, J. Szanyi, C.H.F. Peden, Selective Catalytic Reduction over Cu/SSZ-13: Linking Homo- and Heterogeneous Catalysis, J. Am. Chem. Soc. 139 (2017) 4935–4942. doi:10.1021/jacs.7b01128.

[21] D. Wang, F. Gao, C.H.F. Peden, J. Li, K. Kamasamudram, W.S. Epling, Selective catalytic reduction of NOxwith NH3over a Cu-SSZ-13 catalyst prepared by a solid-state ion-exchange method, ChemCatChem. 6 (2014) 1579–1583. doi:10.1002/cctc.201402010.

[22] F. Gao, E.D. Walter, M. Kollar, Y. Wang, J. Szanyi, C.H.F. Peden, Understanding ammonia selective catalytic reduction kinetics over Cu/SSZ-13 from motion of the Cu ions, J. Catal.

319 (2014) 1–14. doi:10.1016/j.jcat.2014.08.010.

[23] F. Gao, E.D. Walter, E.M. Karp, J. Luo, R.G. Tonkyn, J.H. Kwak, J. Szanyi, C.H.F. Peden, Structure–activity relationships in NH3-SCR over Cu-SSZ-13 as probed by reaction kinetics and EPR studies, J. Catal. 300 (2013) 20–29.

[24] J.H. Kwak, D. Tran, J. Szanyi, C.H.F. Peden, J.H. Lee, The Effect of Copper Loading on the Selective Catalytic Reduction of Nitric Oxide by Ammonia Over Cu-SSZ-13, Catal. Lett. 142 (2012) 295–301.

[25] A.Y. Stakheev, D.A. Bokarev, A.I. Mytareva, T.V.W. Janssens, P.N.R. Vennestrøm, Detailed Study of Cu Migration in the Course of NH3-Facilitated Solid-State Ion-Exchange into *BEA Zeolites, Top. Catal. 60 (2017) 255–259. doi:10.1007/s11244-016-0607-x.

[26] A. Godiksen, O.L. Isaksen, S.B. Rasmussen, P.N.R. Vennestrøm, S. Mossin, Site-Specific Reactivity of Copper Chabazite Zeolites with Nitric Oxide, Ammonia, and Oxygen, ChemCatChem. 10 (2018) 366–370. doi:10.1002/cctc.201701357.

[27] F. Giordanino, E. Borfecchia, K.A. Lomachenko, A. Lazzarini, G. Agostini, E. Gallo, A. V Soldatov, P. Beato, S. Bordiga, C. Lamberti, Interaction of NH3 with Cu-SSZ-13 Catalyst: A Complementary FTIR, XANES, and XES Study, J. Phys. Chem. Lett. 5 (2014) 1552–1559.

[28] A. Godiksen, F.N. Stappen, P.N.R. Vennestrøm, F. Giordanino, S.B. Rasmussen, L.F. Lundegaard, S. Mossin, Coordination Environment of Copper Sites in Cu-CHA Zeolite Investigated by Electron Paramagnetic Resonance, J. Phys. Chem. C. 118 (2014) 23126–23138.

[29] F. Giordanino, P.N.R. Vennestrøm, L.F. Lundegaard, F.N. Stappen, S. Mossin, P. Beato, S. Bordiga, C. Lamberti, Characterization of Cu-exchanged SSZ-13: a comparative FTIR, UV-Vis, and EPR study with Cu-ZSM-5 and Cu-β with similar Si/Al and Cu/Al ratios., Dalt. Trans. 42 (2013) 12741–12761.

[30] E. Borfecchia, K.A. Lomachenko, F. Giordanino, H. Falsig, P. Beato, A. V Soldatov, S. Bordiga, C. Lamberti, Revisiting the nature of Cu sites in the activated Cu-SSZ-13 catalyst for SCR reaction, Chem. Sci. 6 (2015) 548–563. doi:10.1039/c4sc02907k.

[31] E. Borfecchia, P. Beato, S. Svelle, U. Olsbye, C. Lamberti, S. Bordiga, Cu-CHA – a model system for applied selective redox catalysis, Chem. Soc. Rev. (2018). doi:10.1039/C8CS00373D.

[32] A. Martini, E. Borfecchia, K.A. Lomachenko, I. Pankin, C. Negri, G. Berlier, P. Beato, H. Falsig, S. Bordiga, C. Lamberti, Composition-driven Cu-speciation and reducibility in Cu-CHA zeolite catalysts: a multivariate XAS/FTIR approach to complexity, Chem. Sci. 8 (2017) 6836–6851. doi:10.1039/C7SC02266B.

[33] K.A. Lomachenko, E. Borfecchia, C. Negri, G. Berlier, C. Lamberti, P. Beato, H. Falsig, S. Bordiga, The Cu-CHA deNOx Catalyst in Action: Temperature-Dependent NH3-Assisted

Selective Catalytic Reduction Monitored by Operando XAS and XES, J. Am. Chem. Soc. 138 (2016) 12025–12028. doi:10.1021/jacs.6b06809.

[34] C. Paolucci, A.A. Verma, S.A. Bates, V.F. Kispersky, J.T. Miller, R. Gounder, W.N. Delgass, F.H. Ribeiro, W.F. Schneider, Isolation of the Copper Redox Steps in the Standard Selective Catalytic Reduction on Cu-SSZ-13, Angew. Chem. Int. Ed. 53 (2014) 1–7.

[35] L. Chen, J. Jansson, M. Skoglundh, H. Grönbeck, Mechanism for Solid-State Ion Exchange of Cu+ into Zeolites, J. Phys. Chem. C. 120 (2016) 29182–29189. doi:10.1021/acs.jpcc.6b09553.

[36] L. Chen, H. Falsig, T.V.W. Janssens, J. Jansson, M. Skoglundh, H. Grönbeck, Effect of Al-distribution on oxygen activation over Cu-CHA, Catal. Sci. Technol. 8 (2018) 2131–2136. doi:10.1039/c8cy00083b.

[37] L. Chen, H. Falsig, T.V.W. Janssens, H. Grönbeck, Activation of oxygen on (NH3–Cu–NH3)+ in NH3-SCR over Cu-CHA, J. Catal. 358 (2018) 179–186. doi:10.1016/j.jcat.2017.12.009.

[38] J.H. Kwak, D. Tran, S.D. Burton, J. Szanyi, J.H. Lee, C.H.F. Peden, Effects of hydrothermal aging on NH3-SCR reaction over Cu/zeolites, J. Catal. 287 (2012) 203–209.

[39] D.W. Fickel, E. D'Addio, J.A. Lauterbach, R.F. Lobo, The ammonia selective catalytic reduction activity of copper-exchanged small-pore zeolites, Appl. Catal. B. 102 (2011) 441–448.

[40] K. Leistner, L. Olsson, Deactivation of Cu/SAPO-34 during low-temperature NH3-SCR, Appl. Catal. B. 165 (2015) 192–199. doi:10.1016/j.apcatb.2014.09.067.

[41] J. Wang, D. Fan, T. Yu, J. Wang, T. Hao, X. Hu, M. Shen, W. Li, Improvement of low-temperature hydrothermal stability of Cu/SAPO-34 catalysts by Cu2+ species, J. Catal. 322 (2015) 84–90. doi:10.1016/j.jcat.2014.11.010.

[42] P.S. Hammershøi, A.D. Jensen, T.V.W. Janssens, Impact of SO2-poisoning over the lifetime of a Cu-CHA catalyst for NH3-SCR, Appl. Catal. B Environ. 238 (2018) 104–110. doi:10.1016/j.apcatb.2018.06.039.

[43] Y. Cheng, C. Lambert, D.H. Kim, J.H. Kwak, S.J. Cho, C.H.F. Peden, The different impacts of SO2 and SO3 on Cu/zeolite SCR catalysts, Catal. Today. 151 (2010) 266–270.

[44] A. Kumar, M.A. Smith, K. Kamasamudram, N.W. Currier, H. An, A. Yezerets, Impact of different forms of feed sulfur on small-pore Cu-zeolite SCR catalyst, Catal. Today. 231 (2014) 75–82.

Chapter 1

Chapter 2

Importance of the Cu oxidation state for the SO_2-poisoning of a Cu-SAPO-34 catalyst in the NH_3-SCR reaction

This chapter has been published in:
Applied Catalysis B: Environmental 236 (2018) 377-383
https://doi.org/10.1016/j.apcatb.2018.05.038

Applied Catalysis B: Environmental 236 (2018) 377–383

Contents lists available at ScienceDirect

Applied Catalysis B: Environmental

journal homepage: www.elsevier.com/locate/apcatb

Importance of the Cu oxidation state for the SO_2-poisoning of a Cu-SAPO-34 catalyst in the NH_3-SCR reaction

Peter S. Hammershøi[a,b], Peter N.R. Vennestrøm[a], Hanne Falsig[c], Anker D. Jensen[b], Ton V.W. Janssens[a,*]

[a] Umicore Denmark ApS, Nøjsomhedsvej 20, 2800 Kgs. Lyngby, Denmark
[b] Department of Chemical and Biochemical Engineering, Technical University of Denmark, Søltofts Plads B229, 2800 Kgs. Lyngby, Denmark
[c] Haldor Topsoe A/S, Haldor Topsøe's Allé 1, 2800 Kgs. Lyngby, Denmark

ARTICLE INFO

Keywords:
NH_3-SCR
SO_2 poisoning
Deactivation
Cu-CHA
DFT

ABSTRACT

Cu-exchanged zeolites of the CHA structure are state-of-the-art catalysts for selective catalytic reduction of NO_x with NH_3 in diesel aftertreatment systems. However, these catalysts deactivate in the presence of SO_2, which is a constituent of diesel exhaust gas. In this article, the deactivation behavior and mechanisms of a Cu-SAPO-34 catalyst were studied with reactor tests and DFT calculations. Exposure of the catalyst to two different SO_2 concentrations and durations, but with the same total SO_2 exposure, calculated as the product of partial pressure of SO_2 and exposure time, lead to the same degree of deactivation. Exposure of the Cu-SAPO-34 catalyst to SO_2 in the presence and absence of NO and NH_3 at different temperatures between 200–600 °C showed different trends for the deactivation. Below 400 °C, the S/Cu ratio on the catalyst increased with temperature in absence of NO and NH_3, while it decreased with increasing temperature in the presence of NO and NH_3. This is explained by the ability of NO and NH_3 to reduce Cu(II) to Cu(I). DFT calculations show that SO_2 adsorbs more strongly on Cu(I) than on Cu (II). Above 400 °C, the S/Cu ratio decreased with temperature irrespective of the presence of NO and NH_3. In all cases, the S/Cu ratio is lower than 1. This is not compatible with extensive deposition of ammonium sulfate when co-feeding SO_2, H_2O and NH_3. A more likely explanation for the deactivation is that SO_2 is mainly related to the Cu sites. This is further corroborated by DFT calculations showing that SO_2 and SO_3, which is possibly formed by oxidation of SO_2 over Cu sites, interact similar with Cu in Cu-SAPO-34 and Cu-SSZ-13.

1. Introduction

Diesel engines operate with excess air in the combustion, leading to production of nitrogen oxides (NO_x). NO_x emissions from diesel engines are a source of air pollution and are therefore regulated. To meet legislation requirements for NO_x emissions, a modern aftertreatment systems for diesel engines contain one or more catalysts for the reduction of NO_x to N_2 by selective catalytic reduction with NH_3 (NH_3-SCR). The NH_3-SCR proceeds according to the reaction: $4\,NH_3 + 4\,NO + O_2 \rightarrow 4\,N_2 + 6\,H_2O$. Urea injected in the exhaust gas stream is commonly used as a source for NH_3, and, if properly controlled, the NH_3-SCR reaction can reach very high degrees of NO_x removal. The currently applied catalysts for NH_3-SCR are based on V-oxide, Fe-zeolites or Cu-zeolites.

Current zeolite state-of-the-art NH_3-SCR catalysts are based on the CHA structure due to its better hydrothermal stability than other commercial zeolite structures [1]. The CHA structure exists with an overall chemical composition of $H_nAl_nSi_{1-n}O_2$ (SSZ-13) or $H_nSi_nAlP_{1-n}O_4$ (SAPO-34), under the assumption that only P is substituted by Si. Cu ions are introduced into the ion-exchange positions in these materials, and these Cu sites are the source of the catalytic activity of Cu-CHA catalysts. Compared to Fe-zeolites and vanadia-based SCR catalysts, the main advantages of the Cu-CHA catalysts are superior low-temperature SCR activity and lower N_2O selectivity [2,3]. A disadvantage of the Cu-CHA catalysts is their susceptibility towards poisoning by SO_2 [4,5]. SO_2 is an inevitable compound in diesel exhausts, and even at concentration levels below 15 ppm, as in ultra-low sulfur diesel [4,6], the resulting SO_2 in the exhaust gas, typically about 1–2 ppmv, has a significant impact on the performance of Cu-CHA catalysts. It is therefore important to understand how SO_2 affects the Cu-CHA catalysts.

The gas stream that the SCR catalyst is exposed to in a diesel exhaust system consists of several other compounds than SO_2, including but not limited to O_2, H_2O, NO and NH_3. These compounds may affect the

* Corresponding author.
E-mail address: tonv.w.janssens@eu.umicore.com (T.V.W. Janssens).

https://doi.org/10.1016/j.apcatb.2018.05.038
Received 19 February 2018; Received in revised form 9 May 2018; Accepted 14 May 2018
Available online 18 May 2018

interaction of SO_2 with the Cu-CHA catalyst. Several SO_2-poisoning studies have been carried out in gas compositions where NO and NH_3 are omitted [4–11]. Such experiments have shown that the deactivation is due to SO_2 interactions with Cu, which is dependent on the temperature of SO_2 exposure. Adsorption of SO_2 mainly takes place at temperatures around 200 °C [5], while chemical reactions between SO_2 and Cu become more dominating at temperatures around 400 °C [5]. SO_2 reacts at the Cu sites in the CHA, resulting in (Cu,S) species with S in oxidation state +6, which are assigned to isolated Cu-sulfates [4,12]. This assignment is corroborated by their decomposition temperature of around 650 °C, which is consistent with the decomposition of bulk $CuSO_4$ [4,11,13], and by an observed 1:1 correlation between the S/Cu ratio of these species and the deactivation [11]. The formation of sulfates implies that SO_2 is oxidized over the catalyst, and the rate of oxidation increases with temperature [10]. The effect of the gas composition on the deactivation by SO_2 is not fully understood, and therefore, it is important to improve the understanding in order to be able to transfer results to the SO_2-poisoning occurring in real exhausts.

It has been argued that the effect of NO and NH_3 on SO_2-poisoning is the formation of ammonium sulfate, which may infer mass transfer limitations by pore-blocking [14–16]. However, ammonium sulfate decomposes at about 350 °C, and can therefore feasibly be removed [16]. Moreover, the presence of NO and NH_3, or release of NH_3 from ammonium sulfate, has a suggested beneficial effect on the regeneration of SO_2-poisoned catalysts, due to the reducing properties of the SCR gas mixture and NH_3 [8,16].

In this article the SO_2 deactivation behavior of a Cu-SAPO-34 catalyst was investigated. The Cu-SAPO-34 was chosen because of its high hydrothermal stability so that high-temperature regeneration did not result in deterioration of the zeolite structure; something that cannot always be avoided with SSZ-13. We investigated the effect of SO_2 exposure time, SO_2 concentration, and the presence of NO and NH_3 on the deactivation by SO_2. DFT calculations were used to evaluate the interactions between Cu, SO_2 and SO_3 in order to obtain a better understanding of the temperature dependence, and effect of NO and NH_3, on the deactivation.

2. Experimental

2.1. Catalyst material and reactor testing conditions

In this study, we used a Cu-SAPO-34 catalyst with a (P + Al)/Si of 6.5 and a Cu-loading of 1.9 wt%, as determined by ICP-OES. The steady-state conversions of NO in the NH_3-SCR reaction were measured in a fixed-bed quartz reactor with an inner diameter of 2 mm, using 5 mg catalyst on dry matter basis, and a sieve fraction of 150–300 μm. The SCR-feed gas for the activity measurements consisted of 500 ppmv NO, 530 ppmv NH_3, 10% O_2 and 5% H_2O, in N_2 at a total flow of 225 N mL/min- The inlet and outlet gas composition was determined using a Gasmet CX4000 FTIR analyser. Prior to the NH_3-SCR activity measurements, the catalyst was heated for 1 h in the SCR-feed gas at 550 °C. The effect of SO_2 on the NH_3-SCR activity was determined from a comparison of the NO_x conversion before and after exposure of the catalyst to an SO_2-containing feed gas in the same reactor setup.

The catalyst was exposed to SO_2 in a flow with either SCR-feed gas, or with 10% O_2 and 5% H_2O, balanced by N_2 to a total flow rate of 225 N mL/min. The inlet concentrations of SO_2 were 1.5 or 15 ppmv. The temperature and duration of SO_2 exposure were varied and are stated specifically with the results.

The evaluation of the NH_3-SCR activity is based on the rate constant for the NH_3-SCR reaction. The rate constants (k) are derived from measured steady state NO_x conversions, as shown in Eq. (1), assuming plug flow of the gas and that the NH_3-SCR reaction is first order in NO.

$$k = -\frac{F}{W}\ln(1-X) \quad (1)$$

F is the total molar flow rate, W is the total mass of catalyst on a dry matter basis, and X is the NO_x conversion.

The deactivation of the catalyst is calculated from a comparison of rate constants after SO_2 exposure or regeneration with the corresponding rate constant of the fresh catalyst. In this article, we define the deactivation as:

$$\text{Deactivation} = 1-\frac{k}{k_{fresh}} \quad (2)$$

2.2. Computational

Spin polarized Density Functional Theory (DFT) calculations were used to obtain adsorption energies of O_2, SO_2 and SO_3 on Cu species in SAPO-34 and SSZ-13. The calculations were performed with the GPAW package [17,18] using a real space grid-based projector augmented wave method. A grid spacing of h = 0.2 Å and a Fermi smearing of 0.1 K were found sufficient to obtain a satisfactory convergence of the relative energies. To account for Van der Waals interactions the BEEF-vdW functional was used [19]. This functional has shown to produce reliable results for the interaction of molecules with zeolites [20,21]. Both SSZ-13 and SAPO-34 were represented by periodic cells with hexagonal symmetry containing 36 T-atoms (SSZ-13 cell parameters: a,b = 13.886 Å, c = 15.116 Å, α = 120°, β, γ = 90° and SAPO-34 cell parameters: a,b = 14.602 Å, c = 15.287 Å, α = 120°, β, γ = 90°).

3. Results

3.1. Deactivation by SO_2 exposure and scalability

Fig. 1A shows the measured steady state NO_x conversions for the fresh catalyst, after exposure to SO_2, and after regeneration at 550 °C. For the SO_2 exposure, 1.5 ppmv of SO_2 was added to the SCR-feed, which is in the SO_2 concentration range expected in automotive diesel exhaust, and the catalyst was held at 300 °C for 8 h. The regeneration of the catalyst was performed at 550 °C for 1 h in SCR-feed gas without SO_2. Exposure to SO_2 leads to significantly lower steady state NO_x conversions in the temperature range 150–300 °C. Regeneration at 550 °C restores most of the original NO_x conversion in this temperature range. This behavior has also been observed for an aluminosilicate Cu-CHA catalyst, and can be understood in terms of irreversible and reversible deactivation [11]. According to the definitions in [11], the deactivation measured after regeneration at 550 °C is the irreversible deactivation, and the difference in deactivation after SO_2 exposure and regeneration at 550 °C is the reversible deactivation.

For practical reasons when investigating SO_2 deactivation, it is often useful to accelerate the SO_2-poisoning by increasing the SO_2 concentration and proportionally shortening the exposure time. The results are then interpreted in terms of the total SO_2 exposure, calculated as the product of the SO_2 partial pressure and the exposure time, rather than the SO_2 concentration. This interpretation requires that a direct proportionality exists between the exposure time and SO_2 concentration, such that these two parameters can be scaled with respect to SO_2-poisoning. This scalability was investigated by comparing the results of the non-accelerated SO_2 exposure, i.e. exposure to 1.5 ppmv SO_2, to the results from a catalyst exposed to an accelerated SO_2 exposure. For the accelerated SO_2 exposure, the SO_2 concentration was increased by a factor 10 and the exposure time was correspondingly decreased, thus exposing to 15 ppmv SO_2 in SCR-feed gas for 48 min at 300 °C. The steady state NO_x conversions before and after the accelerated SO_2 exposure, and after 1 h regeneration at 550 °C in SCR-feed gas, are plotted in Fig. 1B.

The appearance of the NO_x conversion curve for the accelerated SO_2 exposed catalyst in Fig. 1B, is very similar to that shown in Fig. 1A. The NO_x conversions of the fresh catalyst shown in Fig. 1B are slightly lower than those of the fresh catalyst in Fig. 1A, which is due to small

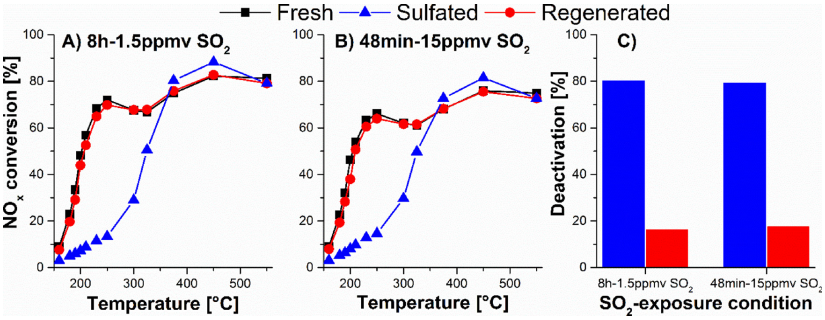

Fig. 1. (A) NO_x conversion as function of temperature for the Cu-SAPO-34 catalyst before and after exposure to 1.5 ppmv SO_2 for 8 h at 300 °C, and after 1 h regeneration at 550 °C. (B) NO_x conversion as function of temperature for the Cu-SAPO-34 catalyst before and after exposure to 15 ppmv SO_2 for 48 min at 300 °C, and after 1 h regeneration at 550 °C. Gas flow conditions for NO_x measurements and regenerations were 500 ppmv NO, 530 ppmv NH_3, 10% O_2, and 5% H_2O in N_2 at 225 N mL/min. The same gas flow conditions, with addition of SO_2, were used for SO_2 exposures. (C) Deactivation of the sulfated (blue bars) and regenerated (red bars) states of the Cu-SAPO-34 catalyst evaluated at 180 °C, after exposure to 1.5 ppmv SO_2 for 8 h and 15 ppmv SO_2 for 48 min (For interpretation of the references to color in this figure legend, the reader is referred to the web version of this article).

differences in the catalyst loads. Therefore, in order to further confirm the similarity of the impact of the accelerated and non-accelerated SO_2 exposure conditions on the SCR performance of the catalyst, the deactivation (evaluated at 180 °C) after SO_2 exposure and regeneration are plotted in Fig. 1C. The degree of deactivation after both treatments are similar, with total deactivations of 80 and 79% and irreversible deactivations of 16 and 18%. This means that the deactivation is the same for the same total SO_2 exposure, and indicates that the SO_2 concentration and exposure time are scalable.

3.2. Regeneration of the irreversible deactivation

A possible explanation for the irreversible deactivation is the formation of Cu-sulfates that are stable up to ~650 °C [4,11,13]. If this is true, a full restoration of the activity of the catalyst by heating to 700 °C should be possible. This was verified by measuring the SCR activity over the Cu-SAPO-34 catalyst after SO_2 exposure and again after regeneration at 550 °C and 700 °C. Fig. 2 shows that at 180 °C, the SCR reaction rate constant is lowest for the sulfated state of the catalyst, and that regeneration first at 550 °C, partially restores the activity, while subsequent regeneration at 700 °C restores the activity to the original level of the fresh catalyst. This result is consistent with Cu-sulfate species causing the irreversible deactivation, since heating to 700 °C, which is above the decomposition temperature of $CuSO_4$, restores the activity of the catalyst completely.

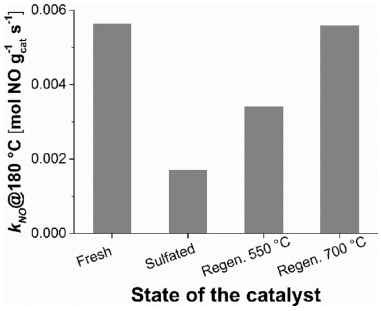

Fig. 2. The NH_3-SCR rate constants of the different states of the Cu-SAPO-34 catalyst, i.e. fresh, sulfated, regenerated at 550 °C, and regenerated at 700 °C. Sulfation was 24 h at 550 °C in 15 ppmv SO_2, 500 ppmv NO, 530 ppmv NH_3, 10% O_2, and 5% H_2O in N_2 at 225 N mL/min. The regenerations were 1 h at 550 °C and 2 h at 700 °C, and were carried out with the same flow conditions as the sulfation, but in absence of SO_2.

3.3. SO_2 exposure in presence of NO and NH_3

The SCR catalyst in a diesel exhaust system is exposed to a wide range of temperatures up to approx. 550 °C, with typical operating temperatures between 200–500 °C. Therefore, the impact of temperature on the deactivation was investigated by exposing the Cu-SAPO-34 catalyst to 1.5 ppmv SO_2 for 8 h in the presence of SCR-feed gas at 200, 300, 400 and 500 °C. The measured steady state NO_x conversions are shown in Fig. 3A–D before and after SO_2 exposure, and after 1 h of regeneration at 550 °C in SCR-feed gas. The NO_x conversion below 325 °C is lower than for the fresh catalyst in all measurements, for both the sulfated and regenerated states of the catalyst. Furthermore, the deactivations in Fig. 4B show that there is a clear trend of more extensive deactivation of the sulfated state of the catalyst at lower SO_2 exposure temperature. The S/Cu ratios of the catalyst shown in Fig. 4A, which were estimated by integration of the measured decrease in SO_2 concentrations in the outlet of the reactor during SO_2 exposure, also increase at lower SO_2 exposure temperature. This is consistent with an interpretation that larger S-uptakes lead to more pronounced deactivation. A different trend is observed for the deactivation of the regenerated states of the catalyst, where only the catalyst exposed to SO_2 at 200 °C stands out with a significantly larger deactivation than the rest.

In order to see if there is a significant impact of NO and NH_3 presence on the uptake of SO_2, the S-uptakes were measured after SO_2 exposure in absence of NO and NH_3 as well. This was done in a separate experiment by measuring the SO_2 desorption during heating to 700 °C after 3 h exposure to 15 ppmv SO_2 in 10% O_2 and 5% H_2O at 200–600 °C. This is possible because all S species desorb as SO_2 [4,13], and the complete restoration of the activity by heating to 700 °C indicates that no sulfur is left on the catalyst (see Fig. 2) [11]. The area of the SO_2 desorption peaks in Fig. 5 reveal that there is a maximum S-uptake at 400 °C, after SO_2 exposure in absence of NO and NH_3, which is different from the SO_2 exposure in the presence of NO and NH_3.

A comparison of the SO_2 uptake at different temperatures in the presence and absence of NO and NH_3 is shown in Fig. 6. Since the SO_2 exposure conditions of the two series are different, the absolute S/Cu ratios are not directly comparable, but the trends with respect to the

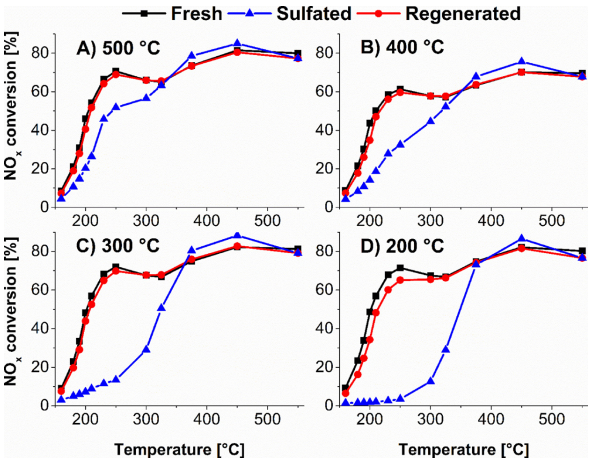

Fig. 3. NO_x conversions as functions of temperature for the Cu-SAPO-34 catalyst before and after SO_2 exposure for 8 h at (A) 500 °C, (B) 400 °C, (C) 300 °C, and D) 200 °C, and after 1 h regeneration at 550 °C. NO_x conversion measurements and regenerations were carried out in 500 ppmv NO, 530 ppmv NH_3, 10% O_2, and 5% H_2O in N_2 at 225 N mL/min, and the same for the SO_2 exposures, but with the addition of 1.5 ppmv SO_2.

exposure temperature are. In the presence of NO and NH_3, the S/Cu ratio decreases monotonically at increased temperature, whereas a maximum for the S/Cu ratio is observed at 400 °C in the absence of NO and NH_3. A possible explanation for the different trends below 400 °C is the deposition of ammonium sulfates in the zeolite pores at low temperatures, which decompose above 350 °C to restore catalytic activity [14–16]. Interestingly, the trends of the S/Cu ratios in the presence and absence of NO and NH_3 appear similar above 400 °C. These results indicate that above 400 °C, the SO_2 exposure conditions are similar despite the different inlet gas compositions. This may be rationalized by the faster SCR reaction rate at higher temperatures, where NO and NH_3 are converted to N_2 and H_2O faster, which means that increasing parts of the catalyst bed are effectively exposed to SO_2 in absence of NO and NH_3 at higher temperatures.

3.4. Stability of reaction products of Cu sites with SO_2 and SO_3

DFT calculations have been carried out to obtain information about the stability of possible SO_x species that can be formed in reactions between different Cu sites in the Cu-SAPO-34 catalyst and SO_2. Because we cannot exclude the formation of some SO_3 when exposing to SO_2 only, especially at higher temperatures, reactions between Cu sites and SO_3 have also been considered in the calculations. The Cu species that are present in the catalyst is determined by the conditions of the SO_2 exposure. In presence of NO and NH_3, Cu(II) can reduce to Cu(I) [22–26], which is modelled as a naked Cu(I) atom charge-balancing a single exchange site, Z-Cu(I). In presence of O_2 and H_2O, only Cu(II) is expected to be present, which can be in two different forms. Either as a single Cu(II) atom charge-balancing two exchange sites, Z_2-Cu(II), or as

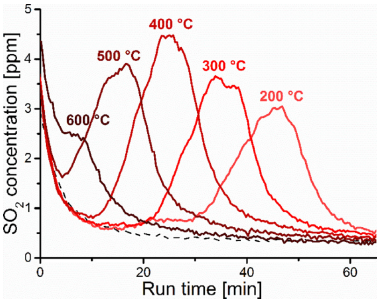

Fig. 5. Outlet SO_2 concentrations during heating to 700 °C after exposing the Cu-SAPO-34 catalyst for 3 h to 15 ppmv SO_2, 10% O_2, and 5% H_2O in N_2 at 225 N mL/min and at 200–600 °C. The dashed line is the zero-desorption line.

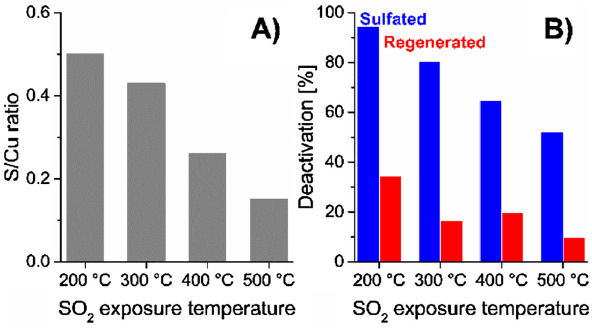

Fig. 4. (A) S/Cu ratios for each SO_2 exposure temperature of the Cu-SAPO-34 catalyst after exposure to 1.5 ppmv SO_2 in SCR-feed gas for 8 h. (B) Deactivation evaluated at 180 °C of the sulfated (blue bars) and regenerated (red bars) states of the Cu-SAPO-34 catalyst for each SO_2 exposure temperature with 1.5 ppmv SO_2 in SCR-feed gas for 8 h (For interpretation of the references to colour in this figure legend, the reader is referred to the web version of this article).

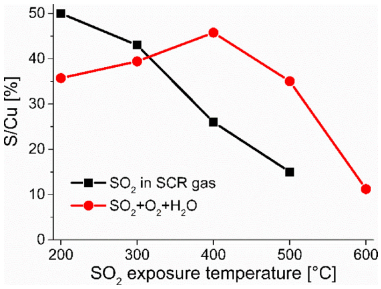

Fig. 6. The S/Cu ratios as functions of the SO_2 exposure temperature for the SO_2 exposures of the Cu-SAPO-34 catalyst in presence and absence of NO and NH_3.

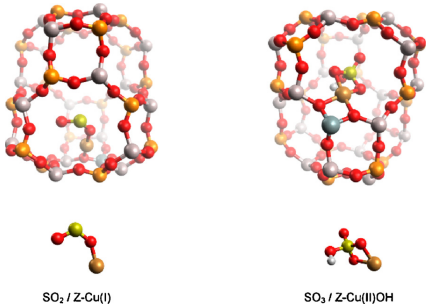

Fig. 7. Calculated structures of SO_2 adsorbed on Z-Cu(I) and SO_3 on Z-Cu(II)OH on Cu-SAPO-34. The atoms are indicated as follows: O (red), P (orange), Al (light purple), Si (grey), Cu (brown), S (yellow), H (white) (For interpretation of the references to colour in this figure legend, the reader is referred to the web version of this article).

a Cu(II) atom with a hydroxide ion charge-balancing a single exchange site, Z-Cu(II)OH. The most stable reaction products from reactions between the three different Cu sites with SO_2 or SO_3, as determined from DFT calculations, are listed in Table 1.

The DFT calculations show that both SO_2 and SO_3 are able to form stable species with Z-Cu(II)OH and with Z-Cu(I), in agreement with previous DFT calulations [12]. The calculated change in energy for adsorption of SO_2, SO_3 and O_2 on Z_2-Cu(II) is positive, indicating that neither of these species adsorb on the Z_2-Cu(II) sites. Interestingly, the most stable reaction product of the Z-Cu(I) site is in reaction with SO_2, while the Z-Cu(II)OH site forms the most stable species in reaction with SO_3. Fig. 7 shows the calculated structures of the resulting Cu species. DFT calculations also indicate that neither SO_2 nor SO_3 bind to the mobile $[Cu(NH_3)_2]^+$ species, which provides the active centers for NH_3-SCR at low temperatures [27,28].

The same calculations of reaction products of Cu sites with SO_2 and SO_3 have also been carried out for an aluminosilicate CHA framework, and the results are similar to those for the silicoaluminophosphate Cu-SAPO-34 structure, but with a tendency to slightly less stable reaction products. This indicates that the deactivation of Cu-CHA catalysts by SO_2 and SO_3 is mainly related to the Cu-SO_x chemistry, and that the framework chemistry, therefore, is of lesser importance.

4. Discussion

It appears that the deactivation level by SO_2 correlates to the total amount of SO_2 that the catalyst is exposed to, as shown in Fig. 1, where the catalyst has been exposed to different SO_2 concentrations and durations at 300 °C. However, this result could also be due to a saturation effect. If a SO_x saturation level is reached, it means that the S-uptake cannot get larger. In Fig. 6 all the S/Cu ratios are plotted as functions of the SO_2 exposure temperature, and the S-uptakes at 200 °C in presence of NO and NH_3, and at 400 °C in only O_2 and H_2O, are both larger than that at 300 °C in presence of NO and NH_3. This shows that larger S-uptakes can be reached at higher and lower temperatures, and, therefore, the catalyst exposed to SO_2 at 300 °C in presence of NO and NH_3 is not saturated, which validates the interpretation that the deactivation by SO_2 is determined by the total exposure to SO_2.

The data in Fig. 6 show that exposure to SO_2 at 200–600 °C results in different amounts of S-uptake by the Cu-SAPO-34 catalyst, dependent on the presence of NO and NH_3. These differences can be related to the different amounts of Cu(I) and Cu(II) and the formation of SO_3. The DFT calculations presented in Table 1 show, that SO_2 adsorbs more strongly than SO_3 on Z-Cu(I) sites. Since a mixture of NO and NH_3 has reducing properties [22–26], the presence of NO and NH_3 leads to a larger fraction of Z-Cu(I) species. This leads to an enhanced driving force for SO_2 adsorption on Cu in the presence of NO and NH_3. The fraction of Z-Cu(I) species decreases with increasing temperature, as a faster SCR reaction leads to lower partial pressures of NO and NH_3 and faster re-oxidation of the Cu, and therefore the SO_2 uptake decreases with increasing temperature in the presence of NO and NH_3, as shown in Fig. 6.

In the absence of NO and NH_3, more Cu is present as Cu(II) species, and therefore, the adsorption of SO_2 on Cu(I) becomes less important. The DFT calculations show that the Z-Cu(II)OH site forms the most stable $CuSO_x$ species in reaction with SO_3, while neither SO_2 nor SO_3 adsorb on the Z_2-Cu(II) sites. Due to the larger amount of Cu(II), the SO_2 uptake is now determined by the formation of SO_3, which then reacts with the Z-Cu(II)OH sites. The increasing SO_2 uptake with temperature in the range 200–400 °C is then a consequence of the increased rate of SO_2 oxidation [10]. Above 400 °C, decomposition and desorption of the $CuSO_x$ species takes place [11], resulting in the lower SO_2 uptake with increasing temperature.

It is noted that both in the presence and in the absence of NO and NH_3, the adsorption of SO_2 or SO_3 always occurs on Cu sites. Therefore, the total SO_2 uptake is limited by the Cu content, in agreement with the observation that the S/Cu ratio does not exceed 1, despite excessive exposure to SO_2 (total exposure of SO_2/Cu is at least 4.8). It has been

Table 1
The stabilities (ΔE) of most stable reaction products from reactions of three different Cu sites in Cu-SAPO-34 or Cu-SSZ-13 with either SO_2 or SO_3. *O_2 does not adsorb on Z_2-Cu(II) in neither Cu-SAPO-34 nor in Cu-SSZ-13. Adsorption energies and standard deviations have been obtained from DFT using BEEF-vdW.

Cu site	+ SO_2 →	ΔE [eV] Cu-SAPO-34	ΔE [eV] Cu-SSZ-13	+ SO_3 →	ΔE [eV] Cu-SAPO-34	ΔE [eV] Cu-SSZ-13
Z-Cu(I)	Z-Cu(I)-SO_2 (*ads*)	−1.07 (+/-0.44)	−1.12 (+/- 0.48)	Z-Cu(I)-SO_3 (*ads*)	−0.80 (+/-0.55)	−0.89 (+/- 0.55)
Z-Cu(II)OH	Z-Cu(II)HSO_3	−0.84 (+/-0.36)	−0.73 (+/- 0.29)	Z-Cu(II)HSO_4	−1.80 (+/- 0.36)	−1.81 (+/-0.32)
Z_2-Cu(II)*	O_2, SO_2, and SO_3 do not adsorb on this site in neither Cu-SAPO-34 nor Cu-SSZ-13					

argued that deposition of ammonium sulfate in the zeolite pores is the cause of deactivation of Cu-CHA catalysts [14–16]. This explanation would be consistent with a larger S-uptake in presence of NO and NH_3 below 400 °C, since ammonium sulfate decomposes at around 350 °C [16]. However, if ammonium sulfate is formed, it is also expected that the amount of sulfur deposited in the catalyst is not limited by the Cu content. Since the S-uptake is limited by the Cu content, formation of ammonium sulfate does not seem to be the cause of the larger SO_2 uptake and deactivation in the low temperature range in the presence of NO and NH_3.

Finally, the chemical nature of the CHA framework (silicoaluminophosphate or aluminosilicate) seems not to have a significant influence on the deactivation by SO_2. As argued in the previous section, the deactivation of the silicoaluminophosphate Cu-SAPO-34 catalyst by SO_2 is related to the chemistry of Cu, SO_2 and SO_3, and therefore, SO_2-poisoning of the two versions of the Cu-CHA catalysts should be comparable. The response of the Cu-SAPO-34 catalyst to SO_2 exposure and regeneration at 550 °C in Fig. 1, is very similar to that observed on a similar aluminosilicate Cu-CHA catalyst [11]. Furthermore, the results from the DFT calculations in Table 1, show that the Cu-SO_x species formed from SO_2 and SO_3, and the interaction energies of SO_2 and SO_3 with the respective Cu(I) and Cu(II) species is similar in both CHA materials. This indicates that the framework chemistry of the two Cu-CHA catalysts does not affect the SO_2-poisoning, and means that SO_2-poisoning is similar on Cu-exchanged aluminosilicate and silicoaluminophosphate CHA materials.

5. Conclusions

The deactivation behavior of a Cu-SAPO-34 catalyst in the NH_3-SCR reaction has been evaluated at simulated operating conditions by comparing the SCR activity before and after exposing to 1.5 ppmv SO_2 in a typical SCR-feed gas feed at 300 °C. The low-temperature activity is significantly lowered by the SO_2 exposure, and regeneration at 550 °C restores the activity to about 80% of the original level. Regeneration at 700 °C restores all activity, which is consistent with decomposition of Cu-sulfates. The degree of deactivation appears to depend on the total SO_2 exposure, calculated as the product of partial pressure and exposure time.

Below 400 °C, the S-uptake increases with temperature in absence of NO and NH_3, and decreases with increasing temperature in the presence of NO and NH_3. This can be explained by the ability of NO and NH_3 to reduce Cu(II) to Cu(I). DFT calculations show that SO_2 binds preferably to Cu(I), while SO_3 binds stronger to Cu(II). This then leads to the higher uptake of SO_2 below 400 °C in the presence of NO and NH_3, since a larger amount of Cu(I) is present under these conditions. Above 400 °C, the S-uptake decreases with increasing temperature, independent of the presence of NO and NH_3.

The S/Cu ratios are always lower than 1, which indicates that the uptake of sulfur is related to adsorption of SO_2 on Cu and that ammonium sulfate does not precipitate in the catalyst when co-feeding SO_2, H_2O and NH_3. Furthermore, DFT calculations also show that SO_2 and SO_3 interactions with Cu is similar for Cu-SAPO-34 and Cu-SSZ-13, indicating that the deactivation by SO_x is mainly associated to the chemistry of the Cu sites. Consequently, the SO_2-poisoning mechanisms for Cu-SAPO-34 and Cu-SSZ-13 are comparable.

Acknowledgement

PSH gratefully acknowledges support from Innovation Fund Denmark [grant number 5139-0023B].

References

[1] J.H. Kwak, D. Tran, S.D. Burton, J. Szanyi, J.H. Lee, C.H.F. Peden, Effects of hydrothermal aging on NH_3-SCR reaction over Cu/zeolites, J. Catal. 287 (2012) 203–209.
[2] I. Nova, E. Tronconi, Urea-SCR Technology for deNOx After Treatment of Diesel Exhausts, 1st ed., Springer-Verlag, New York, 2014.
[3] H.-Y. Chen, Z. Wei, M. Kollar, F. Gao, Y. Wang, J. Szanyi, C.H.F. Peden, A comparative study of N2O formation during the selective catalytic reduction of NOx with NH_3 on zeolite supported Cu catalysts, J. Catal. 329 (2015) 490–498, http://dx.doi.org/10.1016/j.jcat.2015.06.016.
[4] Y. Cheng, C. Lambert, D.H. Kim, J.H. Kwak, S.J. Cho, C.H.F. Peden, The different impacts of SO_2 and SO_3 on Cu/zeolite SCR catalysts, Catal. Today 151 (2010) 266–270.
[5] A. Kumar, M.A. Smith, K. Kamasamudram, N.W. Currier, H. An, A. Yezerets, Impact of different forms of feed sulfur on small-pore Cu-zeolite SCR catalyst, Catal. Today 231 (2014) 75–82.
[6] Y. Cheng, C. Montreuil, G. Cavataio, C. Lambert, Sulfur tolerance and DeSOx studies on diesel SCR catalysts, SAE Int. J. Fuels Lubr. 1 (2008) 471–476.
[7] K. Wijayanti, S. Andonova, A. Kumar, J. Li, K. Kamasamudram, N.W. Currier, A. Yezerets, L. Olsson, Impact of sulfur oxide on NH_3-SCR over Cu-SAPO-34, Appl. Catal. B 166–167 (2015) 568–579, http://dx.doi.org/10.1016/j.apcatb.2014.11.043.
[8] A. Kumar, M.A. Smith, K. Kamasamudram, N.W. Currier, A. Yezerets, Chemical deSOx: an effective way to recover Cu-zeolite SCR catalysts from sulfur poisoning, Catal. Today 267 (2016) 10–16, http://dx.doi.org/10.1016/j.cattod.2016.01.033.
[9] J. Luo, D. Wang, A. Kumar, J. Li, K. Kamasamudram, N. Currier, A. Yezerets, Identification of two types of Cu sites in Cu/SSZ-13 and their unique responses to hydrothermal aging and sulfur poisoning, Catal. Today 267 (2016) 3–9, http://dx.doi.org/10.1016/j.cattod.2015.12.002.
[10] L. Zhang, D. Wang, Y. Liu, K. Kamasamudram, J. Li, W. Epling, SO_2 poisoning impact on the NH_3-SCR reaction over a commercial Cu-SAPO-34 SCR catalyst, Appl. Catal. B 156–157 (2014) 371–377, http://dx.doi.org/10.1016/j.apcatb.2014.03.030.
[11] P.S. Hammershøi, Y. Jangjou, W.S. Epling, A.D. Jensen, T.V.W. Janssens, Reversible and irreversible deactivation of Cu-CHA NH_3-SCR catalysts by SO_2 and SO_3, Appl. Catal. B 226 (2018) 38–45, http://dx.doi.org/10.1016/j.apcatb.2017.12.018.
[12] K.C. Hass, W.F. Schneider, Density functional studies of adsorbates in Cu-exchanged zeolites: model comparisons and SOx binding, Phys. Chem. Chem. Phys. 1 (1999) 639–648.
[13] W. Su, Z. Li, Y. Zhang, C. Meng, J. Li, Identification of sulfate species and their influence on SCR performance of Cu/CHA catalyst, Catal. Sci. Technol. 7 (2017) 1523–1528, http://dx.doi.org/10.1039/C7CY00302A.
[14] K. Wijayanti, K. Leistner, S. Chand, A. Kumar, K. Kamasamudram, N.W. Currier, A. Yezerets, L. Olsson, Deactivation of Cu-SSZ-13 by SO_2 exposure under SCR conditions, Catal. Sci. Technol. 6 (2016) 2565–2579, http://dx.doi.org/10.1039/C5CY01288K.
[15] K. Wijayanti, K. Xie, A. Kumar, K. Kamasamudram, L. Olsson, Effect of gas compositions on SO_2 poisoning over Cu/SSZ-13 used for NH_3-SCR, Appl. Catal. B 219 (2017) 142–154, http://dx.doi.org/10.1016/j.apcatb.2017.07.017.
[16] Y. Jangjou, D. Wang, A. Kumar, J. Li, W.S. Epling, SO_2 poisoning of the NH_3-SCR reaction over Cu-SAPO-34: effect of ammonium sulfate versus other S-containing species, ACS Catal. 6 (2016) 6612–6622, http://dx.doi.org/10.1021/acscatal.6b01656.
[17] J.J. Mortensen, L.B. Hansen, K.W. Jacobsen, Real-space grid implementation of the projector augmented wave method, Phys. Rev. B 71 (2005) 35109, http://dx.doi.org/10.1103/PhysRevB.71.035109.
[18] J. Enkovaara, C. Rostgaard, J.J. Mortensen, J. Chen, M. Dulak, L. Ferrighi, J. Gavnholt, C. Glinsvad, V. Haikola, H.A. Hansen, H.H. Kristoffersen, M. Kuisma, A.H. Larsen, L. Lehtovaara, M. Ljungberg, O. Lopez-Acevedo, P.G. Moses, J. Ojanen, T. Olsen, V. Petzold, N.A. Romero, J. Stausholm-Møller, M. Strange, G.A. Tritsaris, M. Vanin, M. Walter, B. Hammer, H. Häkkinen, G.K.H. Madsen, R.M. Nieminen, J.K. Nørskov, M. Puska, T.T. Rantala, J. Schiøtz, K.S. Thygesen, K.W. Jacobsen, Electronic structure calculations with GPAW: a real-space implementation of the projector augmented-wave method, J. Phys. Condens. Matter 22 (2010) 253202, http://dx.doi.org/10.1088/0953-8984/22/25/253202.
[19] J. Wellendorff, K.T. Lundgaard, A. Møgelhøj, V. Petzold, D.D. Landis, J.K. Nørskov, T. Bligaard, K.W. Jacobsen, Density functionals for surface science: exchange-correlation model development with Bayesian error estimation, Phys. Rev. B 85 (2012) 235149, http://dx.doi.org/10.1103/PhysRevB.85.235149.
[20] R.Y. Brogaard, P.G. Moses, J.K. Nørskov, Modeling van der Waals interactions in zeolites with periodic DFT: physisorption of n-alkanes in ZSM-22, Catal. Lett. 142 (2012) 1057–1060, http://dx.doi.org/10.1007/s10562-012-0870-9.
[21] R.Y. Brogaard, B.M. Weckhuysen, J.K. Nørskov, Guest–host interactions of arenes in H-ZSM-5 and their impact on methanol-to-hydrocarbons deactivation processes, J. Catal. 300 (2013) 235–241, http://dx.doi.org/10.1016/j.jcat.2013.01.009.
[22] T.V.W. Janssens, H. Falsig, L.F. Lundegaard, P.N.R. Vennestrøm, S.B. Rasmussen, P.G. Moses, F. Giordanino, E. Borfecchia, K.A. Lomachenko, C. Lamberti, S. Bordiga, A. Godiksen, S. Mossin, P. Beato, A consistent reaction scheme for the selective catalytic reduction of nitrogen oxides with ammonia, ACS Catal. 5 (2015) 2832–2845, http://dx.doi.org/10.1021/cs501673g.
[23] C. Paolucci, A.A. Verma, S.A. Bates, V.F. Kispersky, J.T. Miller, R. Gounder, W.N. Delgass, F.H. Ribeiro, W.F. Schneider, Isolation of the copper redox steps in the standard selective catalytic reduction on Cu-SSZ-13, Angew. Chem. Int. Ed. 53 (2014) 1–7.
[24] F. Giordanino, P.N.R. Vennestrøm, L.F. Lundegaard, F.N. Stappen, S. Mossin, P. Beato, S. Bordiga, C. Lamberti, Characterization of Cu-exchanged SSZ-13: a comparative FTIR, UV–vis, and EPR study with Cu-ZSM-5 and Cu-β with similar Si/Al and Cu/Al ratios, Dalton Trans. 42 (2013) 12741–12761.
[25] J.-S. McEwen, T. Anggara, W.F. Schneider, V.F. Kispersky, J.T. Miller, W.N. Delgass,

F.H. Ribeiro, Integrated operando X-ray absorption and DFT characterization of Cu–SSZ-13 exchange sites during the selective catalytic reduction of NOx with NH_3, Catal. Today 184 (2012) 129–144.

[26] S. Kieger, G. Delahay, B. Coq, B. Neveu, Selective catalytic reduction of nitric oxide by ammonia over Cu-FAU catalysts in oxygen-rich atmosphere, J. Catal. 183 (1999) 267–280.

[27] F. Gao, D. Mei, Y. Wang, J. Szanyi, C.H.F. Peden, Selective catalytic reduction over Cu/SSZ-13: linking homo- and heterogeneous catalysis, J. Am. Chem. Soc. 139 (2017) 4935–4942, http://dx.doi.org/10.1021/jacs.7b01128.

[28] C. Paolucci, I. Khurana, A.A. Parekh, S. Li, A.J. Shih, H. Li, J.R. Di Iorio, J.D. Albarracin-Caballero, A. Yezerets, J.T. Miller, W.N. Delgass, F.H. Ribeiro, W.F. Schneider, R. Gounder, Dynamic multinuclear sites formed by mobilized copper ions in NOx selective catalytic reduction, Science 357 (2017) 898–903, http://dx.doi.org/10.1126/science.aan5630.

Chapter 3

Reversible and irreversible deactivation of Cu-CHA NH_3-SCR catalysts by SO_2 and SO_3

This chapter has been published in:
Applied Catalysis B: Environmental 226 (2018) 38-45
https://doi.org/10.1016/j.apcatb.2017.12.018

Applied Catalysis B: Environmental 226 (2018) 38–45

Contents lists available at ScienceDirect

Applied Catalysis B: Environmental

journal homepage: www.elsevier.com/locate/apcatb

Reversible and irreversible deactivation of Cu-CHA NH_3-SCRcatalysts by SO_2 and SO_3

Peter S. Hammershøi[a,b,1], Yasser Jangjou[c,d], William S. Epling[c,d], Anker D. Jensen[b], Ton V.W. Janssens[a,*,1]

[a] Haldor Topsoe A/S, Haldor Topsøes Allé 1, 2800 Kgs. Lyngby, Denmark
[b] Department of Chemical and Biochemical Engineering, Technical University of Denmark, Søltofts Plads B229, 2800 Kgs. Lyngby, Denmark
[c] Department of Chemical and Biomolecular Engineering, University of Houston,4800 Calhoun Rd., Houston, TX 77204-4004, United States
[d] Department of Chemical Engineering, University of Virginia, 102 Engineers' Way, Charlottesville, VA 22904-4741

ARTICLE INFO

Keywords:
NH_3-SCR
Cu-CHA
Deactivation
Sulfur oxides
Regeneration

ABSTRACT

Sulfur oxides are a common source for the deactivation of Cu-exchanged CHA zeolite based catalysts used for NO_x reduction in diesel exhausts by selective catalytic reduction with NH_3 (NH_3-SCR). Since water and possible formation of SO_3 affect the deactivation of Cu-CHA catalysts, the deactivation in the presence of SO_2 or a mixture of SO_2 and SO_3 was studied by measuring the SCR activity in wet and dry gas at 200 and 550 °C. The estimated S-content in the catalysts before and after 4 h regeneration at 550 °C in NO, NH_3, O_2 and H_2O was related to the deactivation. The deactivation can be divided into two parts: a reversible deactivation that is restored by the regeneration treatment, and an irreversible part. The irreversible deactivation does not affect the activation energy for NH_3-SCR and display a 1:1 correlation with the S-content, consistent with deactivation by Cu-sulfate formation. The reversible deactivation results in a lower activation energy and a deactivation that is larger than expected from the S-content. The presence of SO_3 at 200 °C leads to higher reversible and irreversible deactivation, but has no significant impact at 550 °C. Furthermore, the irreversible deactivation is always higher when exposed at 200 °C than at 550 °C, and in wet conditions, compared to a dry feed. The deactivation is predominantly reversible, making regeneration at 550 °C a realistic approach to handle S-poisoning in exhaust systems.

1. Introduction

Combustion of diesel fuel in automotive engines produces NO_x (NO and NO_2). Due to the environmentally negative impact of NO_x, emissions of these compounds are subject to strict regulations, which requires NO_x reduction from the exhaust gas. The current technology for the removal of NO_x is selective catalytic reduction (SCR) of NO_x with NH_3. Apart from an NH_3-SCR catalyst, a complete diesel exhaust after-treatment system also contains a diesel oxidation catalyst to oxidize CO and unburnt fuel, a particle filter to remove soot, and an ammonia slip catalyst to remove the ammonia not used in the upstream NH_3-SCR reaction.

The best known NH_3-SCR catalysts are based on V_2O_5, or Cu- or Fe-zeolites. Compared to V_2O_5-based catalyst systems, Cu-zeolites generally work well in a broader temperature region (~150–500 °C) [1]. In particular, the better low temperature activity for Cu-zeolites is of interest for cold-start conditions. Combined with the good hydrothermal stability of small-pore zeolites, these traits have led to commercialization of Cu-zeolites in diesel engine exhaust systems, and Cu-CHA is the current state-of-the-art Cu-zeolite catalyst for diesel emission control.

Another important requirement for NH_3-SCR catalysts is low susceptibility to SO_2-poisoning. Diesel fuels contain a small amount of sulfur, and even ultra-low sulfur fuel will result in SO_2 in the exhaust gas. The performance of NH_3-SCR catalysts, however, can be very sensitive to the presence of SO_2, even at low concentrations, as in ultra-low sulfur diesel [2]. It is therefore important to know the effect of SO_2 on the performance of an NH_3-SCR catalysts.

Unfortunately, Cu-zeolite catalysts deactivate more in the presence of SO_2 in the exhaust gas, while Fe-zeolites are less affected by SO_2 and V_2O_5 is not affected [1,3,4]. Consequently, to be able to exploit the potentially better performance of Cu-zeolite catalysts in an exhaust after-treatment system, it is important to understand how the presence of SO_2 influences the performance of these catalysts. Furthermore, it is also important to know to what degree the deactivation of Cu-zeolites

* Corresponding author.
E-mail address: tonv.w.janssens@eu.umicore.com (T.V.W. Janssens).
[1] Present address: Umicore Denmark ApS, Nøjsomhedsvej 20, DK-2800 Kgs. Lyngby, Denmark.

https://doi.org/10.1016/j.apcatb.2017.12.018
Received 7 September 2017; Received in revised form 5 December 2017; Accepted 8 December 2017
Available online 13 December 2017

induced by SO_2 is reversible versus irreversible.

The current understanding of Cu-zeolite catalyst deactivation by SO_2, and Cu-CHA in particular, is that it originates from SO_2 interaction with the Cu-sites. This can simply be adsorption of SO_2 or could involve a chemical reaction between the SO_2 and Cu-sites [2,5–13]. X-ray photoemission and X-ray absorption spectroscopy indicate that the Cu in the ion-exchange positions reacts to form a $CuSO_4$-like species [2]. The formation of sulfates suggests that some oxidation of SO_2 to SO_3 takes place. In an after-treatment system, oxidation of SO_2 to SO_3 can occur on the diesel oxidation catalyst [2,11], and on the NH_3-SCR catalyst [5]. A higher sulfur uptake and stronger deactivation has been observed in the presence of SO_3 in the feed gas [2,11]. Therefore, a better understanding of the effect of SO_3 on the performance of NH_3-SCR catalysts is needed.

Another mechanism for deactivation of NH_3-SCR catalysts is the formation of ammonium sulfate on the catalyst, which restricts access to the active sites. The presence of SO_2 or SO_3 in a standard, NH_3-containing SCR-gas causes formation of ammonium sulfate, which is a solid below 300 °C, and therefore, deactivation by ammonium sulfate only occurs in the low-temperature range. Ammonium sulfate can be removed by heating the catalyst to above 350 °C, which means that regeneration from this type of deactivation is possible in an exhaust system [5,9,10].

An NH_3-SCR catalyst in a diesel exhaust treatment system is typically operated between 200 and 550 °C, and in the presence of 5–10% water vapor. The effect of temperature on catalyst deactivation by SO_x depends on the presence of SO_3 [2,11]. With SO_2 only, the deactivation is more severe at 200 °C than at 400 °C, while the opposite trend is observed in the presence of SO_3[2,11].

Water also interacts with the Cu ions, changing the environment of and around the active sites in a Cu-CHA catalyst. Water vapor is known to partially hydrolyze the Cu-sites at temperatures below 250 °C [14], affecting the performance for NH_3-SCR. In a similar way, reactions between different Cu-sites with sulfur oxides can be affected by water as well [8,15]. From a mechanistic point of view, the impact of water vapor on the deactivation by SO_2 and SO_3 should be understood, with the additional consideration that SO_3 and H_2O combine and form sulfuric acid below 400 °C [11].

In practice, there are essentially two ways to deal with the presence of SO_x in an exhaust gas. The first one is to design the Cu-CHA SCR catalysts in such a way that the amounts of SO_2 and SO_3 passing through the system during its lifetime can be accommodated in the system. Alternatively, periodic regeneration strategies must be designed that restore at least a part of the catalytic activity. It is therefore important to know how the presence of SO_2 and SO_3 in the exhaust gas stream affects the performance of Cu-CHA catalyst and if regeneration of a Cu-CHA catalyst is possible. In this article, we focus on the effect of the temperature and H_2O and SO_3 on the SO_x-induced deactivation of a monolithic Cu-CHA catalyst for NH_3-SCR. The stability of species formed was studied by comparing the activities of a deactivated catalyst with that after heating to 550 °C, which is a temperature that can be reached in an exhaust system.

2. Experimental

2.1. Preparation of the catalysts

In this study we used both a Cu-CHA powder catalyst and a monolithic Cu-CHA catalyst. For the powdered catalyst, Cu was introduced into the H-CHA zeolite by ion-exchange for 24 h with an aqueous solution of $Cu(CH_3COO)_2$ (5 mmol/kg) at 20 °C, using 20 g H-CHA zeolite powder in 5 kg solution. After ion-exchange the Cu-CHA was filtered and washed with approx. 20 L MilliQ water, which resulted in a colorless filtrate. The Cu-CHA powder was then dried overnight at 95 °C, and calcined at 550 °C for 3 h. The Si/Al ratio was 14.7 and the Cu/Al ratio was 0.5, corresponding to a Cu-loading of 2.8 wt%, as determined by ICP-OES.

The monolithic Cu-CHA catalyst was prepared by washcoating a cordierite monolith with a slurry of H_2O, xanthan gum, colloidal silica and Cu-CHA powder. The Cu-CHA powder was prepared by impregnating 1 kg of H-CHA powder (Si/Al = 16.6) with Cu in 1 kg of an aqueous solution of 0.39 mmol/g $Cu(NO_3)_2{\cdot}3H_2O$ in a rotary evaporator for 4 h at 95 °C. The Cu-loading of the powder was 2.5 wt%, based on the amount of Cu added for the impregnation. After impregnation, the powder was calcined at 550 °C for 3 h. A cordierite monolith (D × L = 25.4 × 10.2 cm, 300 cpsi, 0.13 mm wall thickness) was washcoated with the Cu-CHA slurry to a washcoat-loading of 151 g/L. The Cu-CHA/cordierite monolith was dried at 100 °C, and calcined at 550 °C for 3 h.

2.2. Catalytic test on powder

The NH_3-SCR activity measurements on the Cu-CHA powder were carried out in a fixed-bed quartz reactor with a 2 mm inner diameter, using 5.0 mg catalyst (150–300 µm sieve fraction) on a dry matter basis. The SCR feed gas composition was 500 ppmv NO, 530 ppmv NH_3, 10% O_2, 5% H_2O balanced by N_2, which we hereafter refer to as "SCR-gas". The total flow rate used in the measurements was 0.225 NL/min (10 mmol/min, standard conditions: T = 0 °C, P = 1 atm). The outlet gas was analyzed by a Gasmet CX4000 FTIR analyzer.

The Cu-CHA powder exposure to SO_2 was either done in situ in the reactor at 550 °C for 1 h with 40 ppmv SO_2, 10% O_2, 5% H_2O balanced by N_2 with a total flow rate of 0.2 NL/min (9 mmol/min), or ex situ in a tube furnace at 550 °C for 16 h with 100 ppmv SO_2, 16% O_2 balanced by N_2 with a total flow rate of 0.2 NL/min. Regeneration was always carried out in situ in the reactor at 550 °C with an SCR-gas flow of 0.225 NL/min. 550 °C was chosen, as this is a typical temperature for regeneration of diesel after-treatment systems operating with passive filter regeneration.

2.3. Catalytic test on monoliths

With the purpose of studying the impact of temperature and H_2O and SO_3 gas components on Cu-CHA/cordierite monolith catalyst deactivation by SO_2, steady-state NO_x conversions were measured before and after SO_x exposure, and after regeneration at 550 °C in a laboratory flow reactor system with a horizontal quartz reactor with an inner diameter of 25.4 mm. Upstream and downstream tubing inside surfaces were coated with SilcoNert to minimize adsorption of SO_x (and NH_3). Monolith samples of approx. 20 × 27 mm were cut out from the larger prepared sample (sample masses were between 4.5–5.0 g). The reactor temperature was measured at the inlet, inside, and at the outlet of the monolith samples by thermocouples placed in the radial center of the reactor/sample. The steady-state NO_x conversions were measured at various temperatures (130–250 °C), at a flow of 8.0 NL/min (357 mmol/min). The SCR feed gas composition was 500 ppmv NO, 530 ppmv NH_3, 10% O_2, 5% H_2O balanced by N_2. The outlet gas was analyzed using a MKS MultiGas 2030 FTIR. SO_x exposure was always 3 h in 10% O_2 with 100 ppmv SO_x balanced by N_2 with a total flow rate of 8.0 NL/min. The variations in the SO_x exposure conditions and the assigned sample names, are listed in Table 1. The SO_3 for the SO_x exposures, was produced in an upstream reactor by oxidizing SO_2 over a Pt/Al_2O_3 monolith catalyst. The temperature of the upstream reactor was adjusted to reach a steady-state conversion of SO_2 of 30%, which was added to the main feed prior to the inlet of the quartz reactor containing the Cu-CHA/cordierite catalyst. Regeneration was carried out in the SCR feed gas at 550 °C, heating at 10 °C/min, for 4 h. In order to check if there were S-species remaining on the samples after regeneration, temperature-programmed desorption (TPD) to 900 °C was carried out after the final NO_x conversion measurement that followed the regeneration. The SO_2-TPD was carried out in N_2 at a flow rate of 8.0 NL/min, and with a temperature ramp at 10 °C/min. The

Table 1
Assigned sample names according to variations in SO_x exposure conditions.

SO_x exposure conditions	100 ppm SO_2	70 ppm SO_2 + 30 ppm SO_3
5% H_2O T = 200 °C	SO2-H2O-200	SO3-H2O-200
Dry T = 200 °C	SO2-200	SO3-200
5% H_2O T = 550 °C	SO2-H2O-550	SO3-H2O-550
Dry T = 550 °C	SO2-550	SO3-550

concentrations of H_2O, NO, NO_2, NH_3, SO_2, SO_3 and H_2SO_4 were monitored during regenerations and TPD measurements.

2.4. Evaluation of activity and deactivation

The activities of the catalysts are evaluated by the rate constants, which are derived from the steady-state NO_x conversion measurements. If we assume that the NH_3-SCR reaction is first order in NO, the rate constant is given by:

$$k = -\frac{F}{W}\ln(1 - X) \quad (1)$$

where F is the total molar flow rate, W is the mass of the Cu-CHA powder in both tested catalysts, and X is the conversion of NO. The deactivation is expressed as the relative rate constant of a sulfated or regenerated catalyst with respect to the rate constant for the fresh catalyst:

$$Deactivation = 1 - \frac{k}{k_{fresh}} = 1 - \frac{A\exp\left(-\frac{E_a}{RT}\right)}{A_{fresh}\exp\left(-\frac{E_{a,fresh}}{RT}\right)} \quad (2)$$

Multiplication by 100 then yields the deactivation expressed as a percentage.

3. Results

3.1. Powder experiments

The general behavior of a Cu-CHA catalyst upon exposure to SO_2 and regeneration at 550 °C is illustrated in Fig. 1 for the powder catalyst, which shows the measured NO_x conversions for a fresh catalyst,

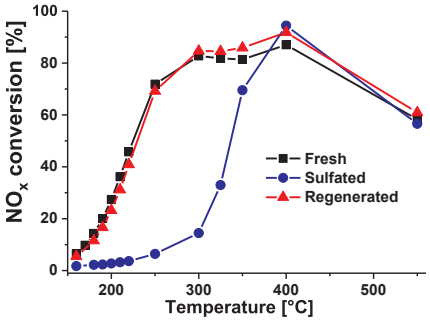

Fig. 1. NO_x conversion as function of temperature of a Cu-CHA catalyst (Si/Al = 14.7, Cu/Al = 0.5, and 2.8 wt% Cu) in fresh, sulfated and regenerated state. SCR conditions: 500 ppmv NO, 530 ppmv NH_3, 10% O_2, 5% H_2O, N_2 balance to 0.225 NL/min on 5.0 mg catalyst in reactor with an inner diameter of 2 mm. SO_x exposure conditions: 100 ppmv SO_2, 16% O_2, N_2 balance to 0.2 NL/min for 16 h at 550 °C. Regeneration conditions: 4.6 h at 550 °C in SCR-gas.

after exposure to 100 ppm SO_2 at 550 °C (sulfated), and after regeneration at 550 °C in SCR-gas (regenerated).

The most significant effect of exposure to SO_2 is seen in the lower temperature range, up to 300 °C, where NO_x conversion was significantly inhibited compared to the fresh sample. Above 300 °C, the NO_x conversion increases rapidly with temperature to slightly above the conversion measured for the fresh catalyst. After regeneration by heating to 550 °C, the conversion above 300 °C was slightly higher, but close to that of the fresh catalyst. Below 300 °C, the conversion remained slightly below that of the fresh catalyst. This shows that exposure to SO_2 results mainly in deactivation of the low-temperature (T < 350 °C) activity of the catalyst, which is consistent with previously reported observations [5,9,11], and regeneration at 550 °C does not fully restore the activity below 300 °C entirely.

To investigate if the incomplete regeneration at 550 °C is due to a too short regeneration time, the regeneration process was monitored by heating the samples at 550 °C for a total of 12 h in intervals, where after each interval the activity at 200 °C was re-evaluated. Fig. 2A shows the measured activity at 200 °C obtained in this way, which indicates that a stable activity level is reached at about 75–80% of the original activity after approximately 4 h of regeneration. This means that a complete regeneration by heating at 550 °C seems not possible.

Fig. 1 shows that the NO_x conversion over a catalyst after exposure to SO_2 increases slightly with temperature up to 300 °C, followed by a steep increase. To determine whether the slight increase below 300 °C is due to a normal temperature dependency of a possible residual activity, or to a slow regeneration in this temperature range, we checked the influence of the temperature on activity of a Cu-CHA catalyst at 200 °C. To do this measurement, a single catalyst sample deactivated by SO_2 was sequentially exposed to heating for 2 h in 5% H_2O/10% O_2/N_2 at a chosen temperature between 200 and 450 °C in increasing order, and then cooled down to 200 °C where the NO_x conversion was then re-measured. Fig. 2B shows the rate constant at 200 °C, determined according to Eq. (1) as a function of the heating temperature. The rate constant at 200 °C does not increase by heating to a temperature of 300 °C or lower, which clearly indicates that the regeneration of a catalyst exposed to SO_2 does not start below 300 °C, and the slight increase in conversion in Fig. 1 is therefore due to the temperature dependence of a residual activity. This also means that measured SCR activities after exposure to SO_2 are not affected by regeneration if the measurements are done at 300 °C or lower.

The observation that the activity after SO_2 exposure cannot be completely restored by heating to 550 °C indicates that there are different forms of deactivation. Based on these data, we define these different forms of deactivation as follows: the part of the deactivation that can be restored by 4 h heating at 550 °C will be referred to as the *reversible deactivation*, and the remaining part as the *irreversible deactivation*. The *total deactivation* is the sum of these two contributions. An activity measured after exposure to SO_x before regeneration, represents the total deactivation, the irreversible deactivation is found from the activity after regeneration. The reversible deactivation can then be determined as the difference in activity of a SO_x-treated catalyst before and after regeneration. The following expression is used to determine the relative reversible deactivation with respect to the activity of the fresh catalyst:

$$1 - \frac{k_{sulfated}}{k_{fresh}} = Reversible\ deactivation + \left(1 - \frac{k_{irreversible}}{k_{fresh}}\right) \quad (3)$$

3.2. Monolith experiments

The effects of SO_3, water and SO_x exposure temperature on the catalyst deactivation and regeneration was studied by measurement of NO conversions over Cu-CHA/cordierite monolith samples after exposure to SO_x at the conditions listed in Table 1, and after subsequent

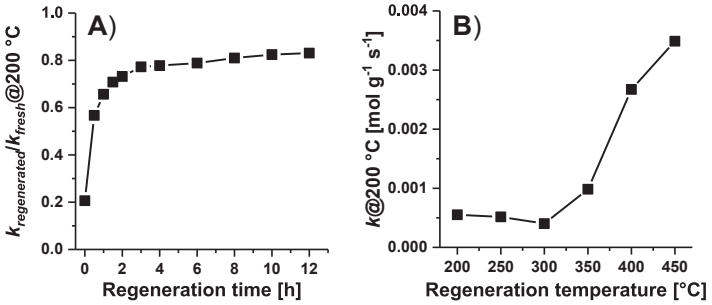

Fig. 2. Cu-CHA catalyst (Si/Al = 14.7, Cu/Al = 0.5, and 2.8 wt% Cu) A) Relative NH_3-SCR activity plotted as function of regeneration time. NO_x conversions measured on 5.0 mg catalyst at 200 °C on fresh catalyst, after SO_2 exposure, and after every regeneration step at 550 °C in SCR-gas. SO_x exposure conditions: 40 ppmv SO_2, 10% O_2, 5% H_2O, N_2 balance to 0.225 NL/min for 1 h at 550 °C. B) NH_3-SCR activity at 200 °C plotted as function of regeneration temperature (2 h at each regeneration temperature). NO_x conversions measured on 5.0 mg catalyst at 200 °C on fresh catalyst, after SO_2 exposure, and after every regeneration step at increasing temperature in SCR-gas. SO_2 exposure conditions: 100 ppmv SO_2, 16% O_2, N_2 balance to 0.2 NL/min for 16 h at 550 °C.

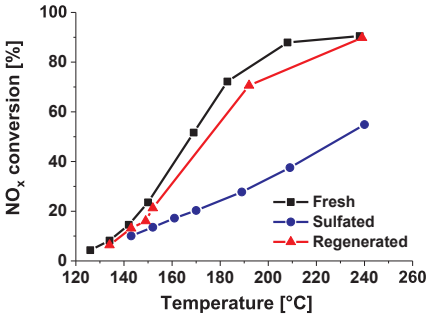

Fig. 3. NO_x conversion as function of temperature of a Cu-CHA/cordierite catalyst (Cu-CHA: Si/Al = 16.6, 2.5 wt% Cu) in fresh, sulfated and regenerated state. SCR conditions: 500 ppmv NO, 530 ppmv NH_3, 10% O_2, 5% H_2O, N_2 balance to 8.0 NL/min on 20 × 27 mm cylindrical monolith catalyst in reactor with an inner diameter of 25.4 mm. SO_x exposure conditions: 100 ppmv SO_2, 10% O_2, 5% H_2O, N_2 balance to 8.0 NL/min for 3 h at 200 °C. Regeneration conditions: 4 h at 550 °C in SCR-gas.

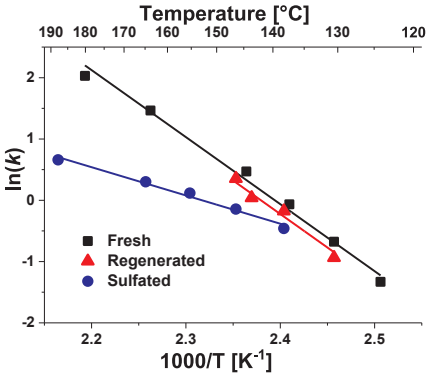

Fig. 4. Arrhenius plot of a Cu-CHA/cordierite catalyst (Cu-CHA: Si/Al = 16.6, 2.5 wt% Cu) in fresh, sulfated and regenerated state. SO_x exposure conditions: 100 ppmv SO_2, 10% O_2, 5% H_2O, N_2 balance to 8.0 NL/min for 3 h at 200 °C. Regeneration conditions: 4 h at 550 °C in SCR-gas.

heating at 550 °C. In all these measurements, the deactivation and regeneration followed the same general trend as observed for the Cu-CHA powder. Fig. 3 shows the measured NO_x conversion in the range 150–250 °C after deactivation in wet SO_2 without SO_3 as an example. Exposure to SO_2 leads to a lower NO_x conversion, which is mostly restored by heating at 550 °C. It is noted that all activity measurements shown in Fig. 3 are obtained below 300 °C, and are therefore not influenced by regeneration during the measurements.

Due to variations in temperature in the different measurements, a common base for comparison of the measured NO_x conversions is needed. To this end, Arrhenius plots were constructed; Fig. 4 shows the Arrhenius plot based on the data in Fig. 3, and represents the general observation for all samples (see supporting information). For all conditions, the slopes of the fresh and regenerated states of the catalyst are nearly the same, while the slope of the sulfated state of the catalyst is always smaller. Our interpretation is that the activation energies for the fresh and regenerated catalysts are the same, and the activation energy was determined from the combined data points of the fresh and regenerated states. Consequently, the differences in activity for fresh and regenerated catalysts are translated to differences in the pre-exponential factor. The relative irreversible deactivation then becomes independent of the temperature for the conditions used here. The assignment of irreversible deactivation to changes in the pre-exponential factor implies a mechanism in which deactivation is caused by loss of active sites, without major changes in the chemistry of the reaction.

The situation is different for the sulfated catalysts, which consistently have lower activation energy than the fresh and regenerated

Table 2
Activation energies of fresh ($E_{a,fresh}$) and sulfated ($E_{a,sulfated}$) states of the tested Cu-CHA/cordierite catalysts, and the ratios of $E_{a,sulfated}/E_{a,fresh}$.

Sample	$E_{a,fresh}$ [kJ mol^{-1}]	$E_{a,sulfated}$ [kJ mol^{-1}]	$E_{a,sulfated}/E_{a,fresh}$(min-max)
SO2-H2O-200	91 ± 8	38 ± 5	0.33–0.53
SO2-200	99 ± 3	53 ± 2	0.50–0.58
SO2-H2O-550	90 ± 7	53 ± 1	0.54–0.65
SO2-550	59 ± 3	30 ± 5	0.41–0.63
SO3-H2O-200	80 ± 26	15 ± 2	0.12–0.32
SO3-200	115 ± 16	39 ± 4	0.27–0.45
SO3-H2O-550	97 ± 4	39 ± 1	0.38–0.43
SO3-550	76 ± 5	31 ± 1	0.36–0.45

catalysts. Table 2 lists the activation energies for the fresh and sulfated samples, and the ratio of the two values. The lower activation energies of the sulfated catalysts also mean that the measured reversible deactivation depends on the temperature of the SCR activity measurement. A change in activation energy cannot be due to a loss of active sites only. Phenomena that could change the activation energy are a change in the chemistry of the NH_3-SCR reaction and diffusion limitations of the NH_3-SCR reaction rate in the zeolite crystals after exposure to SO_x. In the limit of strong pore diffusion limitations, the observed activation energy will be half the value of the intrinsic value. In principle, this is an option for the samples treated with SO_2 alone. For the samples

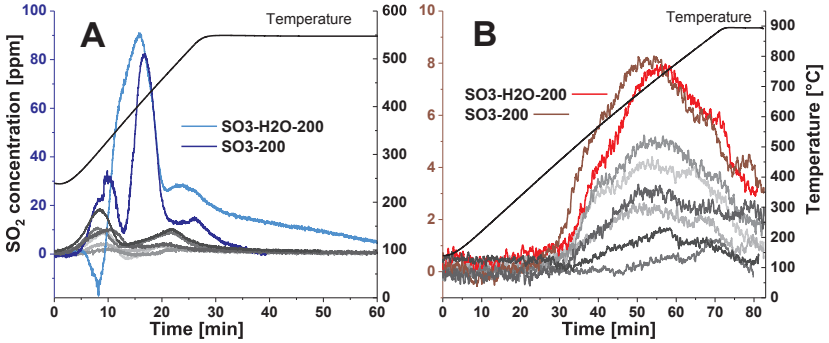

Fig. 5. SO_2 desorption spectra for sulfated Cu-CHA/cordierite catalysts, A) during heating to 550 °C at 10 °C/min in SCR-gas with a total flowrate of 8.0 NL/min, after sulfation, B) during heating to 900 °C at 10 °C/min in 8.0 NL/min N_2, after sulfation and regeneration for 4 h at 550 °C. Curve-smoothing has been applied on the curves in B, using an adjecent-averaging method. In both A and B, legends are only provided for the catalysts exposed to SO_3 at 200 °C. Plots containing legends for all catalysts can be found in supporting information.

treated with SO_3, the activation energy ratios are lower than 0.5, which cannot be explained by internal diffusion limitations alone, suggesting that chemical effects are more pronounced in this case.

3.3. Desorption of SO_2

To determine the amount of sulfur deposited on the catalysts, SO_2 concentrations were measured during the regeneration up to and at 550 °C in SCR-gas, and during heating to 900 °C in N_2 after all activity measurements. The measured SO_2 desorption during the regeneration to 550 °C, shown in Fig. 5A, is related to the reversible deactivation. No SO_3 or H_2SO_4 desorption was observed during the regeneration. Clearly, the two samples exposed to SO_3 at 200 °C stand out with a substantially higher SO_2 desorption around 400 °C. Since the two catalysts exposed to SO_2 at 200 °C did not show a similar high SO_2 desorption around 400 °C, the higher desorption of SO_2 from the two catalysts exposed to SO_3 at 200 °C must be due to decomposition of SO_3 or sulfates [2,11,12]. The desorption temperature of 400 °C is about 200–250 °C lower than the decomposition temperature of bulk Cu sulfate [12]. This indicates that only little Cu sulfate is formed from SO_3 at 200 °C, or that the Cu-sulfate species formed this way in the Cu-CHA catalysts are less stable than bulk Cu-sulfate.

All other samples, exposed to SO_2 at 200 °C or SO_2 + SO_3 at 550 °C, show similar SO_2 desorption peaks at approx. 300 °C and 475 °C. This means that exposure to SO_3 at 550 °C essentially results in similar sulfur species as exposure to SO_2 at 200 or 550 °C, and the influence of water is limited. The observed desorption temperatures are consistent with decomposition of ammonium sulfate [5] and sulfuric acid [12,15]. Ammonium sulfates can possibly have been formed by the exposure of the sulfated samples to NH_3 during the SCR activity measurement directly after the SO_x exposure [10], which would imply a reaction of the adsorbed sulfur species and ammonia.

Fig. 5 B shows the desorption of SO_2 during heating in N_2 to 900 °C after SO_x exposure and regeneration, which represents the sulfur species associated with irreversible deactivation. The catalysts exposed to SO_3 at 200 °C show again the largest amount of SO_2. The desorption peak is centered around 675 °C for all samples, indicating that the same species is formed in all catalysts, but in different amounts, dependent on the conditions for SO_2 exposure. The temperature of 675 °C is consistent with the irreversible deactivation being related to formation of Cu-sulfate [12].

From integration of the curves in Fig. 5, the amounts of sulfur in the sulfated and regenerated catalysts can be estimated, and we highlight the differences in sulfur content between the samples exposed to SO_3 at 200 °C and the other samples. The quality of the measured SO_2 concentrations during regeneration is poor, but the differences between the samples exposed to SO_3 at 200 °C and the other ones are quite clear. We also note that no SO_3 was detected during the temperature programmed desorption, and no sulfur was found in an ICP-OES analysis of the catalysts after heating to 900 °C. This means that the amounts of sulfur detected in the desorption measurements accounts for all sulfur present in the catalysts.

Table 3 lists the SO_2/Cu ratios related to the reversible and irreversible deactivation as derived from integration of the SO_2 desorption curves and the Cu content in the zeolite. The SO_2/Cu ratios of all samples are below 1, which indicates that not all Cu has reacted with SO_x, which would be required for complete formation of Cu-sulfate. The SO_2/Cu ratio after exposure to SO_3 at 200 °C in dry gas is 0.58, and 0.90 in the presence of water, and 70–80% of this amount is released during regeneration at 550 °C. In all other cases, the SO_2/Cu ratio is 0.1-0.2.

3.4. Influence of SO_2/SO_3, water and temperature on deactivation

Having established the general trends in performance and sulfur content after sulfation, and regeneration of the Cu-CHA catalyst, we now turn our attention to the effects of temperature of SO_x exposure, and the presence of water or SO_3. Fig. 6A and B show the reversible and irreversible deactivation for the samples exposed to SO_2 only and SO_2 + SO_3. The reversible deactivation was derived from interpolation of the activity data to 180 °C, using the Arrhenius plots given in Fig. 2 and supporting information. The deactivation is given as a percentage according to Eq. (2).

The effect of SO_3 on deactivation is most noticeable with SO_x exposure at 200 °C, leading to significantly stronger deactivation, compared to exposure to SO_2 alone both in dry and wet feed gases. At 550 °C, the there is no apparent influence of SO_3 in the feed gas. This

Table 3
The reversible, irreversible and total SO_2/Cu ratios of all Cu-CHA/cordierite catalyst samples.

Sample	Reversible SO_2/Cu	Irreversible SO_2/Cu	Total SO_2/Cu
SO2-H2O-200	0.07	0.09	0.16
SO2-200	0.04	0.05	0.09
SO2-H2O-550	0.04	0.12	0.16
SO2-550	0.10	0.02	0.12
SO3-H2O-200	0.74	0.16	0.90
SO3-200	0.40	0.18	0.58
SO3-H2O-550	0.09	0.08	0.17
SO3-550	0.13	0.03	0.16

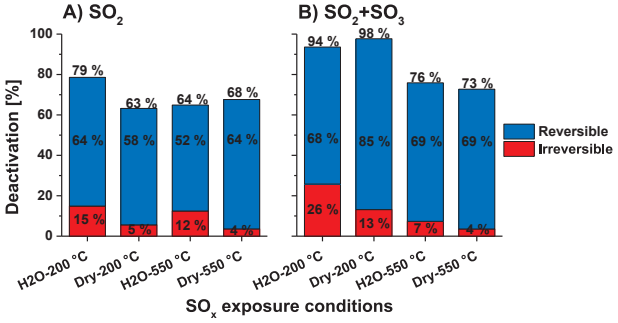

Fig. 6. The reversible deactivation (blue bars), irreversible deactivation (red bars) and total deactivation (sum of red and blue bars) plotted for each SO_x exposure condition of the Cu-CHA/cordierite catalysts. A) samples exposed to 100 ppmv SO_2, B) samples exposed to 70 ppmv SO_2 and 30 ppmv SO_3. (For interpretation of the references to colour in this figure legend, the reader is referred to the web version of this article.)

shows that the specific deactivation by SO_3 is most important in the lower temperature range, and that the effect of SO_3 on deactivation is related to the pronounced decomposition of SO_3 or sulfate at 400 °C, as shown in Fig. 5A.

The presence of H_2O during SO_x exposure always leads to higher irreversible deactivation than the corresponding dry SO_x exposure condition, but appears to have no consistent influence on reversible deactivation. With respect to the impact of temperature, irreversible deactivation is always greater in the samples exposed at 200 °C than the corresponding sample exposed at 550 °C, whereas no consistent impact of temperature is observed on reversible deactivation. The general picture that emerges is that the presence of SO_3 and water at 200 °C has a stronger effect on the deactivation than at 550 °C, in particular on irreversible deactivation.

4. Discussion

The similar activation energies in the SCR reaction for the fresh and regenerated states of the catalysts indicates that irreversible deactivation is the result of having fewer active sites available, and the desorption temperature for SO_2 from the regenerated catalysts points to the formation of Cu-sulfate. If Cu-sulfate formation is the cause of deactivation, a 1:1 correlation should exist between the irreversible deactivation and the sulfur content. Fig. 7 shows the measured irreversible deactivation as a function of the SO_2/Cu ratio, derived from the corresponding SO_2 desorption measurements in Fig. 5B, together with the line for the 1:1 correlation. The measured irreversible deactivation actually follows the 1:1 correlation with the sulfur content fairly well, corroborating the idea that Cu-sulfate formation is responsible for the irreversible deactivation [2,5–13].

A way to envision the irreversible deactivation by formation of a Cu-sulfate species is a reaction of SO_3 with a Cu-ion balanced by a single Al and a hydroxide ligand (Z-Cu-OH), as in reaction Scheme (4).

$$Z{-}\ Cu\ {-}\ OH + SO_3 \rightarrow Z{-}\ Cu\ {-}\ HSO_4 \quad (4)$$

In this case, the hydroxide ligand provides the oxygen required for formation of sulfate. A Cu^{2+} ion balanced by two Al-sites (Z_2-Cu) does not have the hydroxide ligand, but this does not necessarily mean that these Cu-species are incapable of sulfate formation. In the presence of water, a Z_2-Cu can react to a Z-Cu-OH and a Brønsted acid site [14], and the Z-Cu-OH can then react further with SO_3 according to reaction Scheme (4). The overall reaction then becomes:

$$Z_2 - Cu + SO_3 + H_2\ O \rightarrow Z{-}\ Cu\ {-}\ HSO_4 + Z{-}\ H \quad (5)$$

A similar scenario is a reaction with sulfuric acid (H_2SO_4) and a Z_2-Cu site, where the sulfuric acid is formed by reaction of SO_3 and water. Either way, the presence of water would facilitate formation of Cu-sulfate as this leads to a higher amount of Z-Cu-OH-sites compared to dry conditions. The suggested reaction schemes then offer an explanation for the increase in irreversible deactivation in the presence of water. This means that a model that describes the irreversible deactivation by formation of Cu-sulfate is also consistent with the observed effects of the presence of water.

A comparison of measured deactivation and the sulfur content for the sulfated catalysts reveals a different behavior for reversible deactivation. Fig. 8 shows the total deactivation of the sulfated catalysts as a function of their total SO_2/Cu ratios. Clearly, there is no consistent 1:1

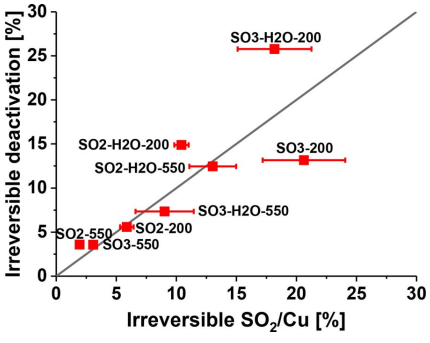

Fig. 7. The irreversible deactivation for the Cu-CHA/cordierite catalysts, determined after SO_x exposure and regeneration for 4 h at 550 °C, plotted as function of the SO_2/Cu ratio of the irreversible S-species.

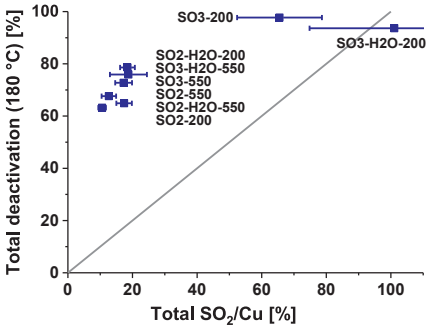

Fig. 8. The total deactivation for the Cu-CHA/cordierite catalysts, determined after SO_x exposure, plotted as function of the SO_2/Cu ratio of the total S-species.

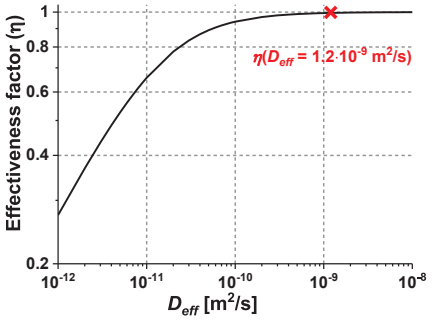

Fig. 9. Double logarithmic plot of the internal effectiveness factor in the zeolite crystals, η, at 180 °C, as a function of the effective diffusion coefficient, D_{eff}. η based on experimental values for D_{eff} of NH_3 in a Cu-CHA catalyst in the range 0–100 °C, is marked, which indicates that the reaction in the fresh catalyst is not limited by diffusion of reactants.

dependence of the total deactivation on SO_2/Cu ratio, with only small SO_2/Cu ratios, between 10 and 20%, leading to degrees of deactivation as high as 60–80%. This indicates that the loss of activity in this case is not caused by a direct interaction of a single sulfur atom with a single Cu ion, as the measured deactivation is 5–10 times higher than expected from a 1:1 correlation.

The lower activation energies of the sulfated catalysts might be due to formation of internal diffusion limitations induced by SO_x deactivation, which can play a role in the deactivation process. In case of increased diffusion limitations, the effectiveness factor should become lower in addition to the loss of sites, resulting in an overall deactivation that is higher than the fraction of Cu sites in contact with sulfur. This agrees, at least qualitatively, with the results shown in Fig. 8. To evaluate a possible effect of diffusion limitations, the effectiveness factor, η, was calculated for the fresh catalyst, assuming spherical zeolite crystals and first order reaction kinetics in NO. For the calculations, the crystal radius was set to 0.5 μm, which is a reasonable value given that the crystal size of the zeolite is on the order of 1 μm. A further description of the calculation of the effectiveness factor is given in supporting information. Fig. 9 shows the effectiveness factor as a function of the effective diffusion coefficient, D_{eff}, at 180 °C. By extrapolation of experimentally determined values for effective diffusion coefficients for NH_3 in a Cu-CHA catalyst, using the corresponding activation energy [16], we find a diffusion coefficient of $1.2{\cdot}10^{-9}$ m^2/s. Using this diffusion coefficient, Fig. 9 shows that the effectiveness factor for the fresh catalyst is close to 1. This implies that no internal diffusion limitation is expected in the crystals of the fresh catalyst. Because the activation energy of the regenerated catalysts is the same as for the fresh, diffusion effects can be excluded for the irreversible deactivation as well.

If the reduction of the effective activation energy to half the intrinsic value would be due to diffusion limitations, the effectiveness factor should decrease to be lower than 0.8, where there is a linear relationship between $\log(\eta)$ and $\log(D_{eff})$ resulting in a straight line in Fig. 9. According to Fig. 9, to obtain an effectiveness factor of 0.8, a decrease of the diffusion coefficient by about a factor of 100 would be required. This would mean that the small amount of sulfur, corresponding to less than 20% coverage of the Cu-sites, reduces the diffusion coefficient by a factor of 100. This seems unlikely, also taking into account that a similar sulfur content in the regenerated catalysts does not affect the activation energy and diffusion.

Alternatively, pore-blocking by possible formation of ammonium sulfates may be considered as a cause for the reversible deactivation behavior. We note that the sulfated catalysts are exposed to SO_2 without ammonia present, and therefore, the resulting sulfur species is most likely bound to the Cu-ions [13]. If ammonium sulfate is formed by subsequent exposure to ammonia, this implies that the ammonium sulfate species is also located close to the Cu-ions. The SO_2/Cu ratios in the sulfated catalysts is about 0.15 (except in those exposed to SO_3 at 200 °C), which is similar to the SO_2/Cu ratio in some of the regenerated catalysts, where it was argued that there is no diffusion limitation. Therefore, it seems unlikely that the presence of these fairly small amounts of ammonium sulfate effectively block access to most of the zeolite. At present, the question of how the limited amount of sulfur can have such a strong impact on the reversible deactivation remains unanswered.

Having ruled out diffusion as a cause for reversible deactivation, the lower activation energy must then be related to changes in the chemistry. An interesting concept is Cu being able to form a mobile diamine species at SCR conditions. These mobile Cu-diamine species are important for the low-temperature activity of Cu-CHA catalysts [17–20]. Possibly, the reversible deactivation by sulfur oxide species inhibits the formation of these mobile Cu diamine complexes, thereby lowering the mobility of Cu and the NH_3-SCR activity, which might lead to the observed high degree of reversible deactivation with low amounts of sulfur.

Finally, our data clearly show that exposure to SO_x at lower temperatures result in the largest deactivation. However, most of the catalytic activity can be regained by heating to 550 °C, even after exposure to SO_3 at 200 °C. This is an interesting result from an application point of view, since it indicates that regeneration strategies based on heating to easily obtainable temperatures in exhaust systems are a feasible solution to handle deactivation of Cu-zeolites by SO_2 and SO_3 [10,13].

5. Conclusion

To evaluate different aspects of sulfur poisoning of NH_3-SCR activity, Cu-CHA catalysts were exposed to SO_2 or a 70:30 mixture of SO_2 and SO_3, in dry or moist conditions and at low and high temperature, and were evaluated before and after regeneration at 550 °C. After SO_x exposure, a high degree of deactivation is observed at temperatures below 300 °C. A major part of this deactivation is reversible by heating to 550 °C for 4 h, while a smaller, but appreciable, level of irreversible deactivation remains.

The mechanisms behind the reversible and irreversible deactivation differs. Irreversible deactivation is proportional to the sulfur content in the catalyst and consistent with the formation of a Cu-sulfate species. Reversible deactivation is not proportional to the sulfur content, and shows a strong deactivation already at low SO_2/Cu ratios.

The presence of water always increases irreversible deactivation, but has no apparent effect on reversible deactivation. Exposure to SO_x at 200 °C, always leads to a higher level of irreversible deactivation compared to exposure at 550 °C. The presence of SO_3 at 200 °C leads to significantly stronger deactivation; at 550 °C, deactivation by SO_3 is not significantly different from that by SO_2. Regeneration of Cu-CHA exposed to SO_3 at 200 °C is accompanied by a decomposition of SO_3 and release of SO_2 around 400 °C.

In all experiments, the reversible deactivation accounts for most of the total deactivation, which makes regeneration by heating to 550 °C, an easily obtainable temperature in exhaust systems, a realistic approach to deal with deactivation by SO_x.

Acknowledgements

PSH gratefully acknowledges support from Innovation Fund Denmark [grant number 5139-0023B]. YJ gratefully acknowledges support from Cummins Inc.

Appendix A. Supplementary data

Supplementary data associated with this article can be found, in the online version, at https://doi.org/10.1016/j.apcatb.2017.12.018.

References

[1] I. Nova, E. Tronconi, Urea-SCR Technology for DeNOx After Treatment of Diesel Exhausts, 1 st, Springer, 2014.
[2] Y. Cheng, C. Lambert, D.H. Kim, J.H. Kwak, S.J. Cho, C.H.F. Peden, Catal. Today 151 (2010) 266.
[3] T. Fushun, Z. Ke, Y. Fang, Y. Lili, X.U. Bolian, Q.I.U. Jinheng, F.A.N. Yining, Chinese J. Catal. 33 (2012) 933.
[4] Y. Cheng, C. Montreuil, G. Cavataio, C. Lambert, SAE Int. J. Fuels Lubr. 1 (2015) 471.
[5] L. Zhang, D. Wang, Y. Liu, K. Kamasamudram, J. Li, W. Epling, Appl. Catal. B 156–157 (2014) 371.
[6] K. Wijayanti, S. Andonova, A. Kumar, J. Li, K. Kamasamudram, N.W. Currier, A. Yezerets, L. Olsson, Appl. Catal. B 166–167 (2015) 568.
[7] K. Wijayanti, K. Leistner, S. Chand, A. Kumar, K. Kamasamudram, N.W. Currier, A. Yezerets, L. Olsson, Catal. Sci. Technol. 6 (2016) 2565.
[8] J. Luo, D. Wang, A. Kumar, J. Li, K. Kamasamudram, N. Currier, Catal. Today 267 (2016) 3.
[9] Y. Jangjou, M. Ali, Q. Chang, D. Wang, J. Li, A. Kumar, W.S. Epling, Catal. Sci. Technol. 6 (2016) 2679.
[10] Y. Jangjou, D. Wang, A. Kumar, J. Li, W.S. Epling, ACS Catal. 6 (2016) 6612.
[11] A. Kumar, M.A. Smith, K. Kamasamudram, N.W. Currier, H. An, A. Yezerets, Catal. Today 231 (2014) 75.
[12] W. Su, Z. Li, Y. Zhang, C. Meng, J. Li, Catal. Sci. Technol. 7 (2017) 1523.
[13] A. Kumar, M.A. Smith, K. Kamasamudram, N.W. Currier, A. Yezerets, Catal. Today 267 (2016) 10.
[14] C. Paolucci, A.A. Parekh, I. Khurana, J.R. Di Iorio, H. Li, J.D.A. Caballero, A.J. Shih, T. Anggara, W.N. Delgass, J.T. Miller, F.H. Ribeiro, R. Gounder, W.F. Schneider, J. Am. Chem. Soc. 138 (2016) 6028.
[15] H. Li, A. Shih, A. Kumar, I. Khurana, C. Paolucci, J.T. Miller, A. Yezerets, R. Gounder, F.H. Ribeiro, W.F. Schneider, Determination of Sulfur Poisoning Pathways across Cu sites in Cu SSZ 13, (2017) NAM-25 meeting June 2017, Denver, O-Fr-D-1.
[16] A.J. O'Malley, I. Hitchcock, M. Sarwar, I.P. Silverwood, S. Hindocha, C.R.A. Catlow, A.P.E. York, P.J. Collier, Phys. Chem. Chem. Phys. 18 (2016) 17159.
[17] F. Gao, D. Mei, Y. Wang, J. Szanyi, C.H.F. Peden, J. Am. Chem. Soc. 139 (2017) 4935.
[18] F. Giordanino, E. Borfecchia, K.A. Lomachenko, A. Lazzarini, G. Agostini, E. Gallo, A.V. Soldatov, P. Beato, S. Bordiga, C. Lamberti, J. Phys. Chem. Lett. 5 (2014) 1552.
[19] S. Shwan, M. Skoglundh, L.F. Lundegaard, R.R. Tiruvalam, T.V.W. Janssens, A. Carlsson, P.N.R. Vennestrøm, ACS Catal. 5 (2015) 16.
[20] C. Paolucci, I. Khurana, A.A. Parekh, S. Li, A.J. Shih, H. Li, J.R. Di Iorio, J.D. Albarracin-Caballero, A. Yezerets, J.T. Miller, W.N. Delgass, F.H. Ribeiro, W.F. Schneider, R. Gounder, Science 357 (2017) 898.

Chapter 3

Chapter 4

STEM-EDX investigation of the S distribution in the zeolite crystals of an SO_2 exposed Cu-CHA catalyst

Introduction

In the previous section of this chapter, the cause of the reduction of the apparent activation energies in the SO_2 exposed catalyst, to about half the value for the fresh catalyst was discussed. Such a decrease to the apparent activation energy can be the result of diffusion limitation. The possibility of introducing diffusion limitations to the SCR reaction by the presence of sulfur was assessed by evaluation of the efficiency factor of the catalyst. In order to get into a diffusion limited regime where the activation energy is affected, the diffusion coefficient had to be lowered by a factor 100. Assuming that sulfur was evenly distributed in the Cu-CHA crystals at the Cu sites, it was argued that the sulfur content corresponding to about 20% coverage of the Cu content could not infer such dramatic changes to the diffusion coefficient. However, if the sulfur is located in the outer shell of the zeolite crystals, it may have a larger impact on the diffusion of the reactants into the zeolite. Therefore, the distribution of sulfur in the Cu-CHA crystals is investigated by scanning transmission electron microscopy with energy dispersive X-ray (STEM-EDX) spectroscopy.

Experimental

For the STEM-EDX measurements, a fresh Cu-CHA catalyst (Si/Al = 14.6 and Cu/Al = 0.42) was exposed to SO_2 at 200 °C for 1 h, resulting in a S/Cu ratio of 0.28, as determined by ICP. The same catalyst was used in Chapter 5, where the SO_2 exposure is described in more detail.

STEM-HAADF (high-angle annular dark-field imagning) images and STEM-EDX measurements were made in a FEI Talos 200FX electron microscope. The fresh Cu-CHA catalyst was mounted on a gold grid, while the SO_2 exposed Cu-CHA catalyst powder was mounted on a Cu grid due to some overlap in the electromagnetic spectrum of gold and sulfur.

Results and discussion

The images of the fresh and SO_2 exposed Cu-CHA catalysts, and distributions of Cu and S from the EDX measurements are shown in Figure 1.

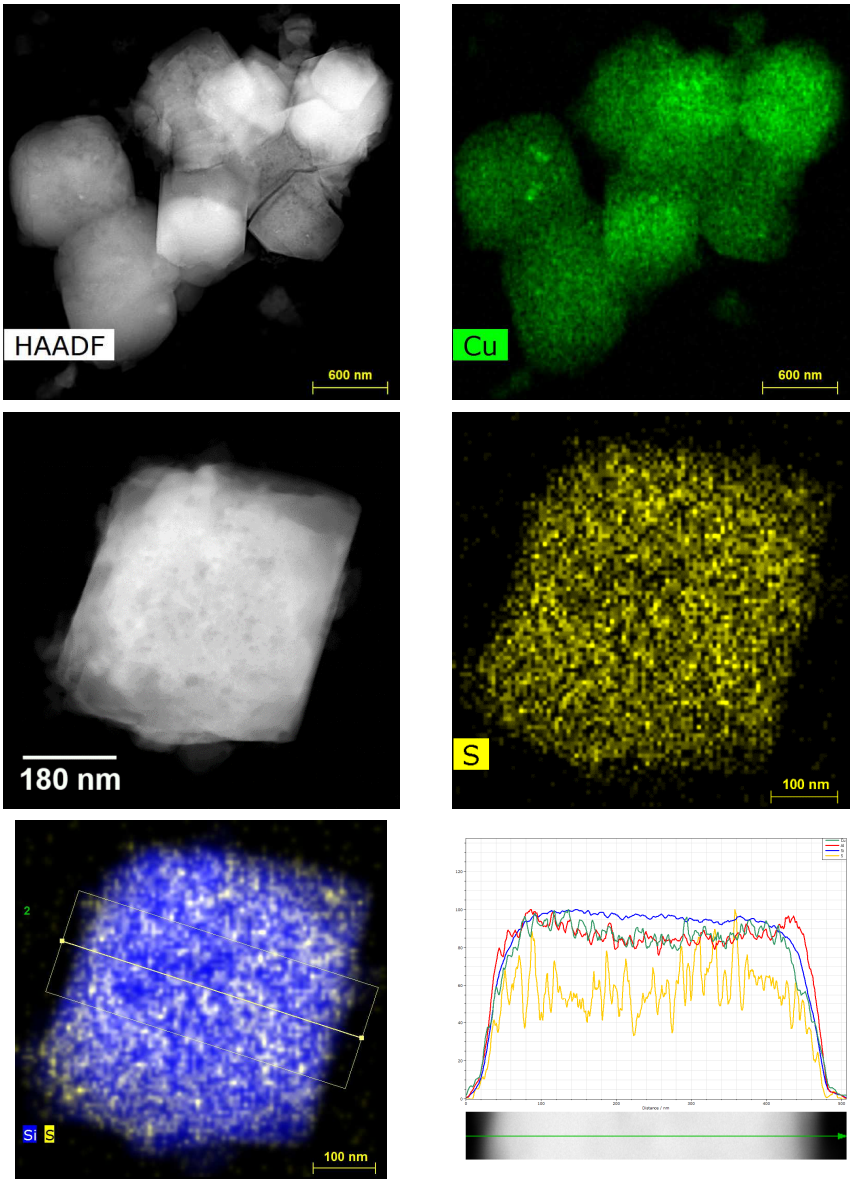

Figure 1 – Top left) STEM-HAADF image of fresh Cu-CHA catalyst, Top right) Cu distribution in fresh Cu-CHA from STEM-EDX, Middle left) STEM-HAADF image of SO_2 exposed Cu-CHA, Middle right) S distribution in SO_2 exposed Cu-CHA from STEM-EDX, Bottom left) S and Si distribution in SO_2 exposed Cu-CHA from STEM-EDX and indication of linescan area, Bottom right) relative concentrations of Cu (green), Al (red), Si (blue) and S (yellow) from the linescan. The relative concentration of S has been scaled, which is the reason for the higher noise level for that element.

In the fresh Cu-CHA catalyst, Cu appears evenly distributed in the crystal with small areas of Cu clustering. Similarly, the S appears to be evenly distributed in the entire zeolite crystal. This is also confirmed by the relative concentrations of S, Si, and Al obtained in the linescan. This indicates that the change in the activation energies of the SO_2 exposed catalysts is not a result of sulfur accumulation in the outer shell of the Cu-CHA zeolite crystals.

With STEM-EDX the Al/S ratio is measured to be 8 in the SO_2 exposed catalyst, and with a Cu/Al ratio of 0.42, it corresponds to a S/Cu ratio of about 0.3, which is close to the S/Cu ratio of 0.28 measured with ICP. This adds to the verification of the STEM-EDX measurements.

Conclusions

The sulfur distribution in an SO_2 exposed Cu-CHA catalyst was measured with STEM-EDX, which showed that sulfur was evenly distributed in the Cu-CHA zeolite crystal. This supports the conclusion in Chapter 3 that the change in the activation energy after SO_2 exposure is not a result of diffusion limitations.

Chapter 5

Impact of SO_2-poisoning over the lifetime of a Cu-CHA catalyst for NH_3-SCR

This chapter has been published in:
Applied Catalysis B: Environmental 238 (2018) 104-110
https://doi.org/10.1016/j.apcatb.2018.06.039

Applied Catalysis B: Environmental 238 (2018) 104–110

Contents lists available at ScienceDirect

Applied Catalysis B: Environmental

journal homepage: www.elsevier.com/locate/apcatb

Impact of SO_2-poisoning over the lifetime of a Cu-CHA catalyst for NH_3-SCR

Peter S. Hammershøi[a,b], Anker D. Jensen[b], Ton V.W. Janssens[a,*]

[a] Umicore Denmark ApS, Nøjsomhedsvej 20, 2800 Kgs. Lyngby, Denmark
[b] Department of Chemical and Biochemical Engineering, Technical University of Denmark, Søltofts Plads B229, 2800 Kgs. Lyngby, Denmark

ARTICLE INFO

Keywords:
Deactivation
Cu-CHA
SO_2
NH_3-SCR

ABSTRACT

Cu-CHA catalysts for NH_3-SCR in exhaust after treatment systems of heavy-duty vehicles, are constantly exposed to SO_2 during their lifetime of about 10,000 h. In order to study the development of deactivation by SO_2, a Cu-CHA catalyst was exposed to SO_2 at 200, 300, 400 and 500 °C for different durations up to 120 h, resulting in total SO_2 exposures that are comparable to that of the lifetime of a Cu-CHA catalyst in an after treatment system. The measured deactivation increases very fast to a steady level in the range 0.85–0.95, dependent on the exposure temperature, which shows the need for frequent regeneration of the catalyst. Regeneration at 550 °C can restore the activity of the catalyst to 80% of its fresh activity level even after 120 h exposure, suggesting frequent regeneration as a feasible method for overcoming SO_2-poisoning. ICP analyses showed that SO_2 exposure led to S/Cu ratios in the range 0.5–1, indicating that sulfur is associated with Cu. After regeneration the S/Cu ratios did not exceed 0.2, suggesting that only certain Cu sites are able to form Cu,S species that are thermally stable above 550 °C. This together with the observations that the deactivation before and after regeneration impact differently on the activation energy of the SCR reaction, and that the deactivation never exceeded 0.95, suggests that SO_2-poisoning of Cu-CHA depends on the structural properties of this material. TGA measurements of the mass uptake during SO_2 exposure was consistent with a process where SO_2 is initially adsorbed on Cu, and then slowly oxidized to SO_3 at 200 °C, whereas the mass uptake at 500 °C was consistent with an immediate adsorption of SO_3, which is accredited to a faster oxidation rate at higher temperature.

1. Introduction

Combustion engines in vehicles produce polluting compounds, and their emissions are restricted by legislation. In particular, the emissions of NO_x (NO and NO_2) from vehicles is strictly regulated, which already has resulted in a significant improvement of air quality [1]. For diesel engines, the most effective method to reduce NO_x emissions to the levels required by legislative regulations, is by selective catalytic reduction with NH_3 (NH_3-SCR), and modern diesel exhaust aftertreatment systems contain one or more catalytic converters for NH_3-SCR [2].

A widely used technique for dosing of NH_3 in exhaust aftertreatment systems is by injection of aqueous urea, which decomposes to NH_3 above 180 °C [2], setting a lower temperature limit for NH_3-SCR in an exhaust system. Furthermore, the improved fuel efficiency of diesel engines that has been achieved in recent years, in order to lower the CO_2 emissions, has resulted in colder exhaust gas. Consequently, it takes longer time to heat the catalysts in the exhaust aftertreatment system, and therefore, the low-temperature activity, in particular around 180 °C, has become more important for the abatement of NO_x emissions.

Currently employed SCR catalysts are V_2O_5-based or zeolites containing Fe or Cu. Especially Cu-zeolites of the CHA topology are very active in the low-temperature range 180–300 °C, which in combination with their high hydrothermal stability and low N_2O selectivity, has made these materials particularly interesting as SCR catalysts for automotive applications [2–4]. The Al centers in the zeolite framework generates locations with negative charge, which are balanced by external cations. In the case of Cu-CHA, Cu in these ion-exchange positions gives rise to the activity of the Cu-CHA catalysts for the NH_3-SCR reaction. Cu-CHA catalysts have two characteristic activity regimes, namely a low-temperature (approx. 200–300 °C) and a high-temperature (> 350 °C) [5], which are separated by a region where the steady state NO_x conversion actually can decrease with increasing temperature [6]. The low-temperature activity of Cu-CHA catalysts is ascribed to the formation of mobile $[Cu(NH_3)_2]^+$ complexes in the presence of NO and NH_3, which enables formation of Cu pairs that efficiently dissociate O_2 [7–14], which is a key step in the NH_3-SCR reaction.

A drawback of Cu-zeolite catalysts is their sensitivity to SO_2. SO_2 is formed by oxidation of sulfur-containing compounds in the fuel and engine lubrication oils. In practice, the formation of SO_2 is limited by

* Corresponding author.
E-mail address: tonv.w.janssens@eu.umicore.com (T.V.W. Janssens).

https://doi.org/10.1016/j.apcatb.2018.06.039
Received 20 April 2018; Received in revised form 8 June 2018; Accepted 13 June 2018
Available online 03 July 2018
0926-3373/

reduction of the sulfur content in diesel fuels, and therefore, the use of ultra-low sulfur diesel (ULSD) has been implemented in USA and Europe. The current maximum allowable sulfur concentration in ULSD is 15 wt ppm in USA and 10 wt ppm in Europe [1]. The use of ULSD results in a typical SO_2 concentration in the exhaust gas in the range 0.5–2 volume ppm SO_2. Even at such low SO_2 concentrations, a considerable deactivation of Cu-CHA catalysts, particularly in the low-temperature regime, is still observed [6,15–22].

The differences in the effect of SO_2 on the performance of the different types of NH_3-SCR catalysts is clearly related to the chemistry of the systems [22]. The high SO_2 sensitivity for Cu-zeolites, compared to Fe-zeolites, is possibly due to the higher stability of Cu-sulfate compared to Fe-sulfate [23]. This is consistent with the observed release of SO_2 and restoration of activity of Cu-CHA by heating to 700 °C, which is above the temperature for thermal decomposition of Cu-sulfate [6,18,22,23]. This suggests that the deactivation induced by SO_2 is at least partially due to the formation of some SO_3. In an aftertreatment system, SO_3 can form from oxidation of SO_2, which can take place over the diesel oxidation catalyst and also in the Cu-CHA catalyst itself [6,15,18,20]. Therefore, to understand the deactivation of Cu-zeolite catalysts by SO_2, the formation and interaction of SO_3 with Cu must be considered as well. This means that the SO_2-induced deactivation of Cu-zeolites is influenced by many factors, such as temperature, gas environment, and oxidation of SO_2 to SO_3 [6,15,18,22], and several Cu,S species of varying stability that can be formed [6,15–18,22,24,25].

A potentially feasible method for treating SO_2-induced deactivation of Cu-CHA catalysts in an exhaust system is by thermal regeneration of the catalyst, which is possible due to the different stabilities of the Cu,S species [6,15,18,20,22,26]. In a typical modern aftertreatment system, an achievable maximum temperature of the SCR catalyst for regeneration is about 550 °C. Regeneration of a Cu-CHA catalyst at this temperature reverses the predominant part of the deactivation [6]. Thus, the total deactivation measured after exposure to SO_x can be divided into a reversible and an irreversible part, by measuring the irreversible deactivation after regeneration at 550 °C [6].

The required lifetime of an SCR catalyst in an aftertreatment system of a heavy-duty diesel vehicle is about 10,000 h. Throughout its lifetime, the SCR catalyst is constantly exposed to low concentrations of SO_2, which makes the deactivation a continuous process persisting over the lifetime of the catalyst. Therefore, it is important to know the impact of these low SO_2 concentrations over long-term SO_2 exposure. The deactivation process can be accelerated by increasing the SO_2 concentration [22], because the deactivation appears to depend on the total SO_2 exposure [22], defined as the product of the SO_2 concentration and the exposure time. In this way, the development of the reversible and irreversible deactivation over the lifetime of the catalyst can be assessed from experiments of significantly shorter exposure times, but with higher SO_2 concentrations.

In this contribution, the deactivation and regeneration of a Cu-CHA catalyst is investigated for SO_2 exposures of increasing duration up to 120 h and with 50 ppmv SO_2, which is comparable to the total SO_2 exposure of a commercial Cu-CHA SCR catalyst during its required lifetime. The deactivation is evaluated by comparing the performance of the catalysts in the NH_3-SCR reaction after SO_2 exposure at 200–500 °C, and after regeneration at 550 °C, to that of the fresh. This is important, in order to assess the impact of the reversible and irreversible deactivation development over long-term SO_2 exposure. Furthermore, the catalytic performance is compared to the S uptake of the catalysts exposed at 200–500 °C, as determined by ICP, and to in situ thermogravimetric measurements of SO_2 exposure at 200 and 500 °C.

2. Experimental

The zeolite material used in this study is a CHA zeolite with a Si/Al ratio of 14.6. Cu was introduced in the zeolite by mixing it with the appropriate amount of an aqueous $Cu(NO_3)_2$ solution to obtain 2.5 wt% Cu in the zeolite. After mixing, the slurry was dried at 120 °C and calcined at 550 °C for 3 h. The calcined catalyst powder was light blue, indicating that Cu is located in the ion-exchange positions of the CHA material. The Si, Al and Cu content were determined by ICP-OES to be 37.5, 2.46, and 2.43 wt%, respectively, corresponding to a Cu/Al ratio of 0.42, and estimated 2.76 wt% Cu on a dry matter basis.

The SO_2 exposures were carried out in a flow reactor setup, equipped with 4 parallel quartz reactor tubes, each with independent control of the temperature. A sample of 1.6 g of fresh catalyst powder (sieve fraction 150–300 µm) was added to each reactor tube and held in place by quartz wool plugs. Prior to SO_2 exposure, all catalyst loadings were heated to 500 °C for 2 h in a flow of 10% O_2, 5% H_2O, and sufficient N_2 to obtain a total flow rate of 1.67 N L/min. Then, one reactor was kept at 500 °C, and the other three reactors were cooled to 200, 300, and 400 °C. For the SO_2 exposure, 50 ppmv SO_2 was added to the reactor feed, while keeping the same total flow rate. In 6 different runs, the duration of SO_2 exposure was varied and chosen as 1, 5, 15, 30, 65, 120 h. In this way, a total of 24 catalyst samples were obtained, each with different SO_2 exposure duration and temperature. Finally, 0.8 g of each of these 24 samples was regenerated in the same parallel reactor setup by exposing to 550 °C for 6 h in a flow of 10% O_2, 5% H_2O, and N_2 to balance the flow to 1.67 N L/min.

This yields a total of 48 treated catalyst samples, 24 exposed to SO_2 and 24 regenerated, which were all analyzed for Cu and S content using ICP-OES in order to determine the S/Cu ratio after each treatment of the catalyst.

The NH_3-SCR activity measurements were done in a microreactor setup, by adding 5 mg (dry matter basis) catalyst powder, 150–300 µm sieve fraction, to a quartz U-tube reactor with an inner diameter of 2 mm, using quartz wool to keep the catalyst in place. The reactor feed gas consisted of 500 ppmv NO, 533 ppmv NH_3, 10% O_2, 5% H_2O, in N_2 at a total flow rate of 225 N mL/min. To measure the NH_3-SCR activity, the catalyst was heated stepwise to 160, 180, 190, 200, 210, 220, 250, 300, 325, 350, 400, and 550 °C and kept at these temperatures for 40 min to ensure stationary conditions. The concentrations of NO, NH_3, NO_2, and N_2O in the reactor exit gas were monitored continuously by a Gasmet CX4000 FTIR analyzer, connected to the reactor outlet. The feed gas concentrations were measured by bypassing the reactor, using the same FTIR analyzer.

To determine the NH_3-SCR activity, the steady state conversion was determined from the activity measurement, and converted to a rate constant according to:

$$k = -\frac{F}{W}\ln(1-X) \tag{1}$$

where F is the total molar flow rate, W is the catalyst mass, and X is the NO conversion. For the deactivation we use our earlier definition [6] in which the rate constants of the catalysts exposed to SO_2 before or after regeneration (k) are related to the corresponding rate constant of the fresh catalyst (k_{fresh}), as expressed in:

$$\text{Deactivation} = 1-\frac{k}{k_{fresh}} \tag{2}$$

Finally, the uptake of sulfur at 200 °C and 500 °C was followed by thermogravimetric analysis (TGA) in two separate measurements. For these measurements, a sample of the fresh catalyst was heated to 550 °C for 1 h in 10% O_2 in N_2, at a total flow rate of 150 N mL/min, to obtain the dry mass of the catalyst. The dry masses of the samples used were 25.9252 mg (S uptake at 200 °C) and 37.6135 mg (S uptake at 500 °C). Then, the catalyst was exposed to SO_2 at 200 °C or 500 °C, using a feed gas consisting of 50 ppmv SO_2, 3% H_2O and 10% O_2 in N_2, also at a total flow rate of 150 N mL/min, while monitoring the change in catalyst mass. Changes in catalyst mass during regeneration were obtained by heating to 550 °C and changing the feed gas to 10% O_2 in N_2, while keeping the same total flow rate. The changes in S uptake are

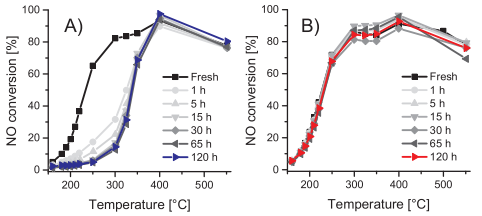

Fig. 1. Steady state NO conversions plotted as function of the temperature in the NH_3-SCR reaction over A) the SO_2 exposed catalysts, and B) the regenerated catalysts. The measurements were carried out with inlet concentrations of 500 ppmv NO, 533 ppmv NH_3, 10% O_2, 5% H_2O and N_2 to a total flow rate of 225 N mL/min.

determined from the weight changes in alternating SO_2 exposure and regeneration phases at a fixed temperature (200 or 500 °C), where catalysts are regenerated after the same cumulative durations of the SO_2 exposure as used in the deactivation measurements given above.

3. Results

Fig. 1 shows the development of the steady state NO conversions as function of the temperature over the duration of exposure to SO_2 at 200 °C, and after subsequent regeneration by heating at 550 °C for 6 h. In all cases, the NO conversion in the temperature range 160–350 °C is considerably lower after exposure to SO_2, compared to the fresh catalyst. Regeneration at 550 °C mostly restores the NO conversion in that temperature range. The same trends are observed after exposure to SO_2 at 300 °C, 400 °C, and 500 °C, see supporting information. This behavior can be described in terms of reversible and irreversible deactivation as defined earlier [6]. The deactivation remaining after regeneration is then the irreversible deactivation, and the reversible deactivation is defined as the difference in deactivation of the SO_2 exposed catalyst before and after regeneration [6].

The total SO_2 exposure, which corresponds to the product of the exposure time and SO_2 concentration, appears to be a good descriptor for deactivation by SO_2 [22], which also allows for estimation of the deactivation over the entire required lifetime of the catalyst. Fig. 2 summarizes the development of the reversible and irreversible deactivation with SO_2 exposure for the exposure temperatures of 200, 300, 400, and 500 °C, along with the corresponding S/Cu ratio measured by ICP. Both the reversible and irreversible deactivation initially show a fast increase with SO_2 exposure, and reach a final level after an SO_2 exposure of 500–1000 ppm h, after which the deactivation remains constant. It is noted that the predominant part of the final deactivation level is reached already after 50 ppm h, which is the first data point in each SO_2 exposure series, indicating that the effect of SO_2 is almost immediate. The final deactivation after SO_2 exposure, before regeneration, is 0.85–0.95 and depends on the temperature of SO_2 exposure. The irreversible deactivation is about 0.2–0.3, independent of the temperature for SO_2 exposure. It is also noted that we have not found any conditions in which a complete deactivation of the Cu-CHA is observed.

In order to relate the measured deactivation of the Cu-CHA catalyst with the sulfur uptake, the deactivation is compared to the measured S/Cu ratios before and after regeneration. The S/Cu ratios of the regenerated states of the catalyst mirrors the observed irreversible deactivation, with a rapid increase during the first 1000 ppm h SO_2, followed by a constant final level of about 0.2, independent of the temperature of SO_2 exposure. This value matches the observed deactivation level of 0.2–0.3 quite well, suggesting that the irreversible deactivation is related to the adsorption of sulfur on the active Cu sites.

The measured S/Cu ratios before regeneration do not appear to reach a final level. The S/Cu ratios initially increase fast, which parallels the fast increase of the deactivation, but after about 1000 ppm h SO_2, the S/Cu ratio continues to increase at a lower rate, except for the catalysts exposed to SO_2 at 500 °C. The measured S/Cu ratios are, in most cases, lower than the observed levels of deactivation, which indicates that the reversible deactivation cannot be directly explained by Cu site blocking with sulfur. Nevertheless, the observation that the S/Cu ratios generally are lower than 1 indicates that the uptake of sulfur is related to the Cu and is consistent with adsorption of sulfur on Cu.

A more detailed comparison of the measured S/Cu ratios and the reversible and irreversible deactivation, is shown in Fig. 3. The reversible deactivation is always disproportionately larger than the corresponding S/Cu ratios, while the irreversible deactivation generally is closer to a 1:1 correlation with the S/Cu ratio, which would be expected for deactivation by single site blocking. This shows that the impact of sulfur uptake on the reversible deactivation is larger compared to the irreversible deactivation. This also suggests that the reversible and irreversible deactivation are related to the formation of different Cu,S species or selective adsorption of sulfur on specific Cu-sites.

The difference between reversible and irreversible deactivation is also reflected in the apparent activation energy for the NH_3-SCR reaction. Fig. 4 shows the apparent activation energies for the different SO_2 exposures before and after regeneration. Clearly, for the catalysts before regeneration, the activation energy is lowered from about 70 kJ/mol to about 30 kJ/mol for an SO_2 exposure of about 1000 ppm h, which coincides with the observed fast increase in deactivation and initial uptake of sulfur. At longer SO_2 exposures, the apparent activation energy remains constant. For the regenerated catalysts, all measured activation energies are about 70 kJ/mol, which is close to the value of the fresh catalyst, independent of SO_2 exposure time or temperature. This means that the level of deactivation of the Cu-CHA catalyst by SO_2 is not only the result of a certain amount of S in the catalyst, but also depends on which Cu,S species that are present. The different trends observed for the activation energies before and after regeneration are also an indication of different mechanisms for the SCR reaction on the reversibly and irreversibly deactivated Cu-CHA catalysts, in agreement with an earlier conclusion [6].

The different influence of the SO_2 exposure temperature on the sulfur uptake related to the reversible or irreversible deactivation is illustrated in Fig. 5, which shows the measured S/Cu ratios as function of the exposure temperatures. As also noted above, the S/Cu ratios related to the irreversible deactivation reach approximately 0.2 for all exposure temperatures, which suggests that the irreversible deactivation is related to the formation of a Cu,S species at certain Cu sites. The S/Cu ratios related to the reversible deactivation in Fig. 5 show a maximum sulfur uptake at 400 °C for short SO_2 exposure (1 and 5 h), and at 300 °C for the longer SO_2 exposures. This trend is similar to that observed on a Cu-SAPO-34 catalyst exposed to SO_2 in O_2 and H_2O at different temperatures [22], and reflects a trade-off between the kinetics of the formation of the Cu sulfate species and the equilibrium adsorption concentration [22].

TGA measurements were used to assess the sulfur uptake during SO_2 exposure at 200 °C and 500 °C in more detail, to better understand the effect of SO_2 at low and high temperature. Fig. 6 shows how the relative mass of the catalyst (with the dry mass of the catalyst before SO_2 exposure as basis) changes with the total SO_2 exposure. Both at 200 °C and 500 °C, SO_2 exposure leads to a steep increase in the catalyst mass at SO_2 exposures below 500 ppm h. At 500 °C, a relative mass of 1.02 is reached, which remains stable after longer exposures to SO_2, while at 200 °C, the relative mass initially increases to 1.01, which then increases further to approximately 1.03 after 6000 ppm h SO_2 exposure. This is qualitatively the same trend as found for the S/Cu ratio (Fig. 2), which is an indication that the observed increase in catalyst mass is indeed due to the uptake of SO_2.

For a more precise interpretation of the observed increase in catalyst mass upon exposure to SO_2 at 200 °C and 500 °C, we need to know in

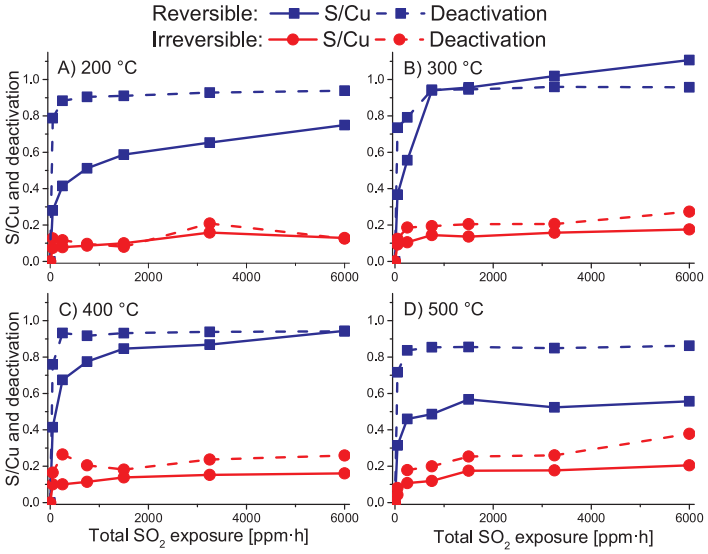

Fig. 2. Reversible (squares) and irreversible (circles) deactivation at 220 °C (dashed lines), and S/Cu ratios (solid lines), plotted as fucntions of the total SO_2 exposure, for the catalysts exposed to SO_2 at A) 200 °C, B) 300 °C, C) 400 °C, and D) 500 °C, and for the corresponding regenerated catalysts.

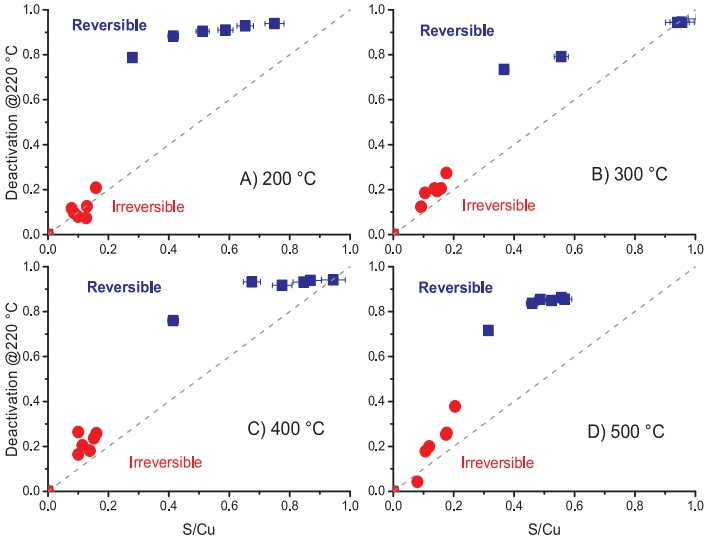

Fig. 3. Reversible (squares) and irreversible (circles) deactivation at 220 °C plotted as functions of the S/Cu ratios for the exposure temperatures A) 200 °C, B) 300 °C, C) 400 °C, and D) 500 °C.

which form the SO_2 is adsorbed on the catalyst. The most obvious options are adsorption of SO_2 or SO_3, and the formation of sulfites and sulfates on the Cu sites [6,15,16,18,22]. By comparing the observed increases in catalyst mass measured in the TGA experiments with the measured S/Cu ratios given in Figs. 2 and 5, it is possible to work out whether the sulfur is adsorbed as SO_2 or SO_3. First, the observed increase in catalyst mass is converted to a molar amount of sulfur, under the assumption that the sulfur is present as either SO_2 or SO_3, which together with the known Cu content, 2.76 wt% on dry matter basis, results in an estimated SO_2/Cu and SO_3/Cu ratio. In Fig. 7, these

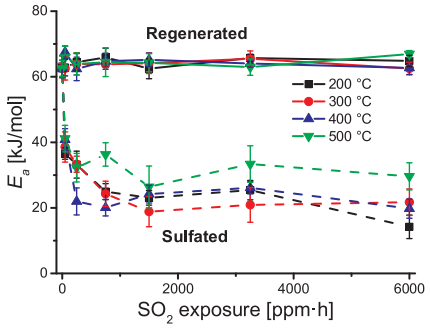

Fig. 4. Activation energies in the NH_3-SCR reaction for the SO_2 exposed (dashed lines) and regenerated (solid lines) catalysts, plotted as functions of the total SO_2 exposure.

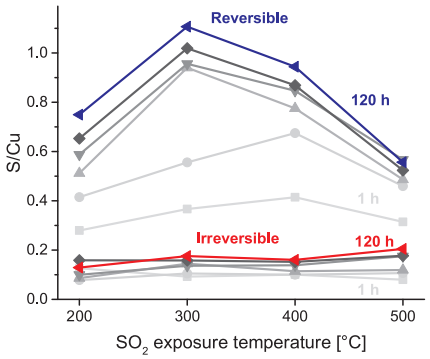

Fig. 5. Development of the reversible and irreversible S/Cu ratios from 1 h to 120 h of SO_2 exposure, plotted for each exposure temperature.

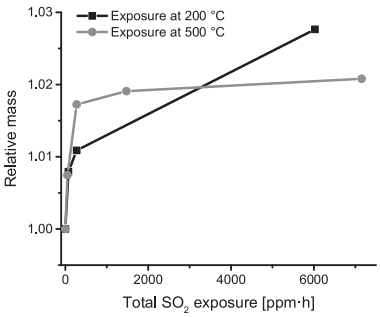

Fig. 6. Relative masses of the catalysts exposed to SO_2 at 200 °C (black) and 500 °C (grey) in the thermogravimetric setup, plotted as functions of the total SO_2 exposure.

estimated SO_2/Cu and SO_3/Cu ratios are compared to the measured S/Cu ratios determined by ICP, for Cu-CHA exposed to SO_2 at 200 °C and 500 °C. At an SO_2 exposure temperature of 200 °C, the SO_2/Cu ratios follow the measured S/Cu ratios to 1000 ppm h of SO_2 exposure. At 6000 ppm h SO_2, the measured S/Cu ratio matches the estimated SO_3/Cu ratio. This indicates that initially it is SO_2 that is adsorbed on the Cu, but it is slowly oxidized to SO_3. With an SO_2 exposure temperature of 500 °C, the estimated SO_3/Cu ratio matches the S/Cu ratio over the entire SO_2 exposure duration. This clearly shows that at 500 °C, oxidation of SO_2 is faster, and adsorption is essentially as SO_3. Adsorption of SO_3 on a Cu-OH species actually corresponds to the formation of a bisulfate species, which have been proposed earlier as being the cause of the irreversible deactivation [6,15,16,18–22,24,25].

4. Discussion

The results presented above clearly show that SO_2 primarily affects the low-temperature activity of Cu-CHA catalysts for SCR, and therefore, the impacts of SO_2 on the high-temperature activity will not be discussed further here.

For an SCR catalyst that has a required lifetime of about 10,000 h, it is important to be able to estimate the performance for the entire lifetime. One way to do this is by comparison of the total SO_2/Cu exposure for the lifetime of the catalyst in a heavy-duty vehicle to similar conditions in a test. The total SO_2/Cu exposure for a Cu-CHA catalyst over its lifetime is about 44, assuming that the vehicle covers 800,000 km with a consumption of 30 L/100 km, using 5 wt ppm S diesel, and with a Cu-loading of 45 g of the Cu-CHA SCR catalyst. The total molar SO_2/Cu exposure in the experiments presented in this article is 41.7 after 120 h, which is similar to the typical SO_2/Cu exposure in an exhaust system. Therefore, we expect that the development of SO_2-poisoning in our experiments reflect that of a Cu-CHA SCR catalyst in an exhaust aftertreatment system.

The results presented in this study shows that the reversible deactivation increases fast to a high level, independent of the SO_2 exposure temperature. This means that the SCR catalyst in an exhaust system requires frequent regeneration in order to maintain an efficient NH_3-SCR performance, especially in the context of cold start where the low-temperature activity is particularly important. Based on the presented results, it is actually possible to restore the predominant part of the original activity of the catalyst throughout its lifetime, by regeneration at 550 °C. This shows that SO_2-poisoning of Cu-CHA catalysts is occurring over the lifetime of the catalyst, but that it can be managed by proper regeneration strategies. Furthermore, the irreversible deactivation seems sufficiently small to be handled by appropriate system design.

The use of Cu-CHA catalysts in exhaust systems appears to rely on the efficiency of regeneration, which likely depends on the SO_2 concentration during regeneration. Thus, exposure to 50 ppmv SO_2 at 500 °C leads to uptake of sulfur by the catalyst, while regeneration at 550 °C in the absence of SO_2 partially removes sulfur from the catalyst. Furthermore, reversible and irreversible deactivation of a Cu-SAPO-34 catalyst have been shown to build up when exposed to SO_2 concentrations as low as 1.5 ppmv at 500 °C [22]. Therefore, it appears that the uptake or removal of sulfur depends on the SO_2 concentration being above or below a critical value, which is somewhere in the range 0–1.5 ppmv SO_2. This could potentially complicate the regeneration if the SO_2 content of the exhaust gas is above the critical concentration, in which case a regeneration would resemble the SO_2 exposure at 500 °C. In that case, the low-temperature activity of Cu-CHA catalysts would be lost relatively fast, and so would the main advantage of using these materials compared to Fe-zeolites or vanadia-based systems. The efficiency of regeneration, and the critical SO_2 concentration, would have to be verified in an actual exhaust system, since reducing compounds in the exhaust gas, such as hydrocarbons and NH_3, have been shown to have a beneficial effect for removing sulfurous compounds from Cu-CHA catalysts [26].

The process for the uptake of sulfur by the Cu-CHA catalyst possibly proceeds by an initial adsorption of SO_2 on Cu where the sulfur is subsequently oxidized to sulfate. This is envisioned because the Cu-CHA

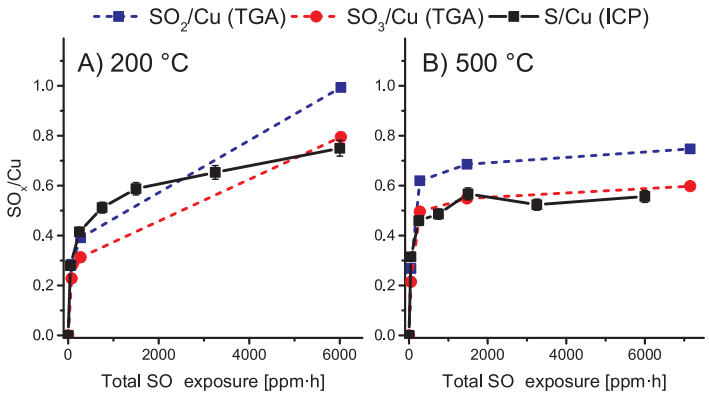

Fig. 7. SO_x/Cu ratios plotted as functions of the total SO_2 exposure for catalysts exposed to SO_2 at A) 200 °C, and B) 500 °C. Black solid lines are S/Cu ratios determined by ICP-OES on catalysts exposed to SO_2 in the reactor setup. Dashed lines are SO_2/Cu ratios (blue squares) and SO_3/Cu ratios (red circles) based on the mass increase measured in the thermogravimetric setup. (For interpretation of the references to colour in this figure legend, the reader is referred to the web version of this article).

catalyst is exposed to SO_2, which must oxidize in order to constitute the forms of sulfate that are associated with the Cu,S species causing the reversible [6,15,16,18,22] and irreversible deactivation [6,22]. The proposed process is consistent with the results from the TGA experiment at 200 °C (Fig. 7), where the initial mass uptake fits with an uptake of SO_2, and over time changes to fit better with an uptake of SO_3. At this temperature (200 °C), there is a clear difference between the initial and final uptake, which indicates that the oxidation of SO_2 is kinetically controlled. In the TGA experiment at 500 °C, the mass uptake fits with a constant uptake of SO_3, which can be explained by a faster oxidation of SO_2 at this temperature [20,22], which both could be on the Cu sites or in the gas phase.

A possible reason for the disproportionally high reversible deactivation, as compared to the S/Cu ratio, is that the adsorption of SO_2 affects the mobility and effective amount of $[Cu(NH_3)_2]^+$ ions in the Cu-CHA zeolite. The current understanding of the low-temperature part of the SCR mechanism is that the mobile $[Cu(NH_3)_2]^+$ complexes allow for the formation of pairs of Cu ions, which are crucial for the dissociation of the oxygen molecules [8,11]. As a consequence, the activity depends on the square of the Cu density below a certain Cu loading, and depends linearly on the Cu density above it [8]. This results in two distinct activity regimes, which may be related to the different impacts of the sulfur loading on the reversible and irreversible deactivation. In principle, the mechanism based on mobile $[Cu(NH_3)_2]^+$ complexes implies that all Cu sites are the same, namely the mobile $[Cu(NH_3)_2]^+$ complex, and contribute equally to the activity. Ultimately, the activity is determined by the amount of Cu pairs that are formed at the given conditions. The different trends for the activation energy of the SCR reaction with reversible and irreversible deactivation, as shown in Fig. 4, and the disproportionately larger reversible deactivation than irreversible deactivation as compared to the S/Cu ratios shown in Fig. 3 can be understood in relation to the two activity regimes. Since the S/Cu ratios related to the irreversible deactivation are always lower than those related to the reversible deactivation, and lower than 0.2, the amount of deactivated Cu in these cases may be sufficiently small to keep the amount of non-deactivated Cu in the linear dependence regime. The activity is then not limited by formation of Cu pairs, and the deactivation would simply correspond to a loss of active sites, which is also consistent with the values of the activation energies close to that of the fresh catalyst. For the reversible deactivation, the S/Cu ratios of 0.3–1 could enforce a situation where the effective Cu content becomes sufficiently low for the activity to be restricted by formation of Cu pairs. In this situation, the activity depends on the square of the effective Cu density, and therefore, it would be expected that the deactivation is disproportionately larger than the S/Cu ratio, as observed in Fig. 3. The lower activation energy is then related to the fact that the rate of the SCR reaction is determined by the limited rate of Cu pair formation.

The observation that similar sulfur contents can result in significantly different levels of reversible and irreversible deactivation [6] is not consistent with the idea that all Cu sites contribute equally to the rate of the NH_3-SCR reaction. Factors like the zeolite structure and Al distribution can also influence the reactivity or mobility of Cu, eventually resulting in Cu sites of different activity. This idea is supported by two observations of the SO_2 exposed and regenerated Cu-CHA catalyst in Fig. 2. The first observation is that the reversible deactivation never exceeds 0.95, indicating that some Cu does not adsorb SO_2 or is not affected by SO_2, and the second observation is that the S/Cu ratio related to the irreversible deactivation is limited to 0.2, suggesting that the more stable Cu sulfate species can only form at certain Cu sites. According to this view, the deactivation and regeneration behavior of Cu-CHA catalysts also depend on the structural properties of the catalyst.

5. Conclusion

A Cu-CHA catalyst for NH_3-SCR has been exposed to SO_2 at different temperatures in the range 200–500 °C, and at durations up to 120 h, resulting in a total SO_2 exposure that is similar to what an SCR catalyst experiences over the entire lifetime in an exhaust aftertreatment system on a heavy-duty vehicle. Activity measurements after SO_2 exposure, and after regeneration at 550 °C, enabled measurement of the extent of deactivation of the catalyst in these two states. The deactivation of the low-temperature activity of the Cu-CHA catalyst in the presence of SO_2 occurs fast in the entire temperature window 200–500 °C to a final deactivation level in the range 0.85–0.95, dependent on the exposure temperature. Heating in SO_2-free gas to 550 °C restores the activity to about 80% of its original level, even after a total S/Cu exposure similar to that of the lifetime of a Cu-CHA SCR catalyst in a heavy-duty diesel after treatment system. This suggests regeneration as a feasible method for handling SO_2-poisoning, since proper dimensioning of the catalyst easily can treat the irreversible deactivation of maximum 0.2–0.3 that develops over long-term SO_2 exposure.

Analogous to the deactivation, the S/Cu ratios also increase fast initially, and the S/Cu ratios of the SO_2 exposed catalysts reach different levels in the range of 0.5–1, dependent on the exposure temperature. The regenerated S/Cu ratios never exceed 0.2, indicating that the irreversible Cu,S species are restricted to certain Cu sites. The mechanism of the sulfur uptake appears to proceed by an initial uptake of SO_2 by the catalyst, followed by oxidation to sulfate on the catalyst, at a rate that increases with temperature.

The reversible and irreversible deactivation have a different impact on the low-temperature SCR mechanism, which is seen by i) a disproportionately larger reversible deactivation relative to the S/Cu ratio as compared with the irreversible deactivation, and ii) by the reversible deactivation causing a change in the activation energy of the SCR reaction, whereas the irreversible deactivation does not. This, together with the observations of a maximum irreversible S/Cu ratio of 0.2, and a maximum deactivation level of 0.95, points to a dependence of the SO_2-poisoning of Cu-CHA catalysts on structural properties of the Cu-CHA material.

Funding

Financial support from Innovation Fund Denmark (grant number 5139-0023B) is gratefully acknowledged by PSH.

Declarations of interest

None.

Acknowledgements

A great part of the practical work with the SO_2 exposures and regenerations was conducted by research specialist Jesper Sargent Larsen (Umicore Denmark ApS) for which he is most thankfully acknowledged.

References

[1] J.D. Miller, C. Façanha, The State of Clean Transport Policy - A 2014 Synthesis of Vehicle and Fuel Policy Developments, ICCT Rep. (2014), p. 73 http://www.theicct.org/sites/default/files/publications/ICCT_StateOfCleanTransportPolicy_2014.pdf.

[2] I. Nova, E. Tronconi, Urea-SCR Technology for deNOx After Treatment of Diesel Exhausts, 1st ed., Springer-Verlag, New York, 2014.

[3] F. Gao, C.H.F. Peden, J.H. Kwak, J. Szanyi, Current understanding of Cu-exchanged chabazite molecular sieves for use as commercial diesel engine DeNO x catalysts, Top. Catal. 56 (2013) 1441–1459, https://doi.org/10.1007/s11244-013-0145-8.

[4] A.M. Beale, F. Gao, I. Lezcano-Gonzalez, C.H.F. Peden, J. Szanyi, Recent advances in automotive catalysis for NOx emission control by small-pore microporous materials, Chem. Soc. Rev. (2015), https://doi.org/10.1039/C5CS00108K.

[5] F. Gao, E.D. Walter, M. Kollar, Y. Wang, J. Szanyi, C.H.F. Peden, Understanding ammonia selective catalytic reduction kinetics over Cu / SSZ-13 from motion of the Cu ions, J. Catal. 319 (2014) 1–14, https://doi.org/10.1016/j.jcat.2014.08.010.

[6] P.S. Hammershøi, Y. Jangjou, W.S. Epling, A.D. Jensen, T.V.W. Janssens, Reversible and irreversible deactivation of Cu-CHA NH3-SCR catalysts by SO2 and SO3, Appl. Catal. B 226 (2018) 38–45, https://doi.org/10.1016/j.apcatb.2017.12.018.

[7] S. Shwan, M. Skoglundh, L.F. Lundegaard, R.R. Tiruvalam, T.V.W. Janssens, A. Carlsson, P.N.R. Vennestrøm, Solid-state ion-exchange of copper into zeolites facilitated by ammonia at low temperature, ACS Catal. 5 (2015) 16–19, https://doi.org/10.1021/cs5015139.

[8] C. Paolucci, I. Khurana, A.A. Parekh, S. Li, A.J. Shih, H. Li, J.R. Di Iorio, J.D. Albarracin-Caballero, A. Yezerets, J.T. Miller, W.N. Delgass, F.H. Ribeiro, W.F. Schneider, R. Gounder, Dynamic multinuclear sites formed by mobilized copper ions in NO x selective catalytic reduction, Science 357 (80-) (2017) 898–903, https://doi.org/10.1126/science.aan5630.

[9] L. Chen, J. Jansson, M. Skoglundh, H. Grönbeck, Mechanism for solid-state ion Exchange of Cu + into zeolites, J. Phys. Chem. C 120 (2016) 29182–29189, https://doi.org/10.1021/acs.jpcc.6b09553.

[10] C. Paolucci, A.A. Parekh, I. Khurana, J.R. Di Iorio, H. Li, J.D.A. Caballero, A.J. Shih, T. Anggara, W.N. Delgass, J.T. Miller, F.H. Ribeiro, R. Gounder, W.F. Schneider, Catalysis in a cage: condition-dependent speciation and dynamics of exchanged Cu cations in SSZ-13 zeolites, J. Am. Chem. Soc. 138 (2016) 6028–6048, https://doi.org/10.1021/jacs.6b02651.

[11] F. Gao, D. Mei, Y. Wang, J. Szanyi, C.H.F. Peden, Selective catalytic reduction over Cu/SSZ-13: linking homo- and heterogeneous catalysis, J. Am. Chem. Soc. 139 (2017) 4935–4942, https://doi.org/10.1021/jacs.7b01128.

[12] T.V.W. Janssens, H. Falsig, L.F. Lundegaard, P.N.R. Vennestrøm, S.B. Rasmussen, P.G. Moses, F. Giordanino, E. Borfecchia, K.A. Lomachenko, C. Lamberti, S. Bordiga, A. Godiksen, S. Mossin, P. Beato, A consistent reaction scheme for the selective catalytic reduction of nitrogen oxides with ammonia, ACS Catal. 5 (2015) 2832–2845, https://doi.org/10.1021/cs501673g.

[13] A. Marberger, A.W. Petrov, P. Steiger, M. Elsener, O. Kröcher, M. Nachtegaal, D. Ferri, Time-resolved copper speciation during selective catalytic reduction of NO on Cu-SSZ-13, Nat. Catal. 1 (2018) 221–227, https://doi.org/10.1038/s41929-018-0032-6.

[14] F. Giordanino, E. Borfecchia, K.A. Lomachenko, A. Lazzarini, G. Agostini, E. Gallo, A.V. Soldatov, P. Beato, S. Bordiga, C. Lamberti, Interaction of NH3 with Cu-SSZ-13 catalyst: a complementary FTIR, XANES, and XES study, J. Phys. Chem. Lett. 5 (2014) 1552–1559.

[15] A. Kumar, M.A. Smith, K. Kamasamudram, N.W. Currier, H. An, A. Yezerets, Impact of different forms of feed sulfur on small-pore Cu-zeolite SCR catalyst, Catal. Today 231 (2014) 75–82.

[16] Y. Jangjou, D. Wang, A. Kumar, J. Li, W.S. Epling, SO2 poisoning of the NH3-SCR reaction over Cu-SAPO-34: effect of ammonium sulfate versus other S-containing species, ACS Catal. 6 (2016) 6612–6622, https://doi.org/10.1021/acscatal.6b01656.

[17] J. Luo, D. Wang, A. Kumar, J. Li, K. Kamasamudram, N. Currier, A. Yezerets, Identification of two types of Cu sites in Cu / SSZ-13 and their unique responses to hydrothermal aging and sulfur poisoning, Catal. Today 267 (2016) 3–9, https://doi.org/10.1016/j.cattod.2015.12.002.

[18] Y. Cheng, C. Lambert, D.H. Kim, J.H. Kwak, S.J. Cho, C.H.F. Peden, The different impacts of SO2 and SO3 on Cu/zeolite SCR catalysts, Catal. Today 151 (2010) 266–270.

[19] Y. Cheng, C. Montreuil, G. Cavataio, C. Lambert, Sulfur tolerance and DeSOx studies on diesel SCR catalysts, SAE Int. J. Fuels Lubr. 1 (2008) 471–476.

[20] L. Zhang, D. Wang, Y. Liu, K. Kamasamudram, J. Li, W. Epling, SO2 poisoning impact on the NH3-SCR reaction over a commercial Cu-SAPO-34 SCR catalyst, Appl. Catal. B 156–157 (2014) 371–377, https://doi.org/10.1016/j.apcatb.2014.03.030.

[21] W. Su, Z. Li, Y. Zhang, C. Meng, J. Li, Identification of sulfate species and their influence on SCR performance of Cu/CHA catalyst, Catal. Sci. Technol. 7 (2017) 1523–1528, https://doi.org/10.1039/C7CY00302A.

[22] P.S. Hammershøi, P.N.R. Vennestrøm, H. Falsig, A.D. Jensen, T.V.W. Janssens, Importance of the Cu oxidation state for the SO2-poisoning of a Cu-SAPO-34 catalyst in the NH3-SCR reaction, Appl. Catal. B 236 (2018) 377–383, https://doi.org/10.1016/j.apcatb.2018.05.038.

[23] J. Mu, D.D. Perlmutter, Thermal decomposition of inorganic sulfates and their hydrates, Ind. Eng. Chem. Process Des. Dev. 20 (1981) 640–646, https://doi.org/10.1021/i200015a010.

[24] K. Wijayanti, K. Xie, A. Kumar, K. Kamasamudram, L. Olsson, Effect of gas compositions on SO2 poisoning over Cu/SSZ-13 used for NH3-SCR, Appl. Catal. B 219 (2017) 142–154, https://doi.org/10.1016/j.apcatb.2017.07.017.

[25] K.C. Hass, W.F. Schneider, Density functional studies of adsorbates in Cu-exchanged zeolites: model comparisons and SOx binding, Phys. Chem. Chem. Phys. 1 (1999) 639–648.

[26] A. Kumar, M.A. Smith, K. Kamasamudram, N.W. Currier, A. Yezerets, Chemical deSOx: an effective way to recover Cu-zeolite SCR catalysts from sulfur poisoning, Catal. Today 267 (2016) 10–16, https://doi.org/10.1016/j.cattod.2016.01.033.

Chapter 6

Site selective adsorption and relocation of SO_x in deactivation of Cu-CHA catalysts for NH_3-SCR

The contents of this chapter has been submitted for publication in:
Reaction Chemistry and Engineering (25-10-2018)

Site selective adsorption and relocation of SO_x in deactivation of Cu-CHA catalysts for NH_3-SCR

Peter S. Hammershøi,[ab] Anita L. Godiksen,[c] Susanne Mossin,[c] Peter N. R. Vennestrøm,[a] Anker D. Jensen[b] and Ton V. W. Janssens*[a]

[a]*Umicore Denmark ApS, Nøjsomhedsvej 20, 2800 Kgs. Lyngby, Denmark*
[b]*Department of Chemical and Biochemical Engineering, Technical University of Denmark, Søltofs Plads B229, 2800 Kgs. Lyngby, Denmark*
[c]*Department of Chemistry, Technical University of Denmark, Kemitorvet B207, 2800 Kgs. Lyngby, Denmark*
*Correponding author e-mail: tonv.w.janssens@eu.umicore.com

Abstract

The presence of SO_2 in diesel exhaust gases causes severe deactivation of the Cu-CHA catalysts for the reduction of NO_x by selective catalytic reduction with ammonia (NH_3-SCR). The deactivation of Cu-CHA catalysts after exposure to SO_2 at 550 °C for 0.5, 4, 8, 16 and 32 h, and subsequent regeneration in SO_2-free gas at 550 °C was related to the site-dependent interactions of SO_2 with Cu ions associated with one or two framework Al centers (Z-CuOH or Z_2-Cu), as determined by electron paramagnetic resonance (EPR). SO_2 primarily interacts with the EPR-silent Z-CuOH sites, but a new, EPR-active Z_2-Cu phase develops with SO_2 exposure time as well. A part of the original Z_2-Cu species remain unaffected by SO_2, which is associated with a maximum deactivation level of about 90%. Regeneration at 550 °C leads to the release of most of the SO_2 from the Z-CuOH sites and some relocation of sulfur to Z_2-Cu sites occurs. The activation energy for NH_3-SCR on the SO_2 exposed catalysts decreases with S content from about 65 kJ/mol to 30 kJ/mol. For the regenerated catalysts, the activation energy is restored to about 65 kJ/mol, showing the importance of the Z-CuOH sites for the NH_3-SCR reaction.

Introduction

The selective catalytic reduction of NO_x (NO and NO_2) with NH_3 (NH_3-SCR) is the predominant method for removal of NO_x from exhaust gas of heavy-duty diesel vehicles. The catalysts used for this reaction are based on V_2O_5, Fe-zeolites or Cu-zeolites. Future legislation will require tighter NO_x emission limits, and therefore, a more efficient removal of NO_x in the low-temperature region becomes crucial. In this respect, the Cu-zeolites with the CHA structure are attractive,[1,2] because of the significantly higher activity of the Cu-CHA catalysts at low temperatures down to 180 °C, which is unmatched by Fe-zeolites and V_2O_5-based catalysts.[1,3,4]

According to the current understanding, the low-temperature activity of Cu-CHA catalysts is related to the ability to form mobile $[Cu(NH_3)_2]^+$ complexes. These complexes facilitate the formation Cu pairs,[5,6] on which the dissociation of oxygen can take place.[5–12]

A drawback of Cu-CHA catalysts, and Cu-zeolite based catalysts in general, is their sensitivity to SO_2 in the exhaust gas that originates from the sulfur present in the fuel. Ultra-low sulfur diesel contains less than 10 wt ppm (Europe) or 15 wt ppm (US) sulfur, and the SO_2 concentration in the exhaust gas typically reaches a few ppmv, which is nevertheless sufficient to reduce the low-temperature activity of the Cu-CHA catalysts significantly.[13,14,23,24,15–22] To be able to preserve the good low-temperature activity, it is important to understand the impact of SO_2 on the NH_3-SCR activity of Cu-CHA based catalysts.

We have recently shown that deactivation of Cu-CHA catalysts depends on the total SO_2 exposure, which is the product of the SO_2 concentration and the exposure time.[14] Deactivation by SO_2 is almost immediate: at about 1% of the total lifetime exposure to SO_2, the activity is reduced to about 30% of the original activity, and it stabilizes at about 10% of the original activity after 5-10% of the lifetime SO_2 exposure.[15] The sulfur uptake in the Cu-CHA catalyst follows a similar pattern as the activity and, dependent on the temperature, a maximum S/Cu molar ratio of 0.5-1 is reached. The observation that the S/Cu ratio usually does not exceed 1 points to the formation of Cu,S species.[13–15] Thermal regeneration at 550 °C, which is feasible in a typical EURO VI exhaust system, can restore most of the activity if carried out in SO_2-free gas.[13–15] During the regeneration, SO_2 is released from the catalyst, but a certain fraction of the sulfur is retained in a stable form that resemble Cu sulfate.[13–17,20] The observations that heating to 550 °C results both in a partial regeneration of Cu-CHA catalysts and in the formation of a certain amount Cu sulfate, indicates that there are distinct Cu sites with a different reactivity towards SO_2.[13,15,20,23]

The most obvious possibility for distinct Cu sites in Cu-CHA catalysts is that the Cu can be associated with either one or two Al centers in the zeolite framework. This leads to two main Cu^{II} sites: Z-CuOH and Z_2-Cu, and these sites have different chemical properties.[10,25–30] The relative amounts of these Cu sites depend on synthesis conditions, the Si/Al ratio of the zeolite, and the Cu loading.[10] Therefore, it is important to understand which role the Z-CuOH sites and Z_2-Cu sites play in the deactivation by SO_2.

Electron paramagnetic resonance (EPR) spectroscopy is a powerful method for selective monitoring of the Z_2-Cu sites in Cu-CHA catalysts, and the presence of sulfur-species on these sites can be detected. In this article, EPR is used in combination with elemental analysis to localize sulfur in SO_2 exposed and regenerated Cu-CHA catalysts after total SO_2 exposures up to 3200 ppm·h at 550 °C. This is compared to the deactivation of the catalysts in the NH_3-SCR reaction, which reveals how Z-CuOH sites and Z_2-Cu sites behave in the deactivation of Cu-CHA catalysts by SO_2.

Experimental

Catalyst preparation

The parent CHA zeolite powder used in this study was prepared according to a previously published procedure,[28] which has been used in other EPR studies as well.[29–31] Cu was introduced by ion-exchange of the parent H-SSZ-13 (Si/Al = 15) with an aqueous solution of $Cu(CH_3COO)_2$ for 24 h at 20 °C. The suspensions consisted of 1 g per 250 mL $Cu(CH_3COO)_2$ solution. To obtain the different Cu loadings in the Cu-CHA, the concentration of the $Cu(CH_3COO)_2$ solution was varied. The concentrations used for the catalysts in this study were 0.5, 1.0, 1.5, 2.0, and 5.0 mM, which resulted in Cu loadings of 0.72, 1.23, 1.63, 1.93, and 2.81 wt%, as determined by ICP-OES analysis.

SO_2 exposure and regeneration

To study the deactivation of Cu-CHA catalysts by SO_2 exposure, 0.5 g portions of the Cu-CHA with 2.81 wt% Cu were exposed to SO_2 for 0.5, 4, 8, 16, and 32 h at 550 °C in a quartz tube furnace. These catalyst samples are referred to as "SO_2 exposed". The gas mixture used in these treatments consisted of 100 ppmv SO_2 and 16 % O_2 in N_2. Prior to the SO_2 exposure, the catalyst samples were de-greened for 1 h at 550 °C in technical air. After the exposure to SO_2, each catalyst portion was divided in two equal parts, and one half of each sample was regenerated in the same tube furnace at 550 °C for 5 h in a flow of 10 % O_2 and 3 % H_2O in N_2 at a flow rate of 200 NmL/min. These catalyst samples are referred to as "regenerated".

NH_3-SCR activity measurements

The NH_3-SCR activities of the fresh, SO_2 exposed, and regenerated catalysts were determined from measurement of steady state NO conversions. For these measurements, a 5 mg sample (on a dry matter basis, sieve fraction 150-300 µm) was loaded in a fixed bed quartz reactor with an inner diameter of 2 mm. The reaction feed consisted of 500 ppmv NO, 530 ppmv NH_3, 10 % O_2 and 5 % H_2O in N_2 at a flow rate of 225 NmL/min. The concentrations of NO, NO_2, N_2O, NH_3 and H_2O were determined online, using a Gasmet CX4000 FTIR analyzer connected to the reactor outlet. For the activity measurements, the reactor temperature was stepwise increased from 160 to 550 °C and allowed to stabilize for 40 min at each temperature.

The activity of the catalysts was derived from the NO conversion as the first order rate constant, *k*, of the SCR reaction:

$$k = -\frac{F}{W\left(1+\frac{\Delta P}{2}\right)}\ln(1-X) \qquad (1)$$

Here, F is the total molar flow rate, W is the dry weight of the catalyst powder, ΔP is the pressure drop over the catalyst bed, and X is the fractional NO conversion. The deactivation of the catalysts is calculated as the relative loss of activity as follows:

$$\text{Deactivation} = 1 - \frac{k}{k_{fresh}} \quad (2)$$

EPR: measurement of the total Cu content

The EPR spectra were collected on a CW X-band Bruker EMX EPR spectrometer with an ER 4102ST cavity and a gunn diode microwave source. To measure the total amount of Cu in the zeolite, the total EPR intensity of a 25 mg of the Cu-CHA sample, placed in a quartz tube, was compared to the measured intensities for a series of samples where $CuSO_4$ is diluted in K_2SO_4 to obtain a known Cu concentration in the range 0.2-5 wt%. In the fresh untreated Cu-CHA samples, the Cu is present as an EPR active hydrated form, allowing for an accurate measurement of the total Cu content.

The measurements were done within the field interval 220-400 mT, with a microwave power of 6.3 mW, a microwave frequency of 9.4-9.6 GHz, a modulation frequency of 100 kHz, and a modulation amplitude of 8 G. The spectra were collected with 2000 points and averaged over 3 scans. The Q-value was noted and carefully observed to be the same for the different samples. The EPR intensity was calculated as the double integral of the measured spectra, after background correction.

In-situ dehydration with EPR

For selective measurement of the Z_2-Cu species present in the Cu-CHA catalysts, the catalysts must be dehydrated. The dehydration was done in a flow of 50 mL/min of 20 % O_2 in He while heating to 250 °C at a rate of 7 °C/min, using a heater attached to the EPR cavity. The EPR spectra were continuously collected, using the parameters as given above, with a time constant of 20.48 msec and conversion time of 15 msec, which results in approximately 41-42 seconds between the start of each spectrum. A final spectrum was collected in pure He atmosphere. All spectra are background corrected by subtracting the spectrum of an empty tube and, if necessary, also by performing a linear baseline correction. The intensity of the EPR spectrum is found by double integration of the background corrected spectrum.

The EPR intensity for the dehydrated samples, I_{rel}, is determined by relating the EPR intensity, $I(T)$, to the intensity of the starting (fully hydrated) EPR spectrum, $I(T_{start})$, and corrected according to the Boltzmann distribution for the temperature differences according to [30,32]:

$$I_{rel} = \frac{I(T)}{I(T_{start})} \cdot \frac{T}{T_{start}} \quad (3)$$

EPR spectra were fitted as a sum of contributions from each Cu species. Each species is modeled using an axial spin Hamiltonian [29] with 4 parameters, $g_{\|}$, $g_{\perp}$, $A_{\|}$, and $A_{\perp}$,. The fittings and simulations are performed using the EasySpin Toolbox in Matlab.[33]

Results

NH_3-SCR activity and impact of SO_2 exposure

The effect of increasing SO_2 exposure time over Cu-CHA on the NH_3-SCR NO conversion is illustrated in Figure 1. Low-temperature activity (<350 °C) of the Cu-CHA catalyst is strongly reduced upon exposure to SO_2 (Figure 1A). The impact of SO_2 at temperatures above 350 °C is clearly less, indicating that deactivation by SO_2 is mainly relevant for the low-temperature performance, in agreement with earlier observations.[13,14,23,24,15–22] The low-temperature activity after SO_2 exposure is partially restored by heating the Cu-CHA catalysts to 550 °C in SO_2-free gas (Figure 1B).[13–15]

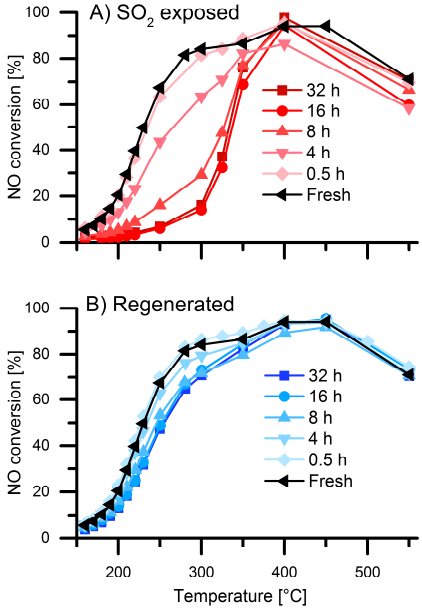

Figure 1 - Steady state NO conversion of the fresh catalyst in comparison with those of A) the SO_2 exposed catalysts after exposure to 100 ppmv SO_2 and 16 % O_2 in N_2 at 550 °C for different durations, and B) the regenerated catalysts after regeneration in 10 % O_2 and 3 % H_2O in N_2 at 550 °C for 5 h.

The changes in the deactivation of NH_3-SCR activity with time of SO_2 exposure are illustrated in Figure 2A, which shows the deactivation, according to Eq. 2, based on the measured NO conversion at 220 °C. About 80% of the activity is lost during the first 8 h of SO_2 exposure, and after 16 h of SO_2 exposure, the loss of activity stabilizes at 90%. This means that the deactivation of the SO_2 exposed catalysts does not reach 100%, but a certain NH_3-SCR activity, although low, is maintained even after prolonged exposure to SO_2.[15] The deactivation of the regenerated catalysts increases with SO_2 exposure in a similar manner, reaching a maximum of 50% deactivation.

To determine the relation of the deactivation with the uptake of sulfur, the sulfur contents of the SO_2 exposed and regenerated catalysts were measured with ICP-OES. The measured S/Cu ratios are also included in Figure 2A. For the SO_2 exposed catalysts, a maximum S/Cu ratio of 0.8 is reached. The fact that the S/Cu ratio does not exceed 1 is consistent with the deactivation being related to interactions between sulfur and Cu.[13–15] After regeneration at 550 °C the S/Cu ratios remain unchanged in the catalysts exposed to SO_2 for up to 4 h, while the S/Cu ratios drops for the catalysts subjected to longer exposures as part of the sulfur is released from the catalyst during regeneration.[13,14] The highest S/Cu ratio for the regenerated catalysts is 0.5. The similar trends in the S/Cu ratio and deactivation curves in Figure 2A suggest a correlation.

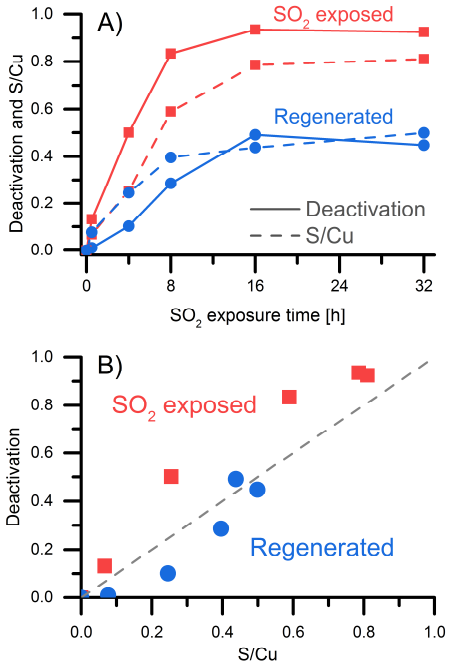

Figure 2 - A) shows the deactivation (full lines) and S/Cu ratios (dashed lines) of the SO_2 exposed (red) and regenerated (blue) catalysts as functions of the exposure time to SO_2. B) shows the deactivation as function of the S/Cu ratio for the SO_2 exposed (red squares) and regenerated (blue circles) catalysts. The grey dashed line indicates the 1:1 correlation between the deactivation and S/Cu. The deactivation in both graphs are at 220 °C.

Figure 2B shows the deactivation as a function of the S/Cu ratios. The grey dashed line represents a 1:1 relation between the deactivation and S/Cu ratio. There is a distinct difference between the SO_2 exposed and regenerated catalysts: All of the SO_2 exposed catalysts have deactivation levels that are above the 1:1 proportionality line, whereas all of the regenerated catalysts are below the line, except for a single catalyst sample. This shows that sulfur causes a stronger deactivation before regeneration than after. This is particularly pronounced when comparing the SO_2 exposed and regenerated catalysts after 0.5 and 4 h of SO_2 exposure. In these catalysts, the deactivation levels are significantly different, but the S/Cu ratios are very similar. This shows that the regeneration is not just a consequence of the release of sulfur from the catalyst. During regeneration, the Cu,S species also changes to a form which affects the NH_3-SCR activity of the catalyst less. This change could be related to the sulfation of different Cu sites.[14,20,23]

The sulfur also affects the activation energy for NH_3-SCR in a different way before and after regeneration. Figure 3 shows the apparent activation energies (190-250 °C) for the SO_2 exposed and regenerated catalysts as a function of the SO_2 exposure time. The activation energies for the SO_2 exposed catalysts decrease with increasing exposure time, while those of the regenerated catalysts remain stable and close to the activation energy of the fresh catalyst. This is consistent with a difference in how the sulfur interacts with the copper before and after regeneration.

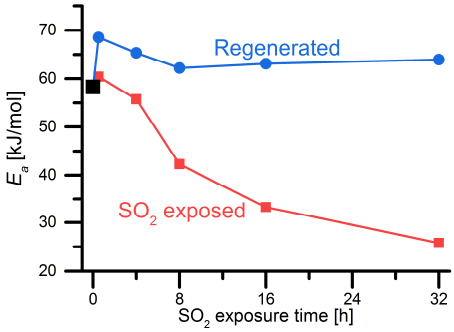

Figure 3 - Activation energies (190-250 °C) for the fresh (black), SO_2 exposed (red), and regenerated (blue) catalysts in the NH_3-SCR reaction, as function of the SO_2 exposure time.

Recently, it was proposed that the NH_3-SCR activity depends on the ability of the catalyst to form Cu pairs from mobile $[Cu(NH_3)_2]^+$ species. [5,6] It was also shown that at low Cu loading, the relation between activity and Cu loading becomes quadratic because it depends on two copper sites to form the active Cu pair site, and that the activation energy increases with increasing Cu loading. In this situation, if single Cu sites were blocked, the deactivation would be disproportionately larger than the amount of affected Cu sites, as observed for the SO_2 exposed catalysts in Figure 2B. A part of the explanation for the observed disproportional effect of sulfur on the activity of the SO_2 exposed catalysts, seems likely to be related to this behavior, as well as the influence on the activation energy.

To understand the consequences of a Cu-site blocking by sulfur better, we compare in Figure 4 the activities and the apparent activation energies of the deactivated catalysts (both SO_2 exposed and

regenerated) to those of fresh Cu-CHA catalysts with various Cu loadings as a function of the sulfur-free Cu density. The sulfur-free Cu density was calculated as the difference between the total molar Cu content of the fresh catalyst and the total molar S content of the deactivated catalysts. The general trends of the rate constants of both the SO_2 exposed and regenerated catalysts are similar to that of the fresh catalysts, but there are some differences as well. In the higher Cu density range, the rate constants of the SO_2 exposed catalysts are slightly lower compared to the fresh catalysts. Furthermore, the rate constants for the SO_2 exposed catalysts show a quadratic dependence on the sulfur-free Cu density up to 0.44 Cu/1000 Å^3. In contrast, the rate constants for the fresh catalysts only appear to follow a quadratic dependence up to about 0.33 Cu/1000 Å^3. The regenerated catalysts generally show a higher rate constant than the corresponding fresh catalysts, and they do not exhibit a quadratic dependence on the sulfur-free Cu density at all.

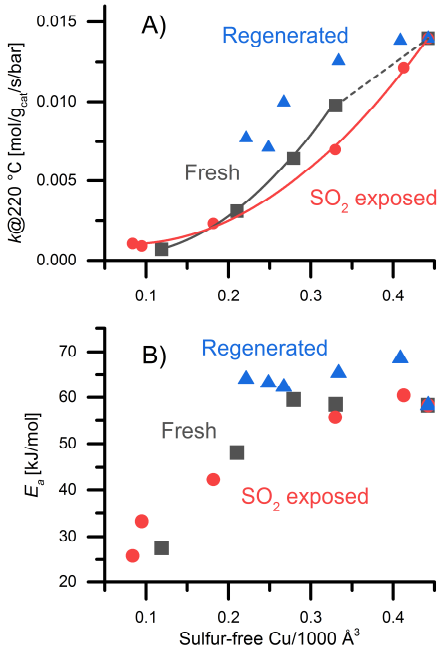

Figure 4 - A) SCR rate constants at 220 °C for the fresh, SO_2 exposed and regenerated catalysts as function of the sulfur-free Cu density, assuming that a single S occupies a single Cu. The black line is a parabolic fit to the 4 fresh catalysts with lowest Cu densities, and the red line is a parabolic fit to all SO_2 exposed catalysts. B) Apparent activation energies for the fresh, SO_2 exposed and regenerated catalysts as function of the sulfur-free Cu density. In both A) and B), the sulfur-free Cu density is calculated from the difference between the total molar Cu content of the fresh catalyst and the molar S content of the deactivated catalysts.

The observed trend in the activation energy for the SO_2 exposed catalysts is similar to that of the sulfur-free catalysts. At Cu densities above 0.3 Cu/1000 Å^3, the activation energy is constant around 65 kJ/mol. Below 0.3 Cu/1000 Å^3, the activation energy gradually decreases to about 30 kJ/mol with Cu density. This indicates that the decrease in activity of the SO_2 exposed catalysts can be explained as a loss of active Cu. The apparent activation energies of the regenerated

catalysts do not show a decrease, but remain at a constant level of about 65 kJ/mol down to 0.22 Cu/1000 Å^3. The change to higher activation energies for the samples with low effective Cu densities, after regeneration, suggests that chemical changes has occurred in the Cu phase, or that certain sites are more affected than others. Although the single site-blocking mechanism does not describe the deactivation to a full extent, it provides a useful framework to assess the deactivation behavior.

EPR results

To address the location of sulfur and possible changes in the Cu phase, catalyst samples were investigated with EPR after SO_2 exposure and regeneration. It has previously been shown that the amount of EPR active Cu in a hydrated and fresh Cu-CHA catalyst sample correlates to the total Cu amount measured by ICP.[28,34,35] The amounts of EPR active Cu in the hydrated fresh, SO_2 exposed and regenerated catalysts were obtained by double integration of the hydrated EPR spectra (not shown). The deviations of total amounts of EPR active Cu in the SO_2 exposed and regenerated catalysts are within the expected error of quantitative EPR results, and we conclude that the SO_2 exposure and subsequent regeneration have no impact on the amount of EPR active Cu in the hydrated catalysts. Therefore, it is assumed that all samples have all Cu present as EPR active Cu^{II} when fully hydrated at room temperature.

In the dehydrated and oxidized state, Cu-CHA contains two principal Cu^{II} sites: one that is charge-balanced by a single framework Al and a hydroxide ion, Z-CuOH, and one that is charge balanced by two framework Al, Z_2-Cu. The EPR spectra of the dehydrated catalysts contain information about the identity and amount of Z_2-Cu sites: After in situ dehydration only the Z_2-Cu sites are EPR active, whereas any Z-CuOH sites formed are EPR silent due to 3-fold coordination around Cu.[29,31] Minority species such as Cu dimers and Cu_xO_y oligomers are also EPR silent due to magnetic coupling between Cu centers.[29,31]

The EPR spectra of the fresh, SO_2 exposed, and regenerated catalysts were recorded after dehydration, and are presented in Figure 5. The total integrated intensity is collected in the two left columns of Table 2. Two sets of quartet hyperfine structure (due to interaction with the $I = 3/2$ Cu nuclei) are easily recognized in the parallel region of the Cu EPR spectrum and reveal the coexistence of at least 2 different Cu species. The hyperfine structure are indicated in Figure 5. All features of the EPR spectra can be simulated assuming two well-resolved Cu^{II} species, A1 and A2, a minority species B and an un-resolved broad species, C. The spin Hamiltonian parameters of each species are determined by simulation in Easyspin [33] and listed in Table 1. The observed species have been identified earlier as follows.[29] The A1 and A2 species are assigned to Z_2-Cu species in which the Cu is located near the 6 membered rings (6mr) of the CHA structure forming 4 bonds to oxygen. The B species are assigned to Cu species forming 5- or 6- bonds. Finally, the C species are assigned to a distribution of non-crystalline Cu^{II} species.[29,31]

From Figure 5 it is seen that the signal from species C (a broad underlying feature) becomes more prominent for samples that have been exposed to SO_2 for longer time. Concurrently, the intensity of the peak related to the A1 species decrease, while the A2 species appears unchanged. A more

detailed analysis using modeling of the EPR spectra is carried out in order to follow the individual species more quantitatively. Therefore, each spectrum was fitted as a linear combination of the 4 species A1, A2, B and C.

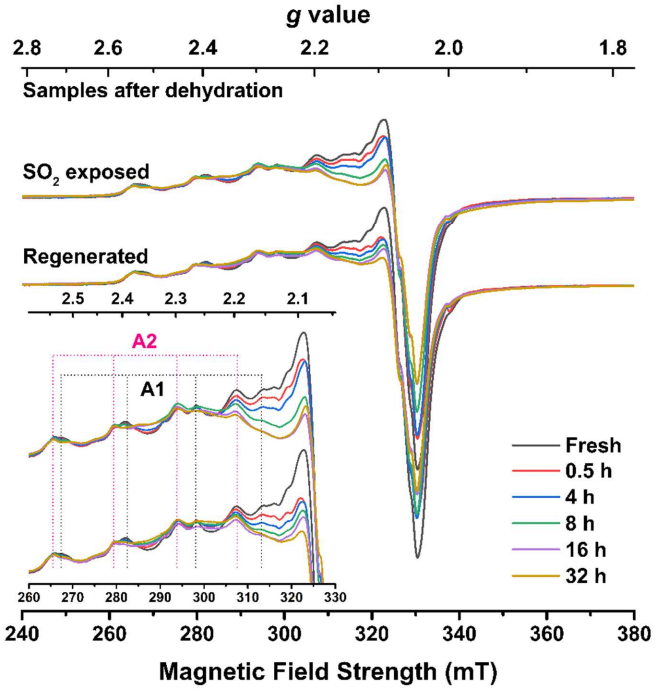

Figure 5 - EPR spectra recorded at 25 ℃ in a flow of He after in-situ dehydration of SO_2 exposed and regenerated Cu-CHA samples. The parallel region of the EPR spectra are expanded in the inset where the quartet hyperfine pattern of the two most well-defined Cu species, A1 and A2 are indicated.

Table 1 - Fitted spin Hamiltonian parameters of different Cu species from the EPR spectra in Figure 5.

Species	**Spin Hamiltonian Parameters**				
	$g_{\parallel}$	$g_{\perp}$	$A_{\parallel}$ (MHz)	$A_{\perp}$* (MHz)	**Line width (FWHM in MHz)**
A1	2.32	2.07	505	45	2.2
A2	2.36	2.07	465	20	1.7-2.8
B	2.26	2.09	490	34	1-2
C	g = 2.16		A = 50		30-42

*These were not well resolved and are based on estimations

The fitted intensity of each Cu^{II} species were related to the corresponding total EPR intensity of the hydrated catalysts that reflect the total Cu content. Thus, the fractions of the four different Cu^{II}

species relative to the total Cu content in each SO_2 exposed and regenerated catalyst were estimated and are listed in Table 2 and graphically displayed in Figure 6.

Table 2 - Intensities of EPR active Cu after dehydration in the fresh, SO_2 exposed and regenerated catalysts. The distributions of EPR active Cu species (A1, A2, B and C) from fittings to the raw EPR spectra after dehydration are also listed.

Sample	EPR intensity after dehydration (%)		Distribution of EPR active Cu* (%)							
	SO_2 exposed	Regenerated	SO_2 exposed				Regenerated			
			A1	A2	B	C	A1	A2	B	C
Fresh	38		13.2	13.8	5.5	5.5				
0.5 h	41	41	14.1	14.7	5.9	5.9	12.0	13.5	4.8	10.7
4 h	42	43	12.6	14.8	5.9	8.9	8.4	14.0	4.2	16.8
8 h	44	44	7.9	13.2	4.0	18.5	7.6	13.6	3.0	19.6
16 h	45	50	4.9	12.4	1.2	26.0	6.2	16.6	2.1	24.9
32 h	58	55	6.7	15.0	1.7	34.9	7.2	16.7	2.4	28.7

*calculated as the amount of Cu in that particular species out of the total Cu content using the amount of EPR active Cu before dehydration.

As seen in Figure 6, the total amount of EPR active Cu in the dehydrated spectra (the sum of the four different Cu^{II} species) increases with SO_2 exposure time, from initially 38% of the total Cu content to about 57%. The amounts of A1 and B species slightly decrease, and the amount of A2 species remains constant. The decrease of A1 and B species occurs in parallel to the increase of the C species. However, the total decrease in A1 and B species, i.e. from approx. 19% to 9%, is less than the increase of C species. Therefore, the increase of C, at least partially, has to arise from EPR silent Cu species becoming EPR active after the exposure to SO_2. This is an indirect indication that SO_2 interacts with the EPR silent Z-CuOH species. This is corroborated by comparing the S/Cu ratios in Figure 2, with the EPR results of the catalysts exposed to SO_2 for 16 and 32 h. The S/Cu ratios are 0.8 while the sulfur-free A1 and A2 Cu species constitute about 20% of the total Cu content, again implying that sulfur is associated with the EPR silent Z-CuOH sites leading to the C species.

The amount of Cu in the Z_2 positions (A1 and A2 combined) decreases with SO_2 exposure time, and stabilize around 8 h of SO_2 exposure. From Figure 2A it can be seen that the S/Cu ratio follows the inverse trend. After regeneration of the catalyst, the S/Cu ratio drops from 0.8 to 0.5, while there are no major changes to the EPR active Cu. This indicates that primarily sulfur associated with the Z-CuOH sites is released during regeneration.

The A2 species in both the SO_2 exposed and regenerated catalysts remain at a constant level of about 15% for all exposure times, indicating that this Cu species is not affected by the SO_2 exposure. This is also consistent with the S/Cu ratio not exceeding 0.8, as seen in Figure 2, and is a possible explanation why a complete deactivation is never observed, even after prolonged SO_2 exposures.[15]

There is an interesting development of the A1 and C species when comparing the SO_2 exposed and regenerated catalysts exposed to SO_2 for 0.5 h and 4 h. The EPR measurements show that the

amount of the A1 species are constant up to 4 h of SO_2 exposure, but after regeneration the amount of A1 species has dropped, which occurs in parallel to an increase of the C species. The corresponding S/Cu ratios measured with ICP (Figure 2) are similar for the SO_2 exposed and regenerated catalysts, implying that sulfur is not removed during regeneration. This indicates that a relocation of sulfur, or Cu,S species, is taking place during regeneration. Such a relocation may also occur during SO_2 exposure, as indicated by the similar amounts of A1 species that are present after 4 h of SO_2 exposure + 5 h of regeneration (effectively 9 h at 550 °C) and after 8 h of SO_2 exposure at 550 °C.

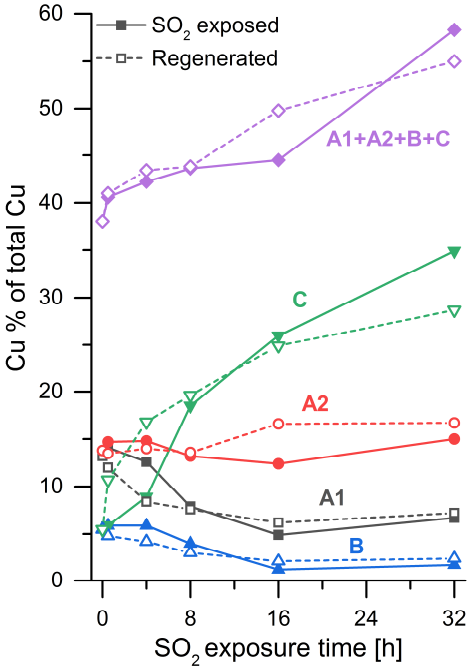

Figure 6 - Fractions of Cu species A1, A2, B and C relative to the total Cu content of the catalysts, plotted as function of the SO_2 exposure time. The values are determined by analysis of the EPR spectra in Figure 5 in the SO_2 exposed (solid lines with full symbols) and regenerated (dashed lines with open symbols) catalysts.

Discussion

In accordance with previous reports,[13–15] the molar S/Cu ratios presented in Figure 2 do not exceed 1. This supports the conclusion that the SO_2 interacts with the Cu sites to form Cu,S species. Density Functional Theory calculations show a clear difference in reactivity of the Z_2-Cu in the 6-membered ring and the Z-CuOH species towards SO_2 and SO_3. According to these calculations, SO_2 and SO_3 form stable Cu,S species on Z-CuOH sites, but do not adsorb on Z_2-Cu in the 6-membered ring.[14] This agrees with our EPR results for the A2 species, which are not influenced by SO_2. The A1 species is also assigned as a Z_2-Cu site, but with another local distribution of Al.

The evidence points to the fact that sulfur interacts to some extent with this species. Also, A1 was previously shown to be more reactive than the A2 species,[30] and this is further demonstrated here. There is the possibility that water plays a role in the interaction of SO_2 with Z_2-Cu and this is enough to activate the A1 species but not the A2 species. Presence of trace water during the SO_2 exposure is likely, and the regeneration was carried out in the presence of water, while the presence of water was not accounted for in the DFT calculations. In line with the DFT calculations, the EPR data also indicate that SO_2 preferably interacts with the Z-CuOH species.

As argued in the results section, a relocation of sulfur or Cu,S species occurs at extended exposure to 550 °C. This relocation appears to be part of a kinetically limited reaction, which leads to more C species, which are argued to be Cu,S that are stable at 550 °C. Such stable Cu,S species in Cu-CHA catalysts are described as certain Cu sulfates.[13–16] Thus, it is plausible that the kinetically limited reaction is an oxidation reaction of SO_2 to SO_3, consistent with TGA measurements,[15] that involves a relocation of sulfur or Cu,S species, and leads to formation of the "irreversible" Cu,S species.

The EPR results presented in Figure 6 shows that the Z_2-Cu sites are largely unaffected by SO_2 exposure and regeneration, constituting about 30% of the total Cu in the fresh catalyst and about 20% after 32 h of SO_2 exposure. Simultaneously, the ICP measurements in Figure 2 reveal that S/Cu ratios as high as 0.8 are reached after SO_2 exposure, which then drops to 0.5 after regeneration. Indirectly, this shows that predominantly the Z-CuOH sites are associated with sulfur after SO_2 exposure, and that the regeneration in SO_2-free gas mainly liberates the Z-CuOH sites from sulfur by desorption or relocation. The concurrent kinetic measurements show that after SO_2 exposure, the apparent activation energies are lowered, and that subsequent regeneration restores the apparent activation energies to the same level as that of the fresh catalyst.

We now put these observations in context with the current understanding of the low-temperature SCR mechanism over Cu-CHA catalysts. The activation energy increases with Cu loading, as shown in Figure 4B. At high Cu loadings and activation energies, the SCR reaction is limited by O_2 dissociation on Cu pairs that are formed by mobile $[Cu(NH_3)_2]^+$ complexes.[5,6,12,36] At low Cu loadings and activation energies, the reaction is limited by the formation of Cu pairs.[5,6] Applying this understanding on the SO_2 exposed catalysts, it suggests that the blocking of Z-CuOH sites by sulfur limits the ability of the catalyst to form Cu pairs. This then leads to the lower activation energies of the SO_2 exposed catalysts and the quadratic dependence of the SCR activity of the SO_2 exposed catalysts on the amount of sulfur-free Cu (Figure 4A). In the regenerated catalysts, where mainly the Z-CuOH sites have released the sulfur, the activation energies are back at the same level as in the fresh catalyst, where O_2 dissociation limits the SCR activity. Therefore, the ability to form Cu pairs appears to be unaffected in the regenerated catalysts, while this ability is noticeably hindered in the SO_2 exposed catalysts with the same exposure to SO_2. This implies that the ability of Cu-CHA catalysts to form Cu pairs depends on the Z-CuOH sites. The observed differences between the impacts of sulfur in the SO_2 exposed and regenerated catalysts, on the overall NH_3-SCR activity, therefore, appear to be linked to the selective deactivation of the Z-CuOH sites and the significance of these sites for Cu pair formation.

Conclusions

The impact of SO_2 on the catalytic performance of a Cu-CHA catalyst in the NH_3-SCR reaction was studied. Exposure of a Cu-CHA catalyst to 100 ppmv SO_2 at 550 °C, for up to 32 h, results in deactivation that increases with exposure time up to a limit of 90%, which is accompanied by a parallel sulfur uptake reaching a maximum S/Cu ratio of 0.8. Consistently, characterization with electron paramagnetic resonance (EPR) spectroscopy showed that certain Z_2-Cu sites, associated with 2 Al centers, were unaffected by sulfur, which added up to about 15% of the total Cu content.

Regeneration at 550 °C in SO_2-free gas lowers the maximum deactivation to 50% and the S/Cu ratio to 0.5. Generally, the impact of sulfur on the activity is higher in the SO_2 exposed catalysts, compared to the regenerated catalysts.

The rate constants and apparent activation energies of the SO_2 exposed catalysts in the NH_3-SCR reaction have a similar dependence on the sulfur-free Cu density as fresh Cu-CHA catalysts with different Cu loadings, indicative of a site-blocking deactivation mechanism.

Parallel measurements with EPR showed that SO_2 mainly interacts with Z-CuOH sites, associated with a single Al center, before regeneration. During regeneration, the Z-CuOH sites are liberated from sulfur by desorption and relocation. The relocation of sulfur or Cu,S species is likely part of the formation of more stable Cu,S species via a kinetically limited oxidation of SO_2.

The preference of sulfur adsorption on Z-CuOH sites before regeneration, and the associated lowering of the apparent activation energy, indicates that the Z-CuOH are more important for Cu pair formation in the Cu-CHA catalysts, compared to Z_2-Cu sites.

References

1 I. Nova and E. Tronconi, *Urea-SCR Technology for deNOx After Treatment of Diesel Exhausts*, Springer-Verlag, New York, 1st ed., 2014.

2 C. Paolucci, J. R. Di Iorio, F. H. Ribeiro, R. Gounder and W. F. Schneider, in *Advances in Catalysis*, Elsevier Inc., 1st edn., 2016, vol. 59, pp. 1–107.

3 F. Gao, J. H. Kwak, J. Szanyi and C. H. F. Peden, *Top. Catal.*, 2013, **56**, 1441–1459.

4 A. M. Beale, F. Gao, I. Lezcano-Gonzalez, C. H. F. Peden and J. Szanyi, *Chem. Soc. Rev.*, 2015, **44**, 7371–7405.

5 C. Paolucci, I. Khurana, A. A. Parekh, S. Li, A. J. Shih, H. Li, J. R. Di Iorio, J. D. Albarracin-Caballero, A. Yezerets, J. T. Miller, W. N. Delgass, F. H. Ribeiro, W. F. Schneider and R. Gounder, *Science*, 2017, **357**, 898–903.

6 F. Gao, D. Mei, Y. Wang, J. Szanyi and C. H. F. Peden, *J. Am. Chem. Soc.*, 2017, **139**, 4935–4942.

7 S. Shwan, M. Skoglundh, L. F. Lundegaard, R. R. Tiruvalam, T. V. W. Janssens, A.

Carlsson and P. N. R. Vennestrøm, *ACS Catal.*, 2015, **5**, 16–19.

8 T. V. W. Janssens, H. Falsig, L. F. Lundegaard, P. N. R. Vennestrøm, S. B. Rasmussen, P. G. Moses, F. Giordanino, E. Borfecchia, K. A. Lomachenko, C. Lamberti, S. Bordiga, A. Godiksen, S. Mossin and P. Beato, *ACS Catal.*, 2015, **5**, 2832–2845.

9 F. Giordanino, E. Borfecchia, K. A. Lomachenko, A. Lazzarini, G. Agostini, E. Gallo, A. V Soldatov, P. Beato, S. Bordiga and C. Lamberti, *J. Phys. Chem. Lett.*, 2014, **5**, 1552–1559.

10 C. Paolucci, A. A. Parekh, I. Khurana, J. R. Di Iorio, H. Li, J. D. A. Caballero, A. J. Shih, T. Anggara, W. N. Delgass, J. T. Miller, F. H. Ribeiro, R. Gounder and W. F. Schneider, *J. Am. Chem. Soc.*, 2016, **138**, 6028–6048.

11 L. Chen, J. Jansson, M. Skoglundh and H. Grönbeck, *J. Phys. Chem. C*, 2016, **120**, 29182–29189.

12 L. Chen, H. Falsig, T. V. W. Janssens and H. Grönbeck, *J. Catal.*, 2018, **358**, 179–186.

13 P. S. Hammershøi, Y. Jangjou, W. S. Epling, A. D. Jensen and T. V. W. Janssens, *Appl. Catal. B Environ.*, 2018, **226**, 38–45.

14 P. S. Hammershøi, P. N. R. Vennestrøm, H. Falsig, A. D. Jensen and T. V. W. Janssens, *Appl. Catal. B Environ.*, 2018, **236**, 377–383.

15 P. S. Hammershøi, A. D. Jensen and T. V. W. Janssens, *Appl. Catal. B Environ.*, 2018, **238**, 104–110.

16 Y. Cheng, C. Lambert, D. H. Kim, J. H. Kwak, S. J. Cho and C. H. F. Peden, *Catal. Today*, 2010, **151**, 266–270.

17 A. Kumar, M. A. Smith, K. Kamasamudram, N. W. Currier, H. An and A. Yezerets, *Catal. Today*, 2014, **231**, 75–82.

18 A. Kumar, M. A. Smith, K. Kamasamudram, N. W. Currier and A. Yezerets, *Catal. Today*, 2016, **267**, 10–16.

19 Y. Jangjou, D. Wang, A. Kumar, J. Li and W. S. Epling, *ACS Catal.*, 2016, **6**, 6612–6622.

20 Y. Jangjou, Q. Do, Y. Gu, L. G. Lim, H. Sun, D. Wang, A. Kumar, J. Li, L. C. Grabow and W. S. Epling, *ACS Catal.*, 2018, **8**, 1325–1337.

21 L. Zhang, D. Wang, Y. Liu, K. Kamasamudram, J. Li and W. Epling, *Appl. Catal. B*, 2014, **156**–**157**, 371–377.

22 K. Wijayanti, K. Leistner, S. Chand, A. Kumar, K. Kamasamudram, N. W. Currier, A. Yezerets and L. Olsson, *Catal. Sci. Technol.*, 2016, **6**, 2565–2579.

23 J. Luo, D. Wang, A. Kumar, J. Li, K. Kamasamudram, N. Currier and A. Yezerets, *Catal.*

Today, 2016, **267**, 3–9.

24 S. Dahlin, C. Lantto, J. Englund, B. Westerberg, F. Regali, M. Skoglundh and L. J. Pettersson, *Catal. Today*, , DOI:10.1016/j.cattod.2018.01.035.

25 C. W. Andersen, M. Bremholm, P. N. R. Vennestrøm, A. B. Blichfeld, L. F. Lundegaard and B. B. Iversen, *IUCrJ*, 2014, **1**, 382–386.

26 C. W. Andersen, E. Borfecchia, M. Bremholm, M. R. V. Jørgensen, P. N. R. Vennestrøm, C. Lamberti, L. F. Lundegaard and B. B. Iversen, *Angew. Chemie - Int. Ed.*, 2017, **56**, 10367–10372.

27 E. Borfecchia, K. A. Lomachenko, F. Giordanino, H. Falsig, P. Beato, A. V Soldatov, S. Bordiga and C. Lamberti, *Chem. Sci.*, 2015, **6**, 548–563.

28 F. Giordanino, P. N. R. Vennestrøm, L. F. Lundegaard, F. N. Stappen, S. Mossin, P. Beato, S. Bordiga and C. Lamberti, *Dalt. Trans.*, 2013, **42**, 12741–12761.

29 A. Godiksen, F. N. Stappen, P. N. R. Vennestrøm, F. Giordanino, S. B. Rasmussen, L. F. Lundegaard and S. Mossin, *J. Phys. Chem. C*, 2014, **118**, 23126–23138.

30 A. Godiksen, O. L. Isaksen, S. B. Rasmussen, P. N. R. Vennestrøm and S. Mossin, *ChemCatChem*, 2018, **10**, 366–370.

31 A. Godiksen, P. N. R. Vennestrøm, S. B. Rasmussen and S. Mossin, *Top. Catal.*, 2017, **60**, 13–29.

32 A. Brückner, *Chem Soc Rev*, 2010, **39**, 4673–4684.

33 S. Stoll and A. Schweiger, *J. Magn. Reson.*, 2006, **178**, 42–55.

34 A. V Kucherov, J. L. Gerlock, H.-W. Jen and M. Shelef, *Zeolites*, 1995, **15**, 15–20.

35 A. V Kucherov, H. G. Karge and R. Schlögl, *Micropor. Mesopor. Mat.*, 1998, **25**, 7–14.

36 L. Chen, H. Falsig, T. V. W. Janssens, J. Jansson, M. Skoglundh and H. Grönbeck, *Catal. Sci. Technol.*, 2018, **8**, 2131–2136.

Chapter 6

Chapter 7

Introducing Temperature-Programmed Reduction with NO as a new characterization of active Cu in Cu-CHA catalysts for NH_3-SCR

Abstract

To measure active Cu in Cu-CHA catalysts for selective catalytic reduction of NO_x with NH_3 (NH_3-SCR), we introduce temperature-programmed reduction with NO (NO-TPR) as a new method. In NO-TPR, the NO consumption is measured in the reduction as it occurs in NH_3-SCR. reaction (NO+NH_3) during reduction of an oxidized Cu-CHA catalyst. The reduction shows NO consumption features at 130 and 230 °C, associated with a Cu-oxide phase and Cu-nitrate phase, respectively. For catalysts with high Cu loadings, the NO consumption at 230 °C is exactly 3 times larger than the Cu content measured with ICP, consistent with the reduction of Cu-nitrate in NH_3-SCR. In catalysts with low Cu loading, not all Cu forms a stable Cu-nitrate. The NH_3-SCR activity appears to be related with the ability to form stable Cu-nitrate. The NO-TPR method was also directly applicable to SO_2 exposed Cu-CHA catalysts after regeneration, while the Cu,S species before regeneration were too unstable to make a consistent measurement.

Introduction

The catalytic properties of chabazite zeolite ion-exchanged with Cu (Cu-CHA) have been studied extensively during the past decade [1–5]. The Cu-CHA typically have a Si/Al ratio in the range 5-20, and the excess charge of the zeolite is compensated by H^+ and Cu ions. The Cu ions have the ability to change the oxidation state between Cu^I and Cu^{II}, dependent on the gas atmosphere and temperature [6], which implies that these ions have specific redox properties that can be exploited for catalysis.

One of the most studied reactions catalyzed by Cu-CHA is the selective catalytic reduction of NO with ammonia in the presence of oxygen (NH_3-SCR) [1–4,7]. For NH_3-SCR, Cu-CHA materials are very efficient and robust catalysts, with both a high activity at around 200 °C, and a high hydrothermal stability up to about 700 °C. These materials are, therefore, well suited for application in automotive diesel exhaust aftertreatment systems, and are already applied today in heavy-duty vehicles. The Cu-CHA catalyst makes it possible to meet the latest requirements (e.g Euro 6/VI) for NO_x (NO and NO_2) emissions from diesel engines [8].

The reduction of NO in the NH_3-SCR reaction follow the reaction $4\ NO + 4\ NH_3 + O_2 \rightarrow 4\ N_2 + 6\ H_2O$; this reaction is often called the 'standard-SCR' reaction. In recent years, significant progress has been made in understanding the reaction mechanism [4,6,7,9–13]. The NH_3-SCR reaction cycle can be performed in steps on Cu-zeolite catalysts, by alternating the oxidation and reduction steps [6,9–11,14,15]. In the reduction step, the Cu starts in the Cu^{II} state and is reduced to Cu^I in a mixture of NO and NH_3, and, dependent on the conditions, a $Cu(NH_3)_2^+$-complex is formed. In the oxidation part, this Cu^I is reoxidized to a Cu^{II} species by a reaction with an NO/O_2 mixture.

The oxidation part of the standard NH_3-SCR reaction involves the dissociation of molecular oxygen, and in the presence of NO, a Cu-nitrate is formed [9,16,17]. According to DFT calculations, molecular oxygen is expected to adsorb exclusively on a Cu^I species [9], which implies that a Cu^{II} species does not contribute to the activation of O_2. The simplest scenario of oxygen dissociation on a Cu ion is then that an oxygen molecule adsorbs on a single Cu ion, where it dissociates. In the presence of NO, this seems a possible reaction path [9,18].

If the O_2 molecule can interact with two Cu^I-ions simultaneously, to form a Cu-O_2-Cu type of species, the dissociation of the O_2 becomes easier [10]. The activation of oxygen over a pair of Cu ions seems to be relevant for the NH_3-SCR reaction at low temperatures [10,11]. Under these reaction conditions, the Cu^I species is present as a linear $Cu(NH_3)_2^+$-complex [6,10,14,19], and DFT calculations indicate that direct dissociation of an O_2 molecule on a single $Cu(NH_3)_2^+$-complex does not occur [11,20]. The observation that the rate of oxidation of $Cu(NH_3)_2^+$-complexes in a CHA zeolite with O_2 shows a second order dependence on Cu-concentration further supports the conclusion that the oxidation of $Cu(NH_3)_2^+$-complexes in a Cu-zeolite involves pairs of $Cu(NH_3)_2^+$-complexes [10,11]. The presence of NO also seems to enhance the activation of O_2 on pairs of bare Cu^I ions or $Cu(NH_3)_2^+$-complexes [20].

An obvious way to form pairs of Cu ions that interact with a single O_2 molecule is by having two Cu ions in positions close enough for a direct interaction with a single O_2 molecule. Since the Cu ions in the ion-exchange positions in a zeolite are linked to the aluminium atoms, the ability to form Cu pairs increases with decreasing Si/Al ratio in the zeolite. This is part of the explanation why Cu-zeolites with a Si/Al ratio in the range 5-20, are generally the preferred catalysts for the NH_3-SCR reaction.

The mobility of the $Cu(NH_3)_2^+$-complex is another way to form the Cu pairs that can activate the O_2 molecule. For Cu-CHA, it has been shown that the $Cu(NH_3)_2^+$-complex has a weak interaction to the zeolite framework [21], and can move up to about 9 Å away from its Si-O-Al anchor point in the zeolite framework [10]. This means that the actual active sites for O_2 activation in NH_3-SCR are formed dynamically under the influence of the NH_3-SCR conditions that are necessary to form the $Cu(NH_3)_2^+$-complex. A consequence is that the NH_3-SCR reaction necessarily follows a different mechanism at temperatures where the mobile $Cu(NH_3)_2^+$ complex is stable and where it is not. This change in the reaction mechanism has been proposed as the reason for the decrease in SCR rate with increasing temperature [9–12,19], which is characteristic for Cu-CHA catalysts and occurs around 300 °C for Cu-CHA catalysts, in good agreement with the measurement of the thermal stability of the $Cu(NH_3)_2^+$-complex [19].

The mobility of the Cu and dynamic formation of the active centers in a Cu-CHA catalyst implies that characterization of the Cu-CHA materials not necessarily gives information that is relevant for the NH_3-SCR reaction. In this chapter, we present temperature-programmed reduction with NO (NO-TPR) as a new method for exploring the reduction and oxidation properties of active Cu in Cu-CHA materials that are relevant for NH_3-SCR. The NO-TPR procedure is based on the ability to perform the NH_3-SCR reaction in alternating oxidation and reduction steps. It has been shown that the reduction of Cu in the NH_3-SCR reaction requires the presence of both NH_3 and NO. By following the consumption of NO under controlled heating, the reduction properties of the Cu in the Cu-CHA catalysts are revealed. Reduction properties of Cu-CHA catalysts have been studied earlier with H_2-TPR [6,22–25], as a method to study the redox properties of Cu-CHA catalysts. Even though the reduction of Cu with H_2 gives some information about the oxidation state of the Cu-CHA materials, and amount of Cu present, these properties cannot necessarily be related to the NH_3-SCR reaction. Since the reduction in a mixture of NO and NH_3 is also part of the NH_3-SCR reaction itself, the reduction as observed in NO-TPR directly reflects the reduction of the active Cu species as it occurs in the NH_3-SCR reaction.

In this chapter, we develop and explore the NO-TPR method in a study of the redox properties for a series of Cu-CHA catalysts with different Cu loadings on the same parent CHA material (Si/Al = 15). The reduction properties of these catalysts are characterized by NO-TPR and we show how the reduction properties of Cu-CHA change with Cu loading. The low-temperature activity at 200 °C of the Cu-CHA catalysts is related to the reduction properties of the Cu-CHA catalysts. Furthermore, the low-temperature activity correlates to the ability of forming stable $Cu(NO_3)$ species, which is affected by the Cu loading. This provides a new possible way of measuring active Cu in Cu-CHA catalysts, as well as a new insight in the NH_3-SCR activity of Cu-CHA catalysts with different Cu loading.

The ability to measure the active Cu, and assess the reduction properties in an SCR related gas composition, is also relevant for studying the deactivation of Cu-CHA catalysts by SO_2. As elaborated in Chapters 2-6, the deactivation by SO_2 is tightly associated with the formation of different Cu,S species. So far, it has only been possible to relate the sulfur in the catalysts to the total Cu content and to the impact on the activity. Important areas for developing a better understanding of the deactivation, is therefore, to ascertain the amount of active Cu sites that are affected by sulfur, and to realize how the sulfur affects the chemistry of the active Cu sites in relation to the SCR reaction mechanism. In this respect, the NO-TPR method could prove a useful tool. Therefore, we also explore the applicability of the NO-TPR method on SO_2-exposed Cu-CHA catalyst before and after regeneration in this chapter. We show that NO-TPR in the current form is directly applicable on the regenerated catalysts, while it still may require adjustments for the sulfated catalysts.

Experimental

NO-TPR: Catalysts

The catalysts used for the development of the NO-TPR method is a series of six Cu-CHA catalysts with Si/Al = 15.1 and a Cu loading ranging from 0.7 to 3.1 wt% Cu. Table 1 gives a more detailed overview of the catalysts. The Cu content, as measured by ICP, was corrected with the measured dry matter content of the catalyst to obtain the Cu content with respect to the amount of dry zeolite. The dry matter content of the catalysts was determined from measurement of the weight loss upon heating to 200 °C, using a Mettler Toledo HX204 moisture analyzer. The Cu/Al ratio is calculated on the basis of the Cu-content on a dry-matter basis and the known Si/Al ratio of 15.1 of the parent material, under the assumption that the Si is present as SiO_2, Al is present as AlO_2H, and Cu is present as CuO. The Cu/Al ratio is then given by

$$\frac{N_{Cu}}{N_{Al}} = \frac{x_{Cu}\left(\frac{N_{Si}}{N_{Al}} M_{SiO_2} + M_{AlO_2H}\right)}{M_{Cu} - x_{Cu} M_{CuO}} \qquad (1)$$

where N_{Si}, N_{Al} and N_{Cu} are the molar amounts of Si, Al, and Cu atoms, x_{Cu} is the weight fraction of Cu on a dry-zeolite basis, and M indicates the molar mass for a unit of SiO_2, AlO_2H, Cu, or CuO.

Table 1 - Measured Cu content by ICP and dry matter content, Si/Al ratio and the corresponding Cu/Al ratio and Cu content on dry matter basis for the catalysts used.

Catalyst	Cu content ICP	Dry matter	Si/Al	Cu/Al	Cu content (dry matter basis)	
	wt%	wt%			wt%	mmol/g
A	0.717	89.7	15.1	0.123	0.799	0.126
B	1.232	90.7	15.1	0.210	1.358	0.214
C	1.629	89.4	15.1	0.284	1.822	0.287
D	1.930	91.9	15.1	0.328	2.100	0.330
E	2.625	91.5	15.1	0.453	2.869	0.451
F	3.142	90.4	15.1	0.554	3.476	0.547

Reactor setup for NH_3-SCR activity and NO-TPR measurements

The NH_3-SCR activity of the Cu-CHA catalysts and NO-TPR measurements were done in a microreactor setup for powder samples, in which the reactor is mounted via a 4-way valve that allows for bypassing the reactor. The concentrations of NO, NO_2, N_2O, H_2O, and NH_3 are monitored with an FTIR spectrometer (Gasmet CX4000) at the reactor outlet; the composition of the feed gas is measured by bypassing the reactor.

For the activity measurement, a 5 mg sample (based on dry matter, sieve fraction 150-300 µm) of the catalysts was filled into a quartz U-tube reactor with an inner diameter of 2 mm. Before starting the measurements, the catalysts were heated at 550 °C in 10% O_2/N_2 for 1 h. Then, the feed gas was changed to 225 Nml/min NH_3-SCR feed gas, consisting of 500 ppm NO, 533 ppm NH_3, 5% water, 10% O_2, and balance nitrogen. The temperature was stepwise lowered to 500, 450, 400, 350, 300, 280, 250, 230, 220, 210, 200, 190, 180, 170, and 160 °C, and at each temperature, the system was allowed to stabilize for 20 min. To evaluate the NH_3-SCR activity, the rate constant for NH_3-SCR at 200 °C is determined from the measured conversion of NO at that temperature, under the assumption that theNH_3-SCR reaction is first order in NO. The rate constant is then given by:

$$k_{200} = \frac{F}{W} \ln(1 - X) \qquad (2)$$

For the NO-TPR measurements, a catalyst powder sample of about 50 or 100 mg on a dry matter basis (150-300 µm sieve fraction) in a quartz U-tube reactor with an inner diameter of 4 mm was used. Various procedures were used for the NO-TPR measurements, which are explained in more detail below.

SO_2-exposed Cu-CHA materials

To determine whether the NO-TPR method can be used to monitor the deactivation of Cu-CHA catalysts by SO_2, the NO-TPR method was applied to some of the SO_2 exposed and regenerated

Cu-CHA catalysts that were made for the investigations of the lifetime impact of SO_2, described in Chapter 5. The specific catalysts that were subjected to NO-TPR are the fresh Cu-CHA (Si/Al = 14.6, ICP: 2.43 wt% Cu), the SO_2 exposed and the regenerated catalyst samples that had been exposed to SO_2 for 1, 5, 15, and 65 h at 300 °C. Detailed information about the SO_2 exposure and regeneration conditions are given in Chapter 5. These catalyst samples were chosen because they contain different amounts of sulfur and show different degrees of deactivation.

NO-TPR Method

It has been shown earlier, that the NH_3-SCR reaction cycle over Cu-zeolite catalysts can be executed by alternating oxidation and reduction steps [9,13]. In the oxidation step, the Cu-zeolite catalyst is exposed to a mixture of NO and O_2, and the Cu is brought into the Cu^{II} oxidation state. Characterization of this Cu^{II} phase by FTIR, XAS, and EPR indicate that a Cu-nitrate species is formed [9,16,17,26,27]. The reduction part of the NH_3-SCR reaction takes place upon exposure of this Cu^{II} state to a mixture of NO and NH_3, and results in the formation of a Cu^{I} state, which is a $Cu(NH_3)_2^+$ complex at sufficiently low temperature [7,11,19]. Reoxidation of the reduced Cu^{I} state with a mixture of NO and O_2 results in the original Cu^{II} state.

The basic idea of the NO-TPR experiments is to exploit the possibility of performing the NH_3-SCR reaction in two steps. In the first part, an oxidized state of the Cu in the catalyst is prepared, which typically, but not necessarily, involves exposure of the catalyst to a mixture of NO and O_2. The reduction step is done by heating the catalyst at a predefined rate in a mixture of NO and NH_3, while following the NO and NH_3 concentrations to give the NO-TPR data. The consumption of NH_3 due to reduction of the Cu is obscured by adsorption and desorption of NH_3 on the zeolite, and hence, it is difficult to obtain reliable quantitative data on the reduction of the Cu from the measured NH_3 consumption. In contrast, NO interacts weakly with the zeolite, and therefore, the reduction of the Cu is clearly observed in the consumption of the NO during reduction.

To ensure a well-defined state of the catalyst in the NO-TPR, the experimental procedure consists of three parts, namely:

1. the preparation of the Cu^{II} state.
2. equilibrating the Cu^{II} state in a mixture of NH_3 and NO at 50 °C, the start temperature for the temperature ramp.
3. heating of the catalyst sample in the mixture of NH_3 and NO to 370 °C with 3°C/min at a flow of 200 Nml/min.

Variations in the preparation of the Cu^{II} state are possible, and this actually affects the final consumption of NO in the NO-TPR. For the NO-TPR data presented here, the exposure to the NO/O_2 mixture is preceeded by a reduction step in NO/NH_3 at 200 °C or by an oxidation in O_2 at 500 °C.

We have chosen to start the reduction at 50 °C, which is the lowest practical temperature that can be achieved in our equipment. Since the NH_3-SCR reaction, and therefore also the reduction in the NO/NH_3 mixture, is already very effective at 200 °C, the reduction must be started at a significantly lower temperature, in order to detect the NO consumption during reduction. To achieve a well-defined and reproducible state of the catalyst before heating the catalyst, the Cu^{II} state is

equilibrated at 50 °C until the adsorption of NH_3 on the zeolite is completed, and the measured concentrations of NO and NH_3 correspond to the inlet concentrations.

Figure 1 gives an overview of the concentrations of NO, NO_2, N_2O, NH_3 and O_2 during the entire procedure for NO-TPR, using 55 mg of catalyst E. The shaded areas indicate the steps in the pretreatment of the catalyst, viz. heating to 500 °C, reduction in NH_3/NO at 200 °C, oxidation in O_2/NO at 50 °C to prepare the Cu^{II} state, exposure to NH_3/NO at 50 °C to equilibrate, and finally the TPR step in NO/NH_3 during heating to 370 °C. Before each step, the reactor was bypassed to mix the feed gas to the appropriate concentration, and to measure the composition of the feed gas at each stage. The analysis of the reduction of the Cu-CHA catalysts is based on the consumption of NO during heating to 370 °C (blue curve in red shaded area).

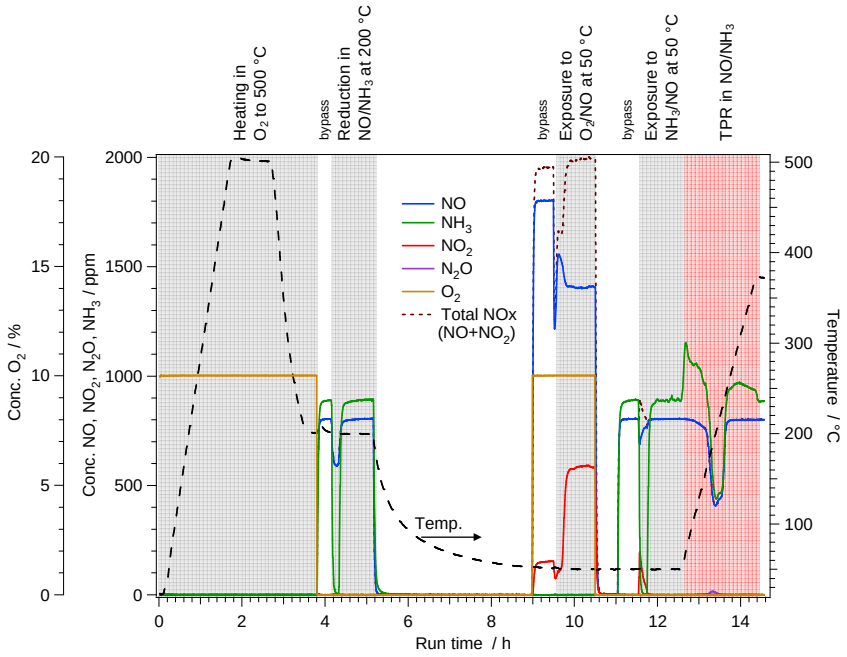

Figure 1 - Concentrations of NO, NH_3, NO_2, N_2O, O_2 and temperature during the entire procedure for an NO-TPR measurement.

Before turning our attention to the analysis of the actual NO-TPR data, we first discuss a few observations that occur during the different reduction and oxidation steps before the actual reduction is done. When the NO/NH_3 mixture is admitted to the reactor at 200 °C in the reduction step, some NO is consumed, indicating that the Cu is in an oxidized state after heating to 500 °C in O_2. Simultaneously, a much larger amount of NH_3 is consumed, even though the reduction of Cu^{II} to Cu^{I} requires equimolar amounts of NO and NH_3. The reasons for the larger consumption

of NH_3, compared to NO, is that additional NH_3 is used for the formation of the linear $Cu(NH_3)_2^+$ complex and that NH_3 adsorbs on the Brønsted sites in the zeolite at 200 °C.

After the reduction at 200 °C, in which the linear $Cu(NH_3)_2^+$ complex is formed, the catalysts are oxidized at 50 °C in a mixture of 2000 ppm NO and 10 % O_2, which yields a Cu^{II}-(N,O) phase. Figure 1 shows that about 60 ppm NO_2 is formed in this mixture while bypassing the reactor, due to the gas phase oxidation of NO that occurs in the mixture. Exposing the reduced catalyst to this NO/O_2 at 50 °C mixture leads to a further oxidation of NO, to yield approximately 160 ppm of NO_2, due to the known oxidation of NO to NO_2 in the confined spaces of the zeolite [28]. For this work, it is important to note that some NO_2 has been present during this oxidation step, but we do not address this formation of NO_2 further. The presence of NO_2 results in a complete oxidation of the $Cu(NH_3)_2^+$ complex, without residual Cu^I phase [10]. Spectroscopic analysis using FTIR, EPR, and XANES has shown that a $Cu(NO_3)$ phase is formed upon oxidation of the $Cu(NH_3)_2^+$-complex with NO_2 or in a mixture of NO and O_2 [9,16,29,30]. We will present further evidence that $Cu(NO_3)$ probably is the major constituent of the Cu^{II}-(N,O) phase formed at 50 °C in this procedure [16].

Finally, before the TPR run can be started, the oxidized Cu^{II}-(N,O) phase must be exposed to the mixture of NO and NH_3 at 50 °C. The ammonia adsorption that occurs under these conditions leads to the delayed breakthrough of the ammonia. Furthermore, a small amount of NO is consumed initially, together with a larger release of NO_2. This shows that at least a part of the Cu^{II}-(N,O) phase reacts with NO and possibly also with NH_3, already at 50 °C, indicating that already at 50 °C, the Cu^{II}-(N,O) species reacts with NH_3 and NO. The release of NO_2, however, is not compatible with a complete NH_3-SCR reaction, which only produces N_2 and H_2O. It may indicate the reaction between a Cu-nitrate species and NO, which can release NO_2 into the gas phase while forming Cu-nitrite; this reaction would not change the oxidation state of the Cu [9].

Results

Figure 2 shows a series of NO-TPR data for the series of Cu-CHA catalysts A-F with different Cu-loading, as specified in Table 1. All data were obtained using the procedure as shown in Figure 1, which means that the Cu^{II}-(N,O) phase is formed in a reaction of Cu^+ (possibly $Cu(NH_3)_2^+$) with the NO/O_2 mixture. The reduction was done by heating to 370 °C at a rate of 3 °C/min in a mixture of 800 ppm NO and 900 ppm NH_3 with 200 Nml/min.

The data in Figure 2 show two distinct temperature ranges for NO consumption for the catalysts with a low Cu loading, with maximum consumptions at around 130 °C and 230 °C. At higher Cu loadings, the NO consumption at around 130 °C is not present, and the peak at 230 °C widens towards the low temperature side, with the maximum NO consumption shifting to just below 200 °C. The disappearance of the NO consumption around 130 °C with increasing Cu loading is highlighted in the right panel of Figure 2, clearly showing the change in the shape of the TPR profile with increasing Cu loading. The total area under the curves increases with Cu loading, which is in line with the expectation that more NO is consumed when more Cu is present. The two distinct regions where NO consumption takes place indicate that there are at least two different forms of oxidized Cu that are reduced in the mixture of NO and NH_3; we designate the Cu species associated with the peak around 130 °C and 230 °C as Cu-*a* and Cu-*b*, respectively.

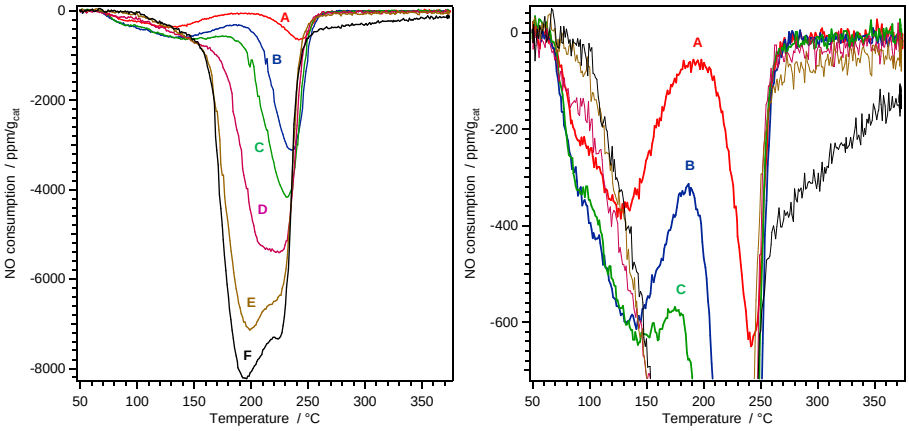

Figure 2 - NO-TPR. Consumption of NO during reduction in 800 ppm NO / 900 ppm NH_3 / N_2 of Cu-CHA catalysts, after reduction in NO/NH_3 at 200 °C and exposure to NO/O_2 at 50 °C. Letters refer to the catalysts listed in Table 1. Right panel is a magnification of the left panel, highlighting the changes in the reduction that takes place around 130 °C.

In the following, we show that Cu-*a* is a Cu^{II} species that does not contain nitrogen, and that Cu-*b* is a Cu(NO_3) species. This assignment is made on the basis of additional NO-TPR measurements, in which the procedure for the formation of the Cu^{II} species has been varied, and a further analysis of the NO-TPR data presented in Figure 2.

The two features corresponding to the Cu-*a* and Cu-*b* species obtained after exposure of the reduced Cu to the O_2/NO mixture on catalyst B are also shown in Figure 3. Furthermore, omitting the exposure to O_2/NO, Figure 3 shows that there is no significant NO consumption over catalyst B. This is expected, since the catalyst has not been oxidized after the initial reduction at 200 °C, leaving the catalyst in the reduced state when performing the NO-TPR measurement.

Figure 3 also presents NO-TPR curves for catalysts B and D, which were measured with and without exposure to the NO/O_2 mixture at 50 °C, after oxidation of the Cu at 500 °C in O_2. The NO-TPR profiles change when an oxidized catalyst is exposed to the NO/O_2 mixture. Heating of the Cu-CHA catalyst to 500 °C in O_2 results in the formation of Cu^{II} species [5,6]. Exposure of this Cu^{II} species to the NO/O_2 mixture at 50 °C results in a peak around 120 °C, and a peak around 230 °C in the NO-TPR profile. At low Cu loadings (catalyst B, 1.35 wt% Cu), the peak at 230 °C remains small, but it becomes clearly visible for catalysts with a higher Cu loading (catalyst D, 2.1 wt% Cu). If the exposure to the NO/O_2 mixture at 50 °C is omitted in these cases, only the peak around 230 °C disappears, while the peak around 130 °C is not affected.

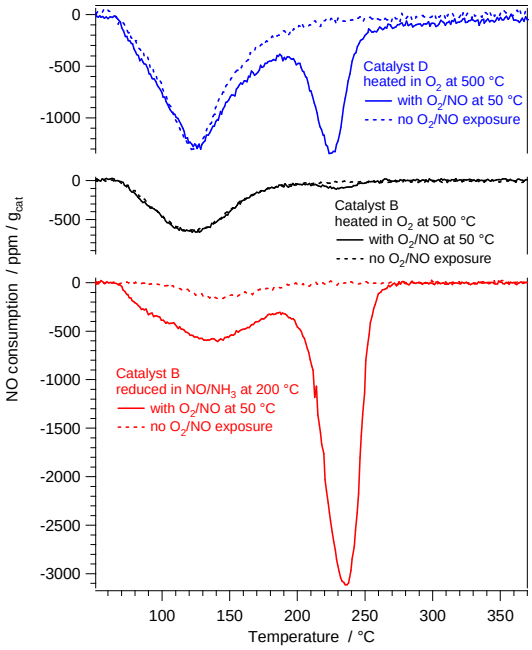

Figure 3 - NO-TPR profiles with and without exposure to the NO/O_2 mixture at 50 °C for oxidized Cu-CHA (catalysts B (black) and D (blue)) and for reduced Cu-CHA (catalyst B (red)) The curves in the panels are drawn to the same scale.

The results shown in Figure 3 lead to several important conclusions:

1. The Cu-*b* species is a nitrogen-containing Cu^{II} species. This is based on the observation that the NO-TPR peak around 230 °C is only observed after oxidation of the catalyst in the NO/O_2 mixture, while it is not present after oxidation in O_2 only.
2. The formation of the Cu-*b* species is enhanced when the NO/O_2 mixture reacts with the reduced Cu^{I} species, probably $Cu(NH_3)_2^+$. This species is formed by reduction in NO/NH_3 at 200 °C. Exposure of oxidized Cu to the NO/O_2 mixture at 50 °C results in a significantly smaller NO-TPR peak around 230 °C, indicating a smaller amount of the Cu-*b* species.
3. The Cu-*a* species is a Cu^{II} species that does not contain nitrogen, since it is present after oxidation in O_2 at 500 °C, and does not require exposure to the NO/O_2 mixture. This result also indicates that the Cu-*a* species does not react with NO alone. The most obvious candidates for the Cu-*a* species are Cu^{II}-oxide or hydroxide species.

We have now established that the Cu-*b* species corresponds to a nitrogen-containing Cu^{II} species. A quantitative analysis of the NO-TPR peak at 230 °C indicates that the nitrogen-containing Cu^{II} species is a $Cu(NO_3)$, as follows. By integration of the NO-TPR data shown in Figure 2, the total consumption of NO in the reduction is determined, and compared with the Cu content in the

catalysts, to obtain the number of NO molecules consumed per Cu atom. Table 2 summarizes these results for the catalysts A-F. We see that the number of consumed NO molecules per Cu atom equals 3 for the catalysts with a higher Cu content (D, E, and F). For the catalysts with a lower Cu-content, the NO/Cu ratio becomes lower. It is noted that precisely the catalysts where the Cu-*a* species is found, are also the catalysts exhibiting NO/Cu ratios lower than 3. A graph of these data is given in Figure 4, showing that the catalysts D, E, and F fall on the dashed line, which indicates the stoichiometric NO/Cu ratio of 3.

Table 2 - Total NO consumption (mmol/g) in NO-TPR of Cu-CHA catalysts and NO/Cu ratio, after exposure of oxidized Cu-CHA catalysts to a mixture of 800 ppm NO and 900 ppm NH_3.

Catalyst	Cu content (dry matter basis)	Total NO consumption TPR	NO/Cu ratio	NO consumption 120 °C (Cu-*a*)	NO consumption 230 °C (Cu-*b*)	Total Cu^{II}*	NOx conversion (200 °C)	SCR rate constant (200 °C)
	mmol/g	mmol/g		mmol/g	mmol/g	mmol/g		10^{-3} mol / g_{cat} s bar
A	0.126	0.129	1.02	0.07	0.059	0.090	0.039	0.92
B	0.214	0.446	2.08	0.13	0.316	0.235	0.104	2.78
C	0.287	0.602	2.10	0.11	0.492	0.274	0.194	4.91
D	0.33	0.990	3.00	0.03	0.96	0.350	0.230	5.98
E	0.451	1.359	3.01	0	1.359	0.453	0.294	8.40
F	0.547	1.630	2.98	0	1.63	0.543	0.316	9.33

* The total amount of Cu^{II} is calculated as the sum of the NO consumption at 120 °C and 1/3 of the consumption at 230 °C.

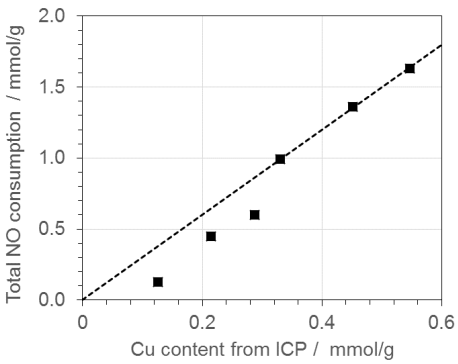

Figure 4 - Total consumption of NO in NO-TPR as a function of the Cu content in Cu-CHA catalysts, after exposure of the reduced state of the Cu-CHA catalysts to a mixture of 800 ppm NO and 900 ppm NH_3. The dashed line corresponds to the stoichiometric ratio NO/Cu of 3.

The stoichiometric NO/Cu ratio of 3 points to the reduction of $Cu(NO_3)$. In an earlier publication, we presented a reaction cycle for NH_3-SCR, in which a $Cu(NO_3)$ species reacts with NO to form a Cu-NO_2 species and an NO_2 (g) molecule, followed by further reduction with NH_3 and NO to Cu^+ [9]. According to that reaction cycle, the net reaction for the reduction of the Z-Cu-(NO_3) can be written as:

$$Z - Cu^{2+} - (NO_3)^- + 3\,NO + 4\,NH_3 \rightarrow\ 4\,N_2\,(g) + 6\,H_2O\,(g) + Z - Cu^+ \quad (3)$$

If we take the formation of the $Cu(NH_3)_2^+$ complex into account, then Eq. (3) is modified to:

$$Z - Cu^{2+} - (NO_3)^- + 3\,NO + 6\,NH_3 \rightarrow\ 4\,N_2\,(g) + 6\,H_2O\,(g) + Z - Cu(NH_3)_2^+ \quad (4)$$

Both equations show that the reduction of a Z-Cu-(NO_3) species in a mixture of NO and NH_3 requires 3 NO molecules per Cu atom. Therefore, the observed consumption of 3 NO molecules per Cu atom indicates that, for the catalysts with a Cu load above 2 wt% (catalysts D,E,F), all Cu is present as $Cu(NO_3)$ species in the NO-TPR measurement. The NO-TPR profile for these catalysts show only the presence of the Cu-*b* species, which therefore can be assigned to a $Cu(NO_3)$ species.

The assignment of the Cu-*b* to $Cu(NO_3)$ is supported by FTIR results for similar Cu-CHA catalysts "CHA15_05" and "CHA15_02" in [16], where a $Cu(NO_3)$ phase is detected after an identical pretreatment. XAS and EPR measurements also indicate that a $Cu(NO_3)$ species is formed in reactions of the $Cu(NH_3)_2^+$ complex with mixtures of NO and O_2 [9]. Furthermore, the NO consumption in a NH_3+NO temperature-programmed selective reduction measurement on a Cu-CHA catalyst with adsorbed nitrates, which is essentially the same as the NO-TPR measurements presented here, shows a consumption of NO that is quite similar to the curves presented here, especially when the nitrate phase is formed at 120 °C [17].

The catalysts with a lower Cu content (catalysts A, B, and C) show the presence of the Cu-*a* species in the NO-TPR profiles (see Figures 2 and 3), which we assign to a Cu^{II}-oxide or hydroxide species. This means that for Cu-CHA catalysts with a lower Cu-loading, not all Cu atoms form a stable $Cu(NO_3)$ species. Since this peak does not correspond to a $Cu(NO_3)$ species, the stoichiometric ratio NO/Cu becomes lower than 3. Starting from a CuO species, which is half of a Cu-O_2-Cu dimeric species, the reduction to $Cu(NH_3)_2^+$ in an NO/NH_3 mixture can be written as follows:

$$CuO + 2\,NO + 4\,NH_3 \rightarrow\ Cu(NH_3)_2^+ + 2\,N_2 + 3\,H_2O \quad (5)$$

The reduction of a Cu-OH species, to $Cu(NH_3)_2^+$ in the NO/NH_3 mixture follows the reaction [6,9,31]:

$$Cu - OH + NO + 3\,NH_3 \rightarrow\ Cu(NH_3)_2^+ + N_2 + 2\,H_2O$$

(6)

This means that the stoichiometric ratio NO/Cu for the reduction of the Cu-*a* species is expected to be between 1 and 2, dependent on the type of Cu-oxide species in the catalyst. In any case, this stoichiometric value lower than 3, is in full agreement with the experimental result (Table 2). Assuming a stoichiometric factor of 1 for the Cu-*a* species, the total amount of Cu^{II} species (see Table 2) matches the Cu content as measured with ICP for all catalysts, except for catalyst A. For catalyst A, the total amount of Cu^{II} from NO-TPR is lower, indicating that either not all Cu has been oxidized, or that there could be another Cu^{II} phase that is not reduced in the mixture of NH_3 and NO up to 370 °C.

To evaluate the catalytic activity of the catalysts A-F, we have measured the NO_x conversion in the temperature range 160-550 °C; the results are shown in the left panel of Figure 5. The first order rate constant for the NH_3-SCR reaction at 200 °C, calculated according to Eq. 1, is used as a measure for the activity. The values for the NO_x conversion and rate constants are also included in Table 2. The development of the rate constants with the total Cu content, as determined by ICP is shown by the red squares in Figure 5, right panel. These data follow the familiar pattern for Cu-CHA catalysts, with a disproportionally low activity for catalysts with low Cu loading [10,11]. This could mean that there exists a critical Cu loading for the low-temperature activity of Cu-CHA catalysts in the NH_3-SCR reaction. There are also indications that the NH_3-SCR activity at low Cu loadings actually is proportional to the square of the Cu-loading, which would also explain this pattern. The latter explanation has led to the conclusion that the NH_3-SCR reaction actually requires pairs of Cu ions, which are formed through diffusion of mobile Cu-$(NH_3)_2^+$ complexes [10,11].

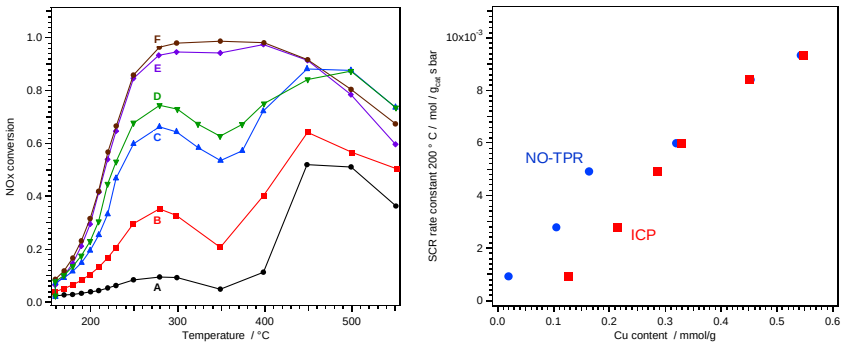

Figure 5 - Left: Measured NO_x conversion for catalysts A-F, (feed gas: 500 ppm NO, 533 ppm NH_3, 5% H_2O, 10% O_2, balance N_2; flow: 225 Nml/min, 5 mg catalyst). Right: NH_3-SCR activity expressed as 1st order rate constants at 200 °C as a function of the total Cu content (ICP, red) and the amount of Cu-b ($Cu(NO_3)$) from NO-TPR (blue).

The NO-TPR results presented above show that the Cu-CHA catalysts with low Cu loading contain both Cu-*a* and Cu-*b* species, while catalysts with a high Cu-loading only have Cu-*b*. Based on this result, it is suggested that only Cu-*b* contributes to the low-temperature activity, implying that only the Cu that is able form $Cu(NO_3)$ contributes to the NH_3-SCR activity. This would explain the

disproportionally low activity of the Cu-CHA catalysts with low Cu loading, since only a fraction of their total Cu loading would be active. To verify this hypothesis, we compare the activity of the Cu-CHA catalysts at 200 °C with respect to the total Cu content of the catalysts (ICP), and with respect to the amount of Cu-*b*. Since it requires 3 NO molecules to reduce a single $Cu(NO_3)$ group, the amount of Cu-*b* is given by 1/3 of the NO consumption in the corresponding NO-TPR peaks, shown in Figure 2. The blue dots in the right panel in Figure 5 show this comparison of the NH_3-SCR activity at 200 °C and the amount of Cu-*b* determined from the NO-TPR measurement. We see, that in the catalysts with low Cu loading, the activity becomes proportional to the amount of Cu-*b*, supporting the hypothesis that only Cu-*b* contributes to the NH_3-SCR activity in these catalysts.

NO-TPR on SO_2-exposed Cu-CHA

The NO-TPR procedure used for the SO_2 exposed and regenerated catalysts is different from those presented above. The first NO-TPR sequence was similar to the procedure shown in Figure 1, except that the reduction step, in the pretreatment, at 200 °C in NO+NH_3 was omitted, which implies that the Cu-nitrate phase is formed by reaction of NO + O_2 at 50 °C with oxidized Cu. The heating ramp during the NO-TPR measurement ended at 270 °C, and the catalyst is then left in the reduced state. The end temperature of 270 °C was chosen to avoid any unwanted regeneration of the SO_2 exposed catalysts. In the second NO-TPR sequence, the reduced catalyst was cooled in 10% O_2, first to 150 °C where it was kept for 1 h, and then further to 50 °C; this procedure leaves the catalyst in the reduced state. From this point on, the sequence is similar to that shown in Figure 1, with a Cu-nitrate formation step and in NO/O_2 followed by the NO-TPR in NO+NH_3.

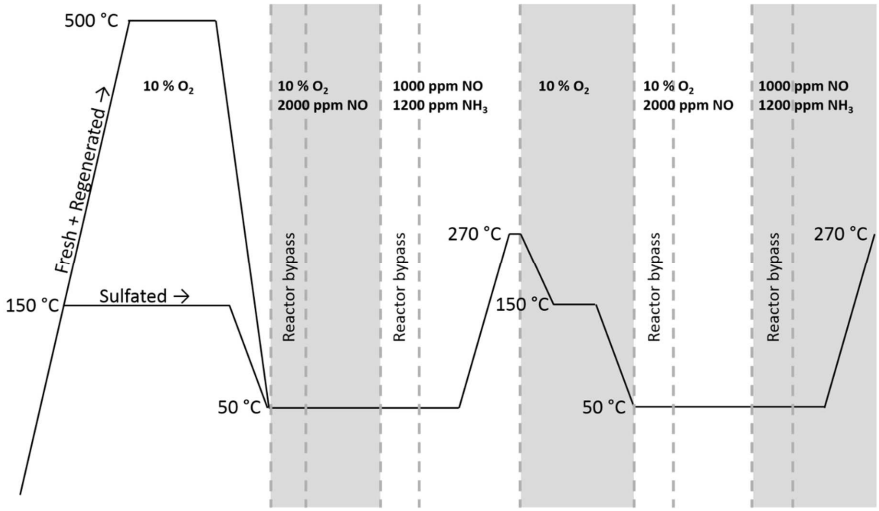

Figure 6 - Schematic illustration of the NO-TPR procedure used on the sulfated and regenerated catalysts, showing the temperature profile (black line) and the employed gas mixtures (white and grey areas). The total flow rate was always 200 Nml/min with N_2 as carrier gas.

An additional change in the NO-TPR procedure was made for the sulfated catalysts due to the thermal stability of the Cu,S species. Therefore, in order to preserve the Cu,S species in the SO_2 exposed catalysts, the initial activation in O_2 was lowered to 150 °C. Since the regenerated catalysts had already been exposed to 550 °C for several hours, the activation at 500 °C was assumed to not to affect the state of the Cu,S species in these catalyst samples.

Since the activity of the Cu-CHA catalysts is related to the NO consumption after exposing the reduced state of the catalyst to the NO/O_2 mixture, only the second NO-TPR measurement of the fresh, SO_2 exposed and regenerated catalysts is considered here, since this procedure is related to Cu-nitrate formation on reduced Cu. The results are summarized in Figure 7. Qualitatively, the trend for both the SO_2 exposed and regenerated catalysts is that the NO consumption peaks becomes smaller with increasing SO_2 exposure time. Table 3 summarizes the total NO consumption found by integration of the NO-TPR peaks, and the relation of the total NO consumption to the Cu content, S content, and measured deactivation.

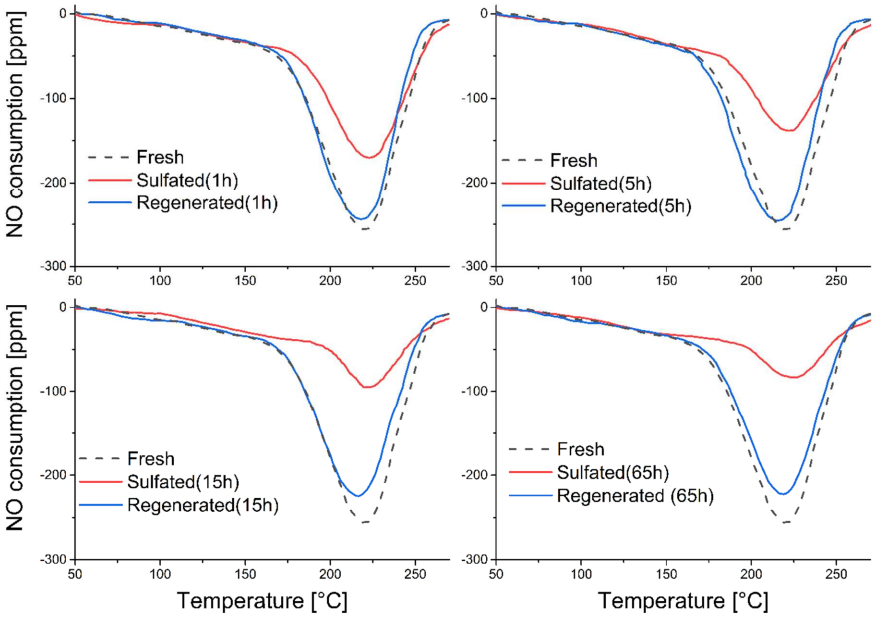

Figure 7 - NO consumption curves for the second NO-TPR sequence of the fresh (black dashed lines), SO_2 exposed (red lines), and regenerated (blue lines) catalysts as functions of the temperature.

The NO consumption in the fresh catalyst corresponds to an active Cu loading of 0.359 mmol/g_{cat}, calculated as 1/3 of the NO consumption. This loading of active Cu in the fresh catalyst accounts for 73% of the total Cu loading measured with ICP (0.494 mmol/g_{cat}).

The amount of active Cu determined from NO-TPR, $Cu_{NO\text{-}TPR}$ loading, in the SO_2 exposed catalysts are in the range 0.109-0.227 mmol/g_{cat}, which overlaps with that of the low Cu loading samples A-C. With this in mind, it is interesting to note that the NO consumption around 130 °C (Cu-*a* species) is not present in the sulfated catalysts (see Figures 2 and 7). This can only be a consequence of the sulfur preventing reduction of the Cu-*a* species.

Table 3 - NO consumption, Cu loading from NO-TPR, S content from ICP and deactivation from SCR activity measurements. The Cu loading for the fresh catalyst as determined by ICP is 0.494 mmol/g_{cat}.

Catalyst	NO consumption	$Cu_{NO\text{-}TPR}$	S/Cu_{ICP}	$S/Cu_{NO\text{-}TPR}$	$Cu_{NO\text{-}TPR} - S_{ICP}$	Deactivation @220 °C
	mmol/g_{cat}	mmol/g_{cat}			mmol/g_{cat}	
Fresh	1.077	0.359	0	0	0.359	0
Sulf(1h)	0.682	0.227	0.37	0.51	0.177	0.73
Sulf(5h)	0.598	0.200	0.56	0.77	0.084	0.79
Sulf(15h)	0.351	0.117	0.94	1.30	-0.107	0.94
Sulf(65)	0.326	0.109	1.02	1.40	-0.145	0.96
Regen(1h)	0.929	0.310	0.09	0.13	0.313	0.12
Regen(5h)	0.924	0.308	0.11	0.14	0.307	0.19
Regen(15h)	0.874	0.291	0.14	0.20	0.287	0.19
Regen(65h)	0.840	0.280	0.16	0.22	0.281	0.21

In the SO_2 exposed and regenerated catalysts, the Cu content does not change, but the uptake of sulfur causes changes to the activity. In Chapters 2-6 it was concluded that the sulfur is associated with the Cu, but so far, it has only been possible to relate the uptake of sulfur to the total Cu content because there was no method available to measure the amount of active Cu. This is now possible with the NO-TPR method.

Under the assumption that a single sulfur species occupies a single Cu site, the remaining active Cu in the SO_2 exposed and regenerated catalysts can be determined in two ways. It can be calculated by subtracting the sulfur content (ICP) from the total active Cu content determined with NO-TPR on the fresh catalyst ($Cu_{NO\text{-}TPR,Fresh} - S_{ICP}$), or it can be measured directly with NO-TPR ($Cu_{NO\text{-}TPR,Sulf/Regen}$). In Figure 8, these two ways of determining the remaining active Cu are compared for the SO_2 exposed and regenerated catalysts by plotting the calculated remaining active Cu against the measured. The grey dashed line is the 1:1 correlation; above this line the amount of measured active Cu is less than anticipated from the sulfur content, and below the measured amount is larger than the calculated. For the regenerated catalysts, the correlation between calculated and measured active Cu falls nicely on the 1:1 line. This suggests that it is possible to measure active Cu in regenerated Cu-CHA catalysts, and corroborates that the deactivation in these catalysts occur via a single site-blocking mechanism.

The SO_2 exposed catalysts are below the 1:1 correlation, indicating that there is more active Cu than expected from the sulfur content measured with ICP. Recalling that the deactivation of the

SO_2 exposed catalysts was disproportionately larger than the S/Cu ratio, it would be expected that the measured active Cu would be less than the calculated, or on the 1:1 line. This indicates that sulfur is not associated with Cu, or that sulfur has been released during the pretreatment. The latter option is consistent with observations of SO_2 desorption around 270 °C during the first NO-TPR sequence. Consistently, such SO_2 desorption was not observed for the regenerated catalysts. The quality of the data was not sufficient for quantification, but qualitatively the SO_2 desorption was largest from the SO_2 exposed catalysts with the longest exposure times. This is consistent with the larger deviation from the 1:1 line of the Sulf(15h) and Sulf(65h) catalysts than the Sulf(1h) and Sulf(5h) catalysts.

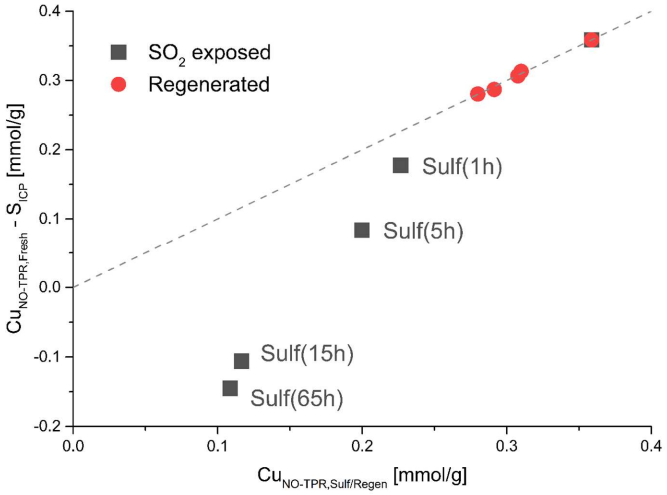

Figure 8 - The calculated active Cu loading assuming 1 S deactivates 1 active Cu, $Cu_{NO\text{-}TPR,Fresh}$ - S_{ICP}, plotted as function of the active Cu loading of the SO_2 exposed (black squares) and regenerated (red dots) catalysts measured with NO-TPR, $Cu_{NO\text{-}TPR,Sulf/Regen}$. The grey dashed line is the 1:1 proportionality line.

For the regenerated catalysts, the deactivation measured in Chapter 5 was slightly higher than the corresponding S/Cu_{ICP} ratios, which is shown by the black squares in Figure 9. The NO-TPR measurement on the fresh catalyst indicated that only 73% of the total Cu loading was active, which may be the reason for the slight offset of the S/Cu_{ICP} from the 1:1 proportionality. Therefore, the S/Cu_{ICP} was corrected for active Cu by dividing by 0.73 to obtain the $S/Cu_{NO\text{-}TPR}$, which are the red dots in Figure 9. As seen, this leads to a better 1:1 correlation between the deactivation and the S/Cu ratio. This emphasizes the applicability of the NO-TPR method for regenerated Cu-CHA catalysts, and the importance of relating sulfur to the active Cu content.

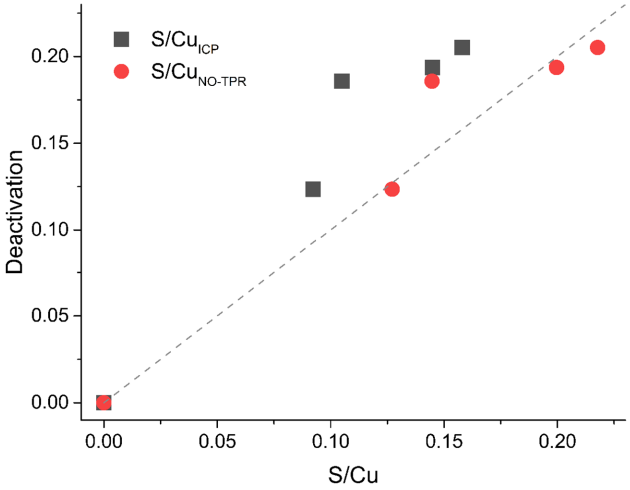

Figure 9 - The deactivation of the regenerated catalysts plotted as function of the S/Cu ratio determined from ICP (black squares) and the S/Cu ratio corrected for active Cu loading as determined from NO-TPR (red dots).

Discussion

The NO-TPR results clearly indicates the presence of two types of Cu in Cu-CHA catalysts, that are distinguished by the reaction product of the oxidation of Cu^+ ($Cu(NH_3)_2^+$) with a mixture of NO and O_2. One type of Cu, Cu-*b*, forms a $Cu(NO_3)$ species, and the other type, Cu-*a*, forms a Cu-oxide or Cu-OH species. If the Cu content is sufficiently high, all Cu in a Cu-CHA catalyst is Cu-*b*, while in catalysts with a lower Cu content, some Cu-*a* is present as well. The NH_3-SCR activity appears to be related to the ability of the Cu-CHA catalyst to form the $Cu(NO_3)$ phase. Since the formation of $Cu(NO_3)$ is enhanced on a reduced Cu-CHA (Figure 3, catalyst B, red curves) containing $Cu(NH_3)_2^+$, it is important that the amount of $Cu(NO_3)$ is measured starting from Cu reduced in $NO+NH_3$.

The reason for the relation between Cu-*b* and the NH_3-SCR activity is that the formation of $Cu(NO_3)$ from Cu^+ or $Cu(NH_3)_2^+$ is part of the NH_3-SCR reaction cycle. In both the formation of $Cu(NO_3)$ and the NH_3-SCR reaction, the dissociation of O_2 on the Cu^+ or $Cu(NH_3)_2^+$ species is an essential step. Dissociation of O_2 on Cu-CHA requires a reduced Cu species, and therefore, the enhanced formation of $Cu(NO_3)$ on reduced Cu shown in Figure 3 is due to a more efficient activation of O_2. This enhanced formation of $Cu(NO_3)$ on reduced Cu-CHA provides additional evidence for the explanation, that the much higher rate of NH_3-SCR, compared to the oxidation of NO to NO_2 on Cu-CHA catalysts, is due to the influence of the oxidation state of the Cu on the dissociation of the O_2. In NH_3-SCR, the dissociation of O_2 takes place on a Cu^I, and it is therefore much more efficient than in NO-oxidation. In NO-oxidation, much less Cu^I, if any, is available, or the dissociation of O_2 takes place on a Cu^{II} phase, and is therefore slower.

The data in Table 2 show that the total amounts of Cu^{II} determined from NO-TPR, assuming a stoichiometric factor NO/Cu-*a* of 1 and NO/Cu-*b* of 3, matches the amounts of Cu found from ICP, suggesting that all Cu is oxidized in the NO-TPR measurements. Recently, it has been shown that in the oxidation of the Cu^{I} species in oxygen, some of the Cu^{I} phase persists, while oxidation in NO_2 leads to a complete oxidation of the Cu^{I} species [10]. Based on this, the conclusion that all Cu has been oxidized in the NO-TPR measurements is probably related to the presence of some NO_2 during the oxidation in the O_2/NO mixture (see Figure 1). This means that at least a part of the Cu^{II} phase in the NO-TPR experiments is formed by a direct reaction between Cu^{I} and NO_2. This means that the oxidic Cu-*a* species in NO-TPR also can be the result of a decomposition of a Cu-(N,O) species, which implies that some Cu in the Cu-CHA catalysts does not form stable $Cu(NO_3)$ or other Cu-(N,O) species. For oxidic Cu species formed by decomposition of Cu-(N,O) species, it can be expected that they do not react with the NO/O_2 mixture, in line with our conclusion for the Cu-*a* species in the NO-TPR measurements. An exception is catalyst A, in which there can be a larger contribution of a CuO phase, according to Eq. (4), or some reduced Cu may be present during the NO-TPR measurement, since there is a difference between the amount of Cu^{II} in NO-TPR and the total amount of Cu found by ICP.

Measurements with EPR also indicate that, at least at low Cu loadings, a part of the visible Cu species are not affected by exposure to NO and O_2, also indicating that not all Cu in Cu-CHA catalysts is able to form stable $Cu(NO_3)$ [32]. The fact that such a Cu species is observed in EPR also means that it is a Cu^{2+} species, since Cu^{+} species are EPR silent. This matches the assignment of the Cu-*a* species well: it must be a Cu^{2+} species, because NO-TPR shows that it can be reduced in the NO/NH_3 mixture, but it is not affected by the exposure to the NO/O_2 mixture. Furthermore, the Cu-*a* species is only observed for the Cu-CHA catalysts with a low Cu content. Therefore, the Cu-*a* species observed in NO-TPR can very well be the same Cu species that does not form a $Cu(NO_3)$ species in EPR.

The dependence of the NH_3-SCR activity at 200 °C on the Cu density, as also shown by the red dots in Figure 5, is divided in two ranges. At high Cu loadings, the activity depends linearly on the total Cu loading. This agrees well with the interpretation of the NO-TPR data, that only the Cu-*b* species contributes to the NH_3-SCR activity, since the amount of $Cu(NO_3)$ formed just corresponds to the Cu-content at higher Cu loadings. At low Cu-loadings, the NH_3-SCR activity becomes disproportionally low, and the data indicate that a critical amount of about 0.1 mmol/g Cu is needed to obtain activity at 200 °C. For low Cu loadings, it has been argued that there is a 2^{nd} order dependence of the NH_3-SCR activity on the Cu loading, which indicates that the NH_3-SCR rate involves the formation of Cu-pairs. The distinction between a critical Cu loading and a 2^{nd} order dependence cannot reliably be made, since it entirely depends on the measured amounts of Cu-*a* and Cu-*b* in a single data point (catalyst C). The NO-TPR data, however, clearly show that the NH_3-SCR activity becomes 0 when the amount of Cu-*b* becomes 0, indicating that the ability to form a stable $Cu(NO_3)$ species is critical for the NH_3-SCR activity of Cu-CHA catalysts.

We note that the relative amount of the Cu-*a* species becomes smaller, and that all Cu is present as a Cu-*b* species at higher Cu loadings, probably with a slightly lower reduction temperature, as indicated by the widening of the NO-TPR peak at the low-temperature edge. This implies that it is possible to transform the inactive Cu-*a* species to a Cu-*b* species by increasing the Cu density.

This suggests that the formation of the Cu-*b* species follows from interaction of two Cu atoms. It is known that the dissociation of an oxygen molecule on a Cu-CHA catalyst becomes easier on a pair of Cu ions [10,18,20], and therefore, pairs of Cu ions are important intermediates for NH_3-SCR. The fact that a $Cu(NH_3)_2^+$ ion is mobile facilitates Cu pair formation, which gives rise to the high SCR activity of Cu-CHA at low temperatures. If we follow the idea that the activation of oxygen is the same for both $Cu(NO_3)$ formation and for NH_3-SCR, then the amount of $Cu(NO_3)$ in NO-TPR should reflect the amount of Cu that can form Cu-pairs. Because formation of Cu-pairs depends on the mobility of the $Cu(NH_3)_2^+$ complex [10], it can be expected that a certain fraction of the Cu is not able to form the Cu-nitrate species, and this fraction becomes smaller as the Cu-density increases. In NO-TPR, we find that the fraction of Cu that is able to form $Cu(NO_3)$ increases with Cu content (see Table 2), which is, at least qualitatively, in agreement with the scenario that $Cu(NO_3)$ formation also proceeds via O_2 activation on Cu pairs.

The fact that a clear reduction is observed in NO-TPR after exposure of a reduced Cu to a mixture of NO and O_2 at 50 °C (Figure 3), means that the oxidation of Cu^I already takes place at that temperature. The reduction associated with the Cu-*b* species, which determines the NH_3-SCR activity, starts at around 150 °C, which is close to the light-off of the NH_3-SCR reaction on Cu-CHA catalysts. This is not consistent with earlier conclusions that the dissociation of oxygen is the rate-limiting step for the NH_3-SCR reaction. It seems that the unavoidable presence of NO_2 in the mixture of NO and O_2 is important here, and that NO_2 facilitates the oxidation of Cu^I, in agreement with the observation that a complete oxidation of Cu is observed in the presence of NO_2. A lower temperature for oxidation of Cu^I with NO_2, compared to the reduction in NO/NH_3, indicates that the NO_2 indeed can enhance the rate of the NH_3-SCR reaction to give the fast-SCR reaction, with a more rate-determining character for the reduction part of the NH_3-SCR reaction [9].

An oxidation of Cu^I with NO_2 would initially lead to a Cu^{II}-NO_2^- species, and the nitrate species is then formed in a second reaction step with NO_2 to release an NO molecule, according to the known nitrite/nitrate equilibrium [17,27,33,34]:

$$Cu - NO_2^- + NO_2\,(g) \leftrightarrow Cu - NO_3^- + NO\,(g) \qquad (7)$$

The NO-TPR data indicate that all Cu is present as a $Cu(NO_3)$ species at high Cu loadings, while at low Cu loadings, the nitrate is not stable on all Cu sites, as also indicated by previous EPR measurements [32]. Apparently, the $Cu(NO_3)$ species can be stabilized by increasing the Cu loading, suggesting that the formation of Cu pairs not only facilitates the dissociation of O_2, but also plays a role in the stabilization of the $Cu(NO_3)$ species. Following the results presented in this chapter, the sites where this stabilization occurs are then also the active sites for NH_3-SCR. The configurations of the Cu, where the $Cu(NO_3)$ species is not stable, cannot be derived from the NO-TPR measurements, but are most probably related to the way Cu is bound to the zeolite (e.g. Z-CuOH vs Z_2-Cu), and the location of the Cu ions in the zeolite (6-ring or 8-ring).

NO-TPR on SO_2-exposed Cu-CHA

The NO-TPR method applied here appeared to be fully applicable on the regenerated catalysts, which is probably due to the stable Cu,S species in these catalysts. This is not the case in the SO_2 exposed catalysts, which is possibly due to the combination of the employed NO-TPR pretreatment

and the less stable Cu,S species in SO_2 exposed catalysts. To accomodate this in the NO-TPR method on the SO_2 exposed catalysts, the O_2 activation at 500 °C was avoided and the NO-TPR measurement was stopped at 270 °C instead of 370 °C. However, some SO_2 desorption was still observed around 270 °C during the first NO-TPR sequence, indicating some unintended loss of sulfur. In Figure 2B (Chapter 3) it can be seen that the SCR activity of an SO_2 exposed catalyst is unaffected by exposure up 300 °C in SCR gas, and in Figure 5A (Chapter 3) the SO_2 desorption from SO_2 exposed Cu-CHA monolith catalysts in a typical SCR reaction gas mixture starts around 270 °C. Furthermore, it has been suggested that the desorption of SO_2 from SO_2 exposed Cu-CHA catalysts is enhanced under more reducing conditions [32], which are closer to the conditions used in the actual NO-TPR measurement. Therefore, it is plausible that the unexpected results of the NO-TPR measurements on the SO_2 exposed catalysts is due to SO_2 desorption during the first NO-TPR sequence. It may be possible to avoid this by carrying out the reduction step at 200 °C, as presented in the general NO-TPR method, but a further development of the NO-TPR method is needed to resolve this.

Conclusions

We have introduced temperature programmed reduction with NO (NO-TPR) as a method to obtain direct and quantitative information about the reduction of Cu^{II} species as it takes place in the NH_3-SCR reaction. In NO-TPR a mixture of NO and NH_3 is used to reduce the Cu^{II} species, and the consumption of NO is measured as a function of the temperature. Since this procedure reflects the reduction part of the NH_3-SCR reaction, the observed reduction profiles are a direct reflection of the relevant reduction properties of Cu for NH_3-SCR.

The NO-TPR procedure consists of three phases, namely (1) the preparation of the Cu^{II} phase, (2) exposure of the Cu^{II} phase to a mixture of NO and NH_3 at the start temperature for the TPR procedure, and (3) the reduction of the Cu^{II} phase in the mixture of NO and NH_3 during controlled heating. The results of the NO-TPR measurement depend on the way the Cu^{II} phase is prepared. The most relevant results for the NH_3-SCR reaction were obtained by first preparing a Cu^{I} phase in a mixture of 800 ppm NO and 900 ppm NH_3 followed by oxidation at 50 °C in a mixture of 2000 ppm NO in 10% O_2/N_2.

The NO-TPR results for series of Cu-CHA catalysts for NH_3-SCR, with different Cu loadings, ranging from 0.7 to 3.0 wt%, on the same parent material (Si/Al = 15), show a distinction between catalysts with a low and high Cu loading. At high Cu loadings, the NO consumption in the NO-TPR takes place between 150 and 250 °C, in a single broad peak with a maximum consumption at around 230 °C. In these cases, the total NO consumption corresponds to exactly 3 times the Cu content in the catalysts, which indicate that all Cu in the catalyst is present as a $Cu(NO_3)$ species. At lower Cu-loadings the reduction occurs in two stages, with a reduction peak around 130 °C, and the $Cu(NO_3)$ species around 230 °C, as also observed at higher Cu loadings. The reduction around 130 °C is due to the formation of a Cu^{II}-oxide or Cu^{II}-hydroxide phase in the zeolite. This means that for at low Cu loadings, not all Cu forms a stable $Cu(NO_3)$ phase at 50 °C.

The low-temperature activity of the Cu-CHA catalysts is related to the amount of stable $Cu(NO_3)$ that is observed in the NO-TPR measurement. For Cu-CHA with a low Cu-loading, this means that a certain fraction of the Cu does not contribute to the low-temperature NH_3-SCR activity; at

higher Cu loadings, all Cu contributes to the NH_3-SCR activity. The $Cu(NO_3)$ phase is apparently stabilized at higher Cu loadings, indicating that Cu-Cu interactions play a role in the formation of the stable $Cu(NO_3)$ phase.

The applicability of the NO-TPR method was also tested on SO_2 exposed and regenerated Cu-CHA catalysts. For the regenerated catalysts, the method appeared to be directly applicable, and lead to an improved relation between sulfur content and deactivation. For the sulfated catalysts, the NO-TPR method should be changed to accommodate the loss of sulfur from less stable Cu,S species.

References

[1] F. Gao, J.H. Kwak, J. Szanyi, C.H.F. Peden, Current Understanding of Cu-Exchanged Chabazite Molecular Sieves for Use as Commercial Diesel Engine DeNOx Catalysts, Top. Catal. 56 (2013) 1441–1459.

[2] A.M. Beale, F. Gao, I. Lezcano-Gonzalez, C.H.F. Peden, J. Szanyi, Recent advances in automotive catalysis for NOx emission control by small-pore microporous materials, Chem. Soc. Rev. 44 (2015) 7371–7405. doi:10.1039/C5CS00108K.

[3] C. Paolucci, J.R. Di Iorio, F.H. Ribeiro, R. Gounder, W.F. Schneider, Catalysis Science of NOx Selective Catalytic Reduction With Ammonia Over Cu-SSZ-13 and Cu-SAPO-34, in: Adv. Catal., 1st ed., Elsevier Inc., 2016: pp. 1–107. doi:10.1016/bs.acat.2016.10.002.

[4] F. Gao, C.H.F. Peden, Recent Progress in Atomic-Level Understanding of Cu/SSZ-13 Selective Catalytic Reduction Catalysts, Catalysts. 8 (2018) 140. doi:10.3390/catal8040140.

[5] E. Borfecchia, K.A. Lomachenko, F. Giordanino, H. Falsig, P. Beato, A. V Soldatov, S. Bordiga, C. Lamberti, Revisiting the nature of Cu sites in the activated Cu-SSZ-13 catalyst for SCR reaction, Chem. Sci. 6 (2015) 548–563. doi:10.1039/c4sc02907k.

[6] C. Paolucci, A.A. Parekh, I. Khurana, J.R. Di Iorio, H. Li, J.D.A. Caballero, A.J. Shih, T. Anggara, W.N. Delgass, J.T. Miller, F.H. Ribeiro, R. Gounder, W.F. Schneider, Catalysis in a Cage: Condition-Dependent Speciation and Dynamics of Exchanged Cu Cations in SSZ-13 Zeolites, J. Am. Chem. Soc. 138 (2016) 6028–6048. doi:10.1021/jacs.6b02651.

[7] E. Borfecchia, P. Beato, S. Svelle, U. Olsbye, C. Lamberti, S. Bordiga, Cu-CHA – a model system for applied selective redox catalysis, Chem. Soc. Rev. (2018). doi:10.1039/C8CS00373D.

[8] The International Council on Clean Transportation, A technical summary of Euro 6/VI vehicle emission standards, 2016.

[9] T.V.W. Janssens, H. Falsig, L.F. Lundegaard, P.N.R. Vennestrøm, S.B. Rasmussen, P.G. Moses, F. Giordanino, E. Borfecchia, K.A. Lomachenko, C. Lamberti, S. Bordiga, A. Godiksen, S. Mossin, P. Beato, A Consistent Reaction Scheme for the Selective Catalytic Reduction of Nitrogen Oxides with Ammonia, ACS Catal. 5 (2015) 2832–2845.

doi:10.1021/cs501673g.

[10] C. Paolucci, I. Khurana, A.A. Parekh, S. Li, A.J. Shih, H. Li, J.R. Di Iorio, J.D. Albarracin-Caballero, A. Yezerets, J.T. Miller, W.N. Delgass, F.H. Ribeiro, W.F. Schneider, R. Gounder, Dynamic multinuclear sites formed by mobilized copper ions in NOx selective catalytic reduction, Science 357 (2017) 898–903. doi:10.1126/science.aan5630.

[11] F. Gao, D. Mei, Y. Wang, J. Szanyi, C.H.F. Peden, Selective Catalytic Reduction over Cu/SSZ-13: Linking Homo- and Heterogeneous Catalysis, J. Am. Chem. Soc. 139 (2017) 4935–4942. doi:10.1021/jacs.7b01128.

[12] F. Gao, E.D. Walter, M. Kollar, Y. Wang, J. Szanyi, C.H.F. Peden, Understanding ammonia selective catalytic reduction kinetics over Cu/SSZ-13 from motion of the Cu ions, J. Catal. 319 (2014) 1–14. doi:10.1016/j.jcat.2014.08.010.

[13] C. Paolucci, A.A. Verma, S.A. Bates, V.F. Kispersky, J.T. Miller, R. Gounder, W.N. Delgass, F.H. Ribeiro, W.F. Schneider, Isolation of the Copper Redox Steps in the Standard Selective Catalytic Reduction on Cu-SSZ-13, Angew. Chem. Int. Ed. 53 (2014) 1–7.

[14] S. Shwan, M. Skoglundh, L.F. Lundegaard, R.R. Tiruvalam, T.V.W. Janssens, A. Carlsson, P.N.R. Vennestrøm, Solid-State Ion-Exchange of Copper into Zeolites Facilitated by Ammonia at Low Temperature, ACS Catal. 5 (2015) 16–19. doi:10.1021/cs5015139.

[15] S. Kieger, G. Delahay, B. Coq, B. Neveu, Selective Catalytic Reduction of Nitric Oxide by Ammonia over Cu-FAU Catalysts in Oxygen-Rich Atmosphere, 183 (1999) 267–280.

[16] C. Negri, P.S. Hammershøi, T.V.W. Janssens, P. Beato, G. Berlier, S. Bordiga, Investigating the Low Temperature Formation of CuII-(N,O) Species on Cu-CHA Zeolites for the Selective Catalytic Reduction of NOx, Chem. - A Eur. J. 24 (2018) 12044–12053. doi:10.1002/chem.201802769.

[17] M. Colombo, I. Nova, E. Tronconi, Detailed kinetic modeling of the NH3-NO/NO2 SCR reactions over a commercial Cu-zeolite catalyst for Diesel exhausts after treatment, Catal. Today. 197 (2012) 243–255. doi:10.1016/j.cattod.2012.09.002.

[18] H. Falsig, P.N.R. Vennestrøm, P.G. Moses, T.V.W. Janssens, Activation of Oxygen and NO in NH3-SCR over Cu-CHA Catalysts Evaluated by Density Functional Theory, Top. Catal. 59 (2016) 861–865. doi:10.1007/s11244-016-0560-8.

[19] K.A. Lomachenko, E. Borfecchia, C. Negri, G. Berlier, C. Lamberti, P. Beato, H. Falsig, S. Bordiga, The Cu-CHA deNOx Catalyst in Action: Temperature-Dependent NH3-Assisted Selective Catalytic Reduction Monitored by Operando XAS and XES, J. Am. Chem. Soc. 138 (2016) 12025–12028. doi:10.1021/jacs.6b06809.

[20] L. Chen, H. Falsig, T.V.W. Janssens, H. Grönbeck, Activation of oxygen on (NH3–Cu–NH3)+ in NH3-SCR over Cu-CHA, J. Catal. 358 (2018) 179–186. doi:10.1016/j.jcat.2017.12.009.

[21] F. Giordanino, E. Borfecchia, K.A. Lomachenko, A. Lazzarini, G. Agostini, E. Gallo, A. V Soldatov, P. Beato, S. Bordiga, C. Lamberti, Interaction of NH3 with Cu-SSZ-13 Catalyst:

A Complementary FTIR, XANES, and XES Study, J. Phys. Chem. Lett. 5 (2014) 1552–1559.

[22] J.H. Kwak, D. Tran, S.D. Burton, J. Szanyi, J.H. Lee, C.H.F. Peden, Effects of hydrothermal aging on NH3-SCR reaction over Cu/zeolites, J. Catal. 287 (2012) 203–209.

[23] J.H. Kwak, H. Zhu, J.H. Lee, C.H.F. Peden, J. Szanyi, Two different cationic positions in Cu-SSZ-13?, Chem. Commun. 48 (2012) 4758–4760.

[24] F. Gao, N.M. Washton, Y. Wang, M. Kollár, J. Szanyi, C.H.F. Peden, Effects of Si/Al ratio on Cu/SSZ-13 NH3-SCR catalysts: Implications for the active Cu species and the roles of Brønsted acidity, J. Catal. 331 (2015) 25–38. doi:10.1016/j.jcat.2015.08.004.

[25] F. Gao, E.D. Walter, E.M. Karp, J. Luo, R.G. Tonkyn, J.H. Kwak, J. Szanyi, C.H.F. Peden, Structure–activity relationships in NH3-SCR over Cu-SSZ-13 as probed by reaction kinetics and EPR studies, J. Catal. 300 (2013) 20–29.

[26] A. Grossale, I. Nova, E. Tronconi, D. Chatterjee, M. Weibel, NH3-NO/NO2 SCR for diesel exhausts aftertreatment: Reactivity, mechanism and kinetic modelling of commercial Fe- and Cu-promoted zeolite catalysts, Top. Catal. 52 (2009) 1837–1841. doi:10.1007/s11244-009-9354-6.

[27] M. Colombo, I. Nova, E. Tronconi, A comparative study of the NH3-SCR reactions over a Cu-zeolite and a Fe-zeolite catalyst, Catal. Today. 151 (2010) 223–230.

[28] J.A. Loiland, R.F. Lobo, Low temperature catalytic NO oxidation over microporous materials, J. Catal. 311 (2014) 412–423. doi:10.1016/j.jcat.2013.12.013.

[29] J.M. Fedeyko, B. Chen, H.-Y. Chen, Mechanistic study of the low temperature activity of transition metal exchanged zeolite SCR catalysts, Catal. Today. 151 (2010) 231–236.

[30] H.-Y. Chen, Z. Wei, M. Kollar, F. Gao, Y. Wang, J. Szanyi, C.H.F. Peden, A comparative study of N2O formation during the selective catalytic reduction of NOx with NH3 on zeolite supported Cu catalysts, J. Catal. 329 (2015) 490–498. doi:10.1016/j.jcat.2015.06.016.

[31] T. Günter, H.W.P. Carvalho, D.E. Doronkin, T. Sheppard, P. Glatzel, A.J. Atkins, J. Rudolph, C.R. Jacob, M. Casapu, J.D. Grunwaldt, Structural snapshots of the SCR reaction mechanism on Cu-SSZ-13, Chem. Commun. 51 (2015) 9227–9230. doi:10.1039/c5cc01758k.

[32] A. Godiksen, O.L. Isaksen, S.B. Rasmussen, P.N.R. Vennestrøm, S. Mossin, Site-Specific Reactivity of Copper Chabazite Zeolites with Nitric Oxide, Ammonia, and Oxygen, ChemCatChem. 10 (2018) 366–370. doi:10.1002/cctc.201701357.

[33] D. Wang, L. Zhang, K. Kamasamudram, W.S. Epling, In Situ-DRIFTS Study of Selective Catalytic Reduction of NOx by NH 3 over Cu-Exchanged SAPO-34, ACS Catal. 3 (2013) 871–881. doi:10.1021/cs300843k.

[34] C. Tyrsted, E. Borfecchia, G. Berlier, K.A. Lomachenko, C. Lamberti, S. Bordiga, P.N.R. Vennestrøm, T.V.W. Janssens, H. Falsig, P. Beato, A. Puig-Molina, Nitrate-nitrite

equilibrium in the reaction of NO with a Cu-CHA catalyst for NH3-SCR, Catal. Sci. Technol. 6 (2016) 8314–8324. doi:10.1039/c6cy01820c.

Chapter 7

Chapter 8

Summary, conclusions and future perspectives

Summary and Conclusions

The important task of efficiently removing NO_x from diesel exhaust of heavy-duty vehicles is improved by the use of Cu-CHA NH_3-SCR catalysts. However, the presence of SO_2 in diesel exhaust significantly deactivates Cu-CHA catalysts, and thereby diminish their ability to remove NO_x. With the motivation of developing robust Cu-CHA catalysts to ensure the efficient removal of NO_x, a solid fundamental understanding of the deactivation behavior of Cu-CHA catalysts by SO_2 was obtained. Supported by this fundamental understanding, it was concluded that the impact of SO_2 over the lifetime of the catalyst is not prohibitive for practical application. The anchor of the investigations was the assessment of the impact of different SO_2 treatments on the performance of the catalysts in the NH_3-SCR reaction, further supported by several characterization techniques.

As Cu-CHA catalysts are exposed to SO_2, particularly the low-temperature SCR activity of the catalysts is affected. It has been established that the deactivation of Cu-CHA catalysts by SO_2 is a consequence of chemical interactions between SO_2 and Cu sites, leading to formation of various Cu,S species. Consistently, the S/Cu ratios after exposure of Cu-CHA catalysts to SO_2 or mixtures of SO_2 and SO_3, never exceeds 1 in any of the experiments conducted during this PhD work. This indicates that SO_2 selectively interacts with Cu sites in the catalysts, and precipitation of ammonium sulfate is not considered responsible for the deactivation of Cu-CHA catalysts by SO_2. The direct Cu,S interactions also mean that the chemical composition of the zeolite framework ($H_nAl_nSi_{1-n}O_2$ vs $H_nSi_nAlP_{1-n}O_4$), has little impact on the deactivation behavior.

The affinity of SO_2 for Cu depends on the oxidation state of Cu. SO_2 adsorbs more stably on Cu^I than on Cu^{II}, while SO_3 has a higher affinity for Cu^{II} than for Cu^I. In the relevant temperature interval for SCR in heavy-duty vehicles (180-550 °C), SO_3 is formed via oxidation of SO_2. The rate of the oxidation increases with temperature to such an extent that the effect of admitting SO_3 together with SO_2 is only measurable at lower temperatures. Furthermore, since the presence of NO and NH_3 determines the oxidation state of the Cu, the effect of SO_x and the formation of Cu,S species also depend on the reaction conditions.

In Cu-CHA catalysts, the main Cu^{II} sites are Z-CuOH and Z_2-Cu, which are Cu charge-balancing one or two framework Al atoms, respectively. SO_2 and SO_3 mainly interacts with the Z-CuOH sites, while certain Z_2-Cu sites are unaffected by SO_x. The SO_2 resistant Z_2-Cu sites are conceivably the reason why a 100% deactivation of the low-temperature activity has not been observed.

During exposure to SO_2 concentrations as low as 1.5 ppmv, Cu,S species are primarily formed on the Z-CuOH sites. The majority of the formed Cu,S species are unstable at 550 °C, and these Cu,S species are denoted reversible. Heating to 550 °C in SO_2-free gas for minimum 4 h liberates the Z-CuOH sites fully from the reversible Cu,S species. The decomposition of the reversible Cu,S species begins close to 300 °C.

In parallel to the formation of the reversible Cu,S species, a more thermally stable Cu sulfate (denoted irreversible) is also formed, which has a decomposition temperature around 650 °C.

Hence, a full restoration of the low-temperature activity can be achieved by heating to 700 °C. Formation of the irreversible Cu sulfate appears to occur via a kinetically limited reaction that is enhanced by the presence of H_2O. The formation involves a relocation of sulfur from Z-CuOH sites to certain Z_2-Cu sites, and chemical changes to the Cu,S species on Z-CuOH sites. The irreversible Cu sulfate is only formed on a restricted fraction of the total Cu content.

Both the reversible and irreversible Cu,S species are suggested to deactivate Cu-CHA catalysts by a single site-blocking mechanism. However, the reversible and irreversible Cu,S species have significantly different impacts on the low-temperature SCR activity of Cu-CHA catalysts. Comparing the deactivation with the amount of Cu,S species in the catalyst, the reversible Cu,S species induces a disproportionately large deactivation for a single site-blocking mechanism. In contrast, the irreversible Cu,S species causes a 1:1 correlation between the deactivation and S/Cu ratio. Furthermore, the reversible Cu,S species leads to a change in the apparent activation energy for NH_3-SCR, whereas the apparent activation energy is unaffected by the irreversible Cu,S species. These different impacts are explained by a more significant contribution of the Z-CuOH sites than the Z_2-Cu sites to Cu pair formation that is important for the low-temperature SCR activity of Cu-CHA catalysts.

The deactivation of Cu-CHA catalysts by SO_2, appears to depend on the total SO_2 exposure, which is calculated as the product of the SO_2 concentration and the exposure time. It implies that the formation rate of the deactivating Cu,S species has a similar dependence on the exposure conditions. This dependency can be exploited to estimate the development and impact of Cu,S species via accelerated SO_2 exposures with higher SO_2 concentrations. During SO_2 exposures similar to those expected within the full lifetime of a Cu-CHA catalyst in a heavy-duty vehicle aftertreatment system, the formation of reversible Cu,S species occurs fast. The formation rate has a volcano-like dependence on the exposure temperature. Within the range 200-500 °C, the fastest formation rates are at intermediate temperatures of 300-400 °C. Despite this influence of exposure temperature, S/Cu ratios 0.5 are reached for all exposure temperatures within the first 13% of the lifetime SO_2 exposure. Due to the disproportionately large impact of the reversible Cu,S species on the low-temperature activity, the deactivation builds up even faster than the reversible Cu,S species. Thus, deactivation levels of at least 80% for all exposure temperatures, are reached already within 5% of the lifetime SO_2 exposure. The formation of irreversible Cu sulfate is similarly fast, but restricted to a minor fraction of Cu. This is regardless of exposure time and independent of the exposure temperature, which is likely a consequence of the similar regeneration treatments at 550 °C that all catalyst samples were exposed to before measurement of the irreversible Cu sulfate amounts. The deactivation by the irreversible Cu sulfate is therefore, restricted to about 30% throughout the lifetime SO_2 exposure.

In terms of the applicability of Cu-CHA catalysts in exhaust aftertreatment systems of heavy-duty vehicles, the results presented in this thesis show that the significant impact of low concentrations of SO_2 on the low-temperature activity is a present issue. Therefore, Cu-CHA catalysts are best employed when diesel with low sulfur content, as in ultra-low sulfur diesel, is used as fuel. Despite the use of ultra-low sulfur diesel, deactivation occurs fast, and hence, application of Cu-CHA catalysts are contingent on effective regeneration strategies in order to maintain efficient use of the catalysts' good low-temperature activity. The potential impact of SO_3 exposure, formed via

SO_2 oxidation on upstream aftertreatment components, appears only to be concern at low temperatures. However, under SCR conditions at low temperature, a significant fraction of Cu will be present as Cu^I on which SO_2 adsorbs more stably, and therefore, the impact of SO_3 may also be of little importance at low temperatures.

Finally, temperature programmed reduction of NO (NO-TPR) has been developed as a new method to measure the active amount of Cu in Cu-CHA catalysts in NH_3-SCR. The NH_3-SCR activity depends on the ability of the Cu-CHA catalysts to form a stable Cu-nitrate species. Initial explorative tests of the NO-TPR method on SO_2 exposed Cu-CHA catalysts indicate that the irreversible deactivation that remains after regeneration at 550 °C, most likely caused by the formation of Cu sulfate, can be monitored by the NO-TPR method. For the SO_2 exposed samples, the method needs to be developed further, since the changes to the reversible Cu,S phases and the interactions with the ammonia and NO in the reduction are not well understood yet.

Future perspectives

The use of Cu-CHA catalysts for NH_3-SCR is especially promoted by their better activity in the low-temperature region for SCR in automotive aftertreatment systems, compared to other SCR catalysts. Maintaining the better low-temperature activity in the presence of SO_2 is contingent on efficient regeneration. In this work regeneration has typically been carried out for at least 4 h at 550 °C in SO_2-free gas, to achieve the maximum possible regeneration at 550 °C. However, these regeneration conditions are unrealistic in an actual aftertreatment system. Therefore, several topics within regeneration should be explored to establish how efficiently regeneration in aftertreatment systems can be carried out. The first topic, which may be the most important, is to identify the "critical" SO_2 concentration for regeneration. As shown in this thesis, even at 500 °C the deactivation builds up in the presence of 1.5 ppmv SO_2, but is lowered in SO_2-free gas. This means that somewhere in the SO_2 concentration range 0-1.5 ppmv, there is a critical concentration of SO_2 where regeneration occurs, which would be an important parameter for developing regeneration strategies. It is possible that this concentration is lower than what is practically achievable, and hence, other approaches for efficient regeneration should be explored. Furthermore, as engine operating temperatures are generally lowered, thermal regeneration may not be an option in the future. An alternative approach could be to increase the reduction properties of the exhaust gas, since there are indications that more reducing gas atmospheres promote the decomposition of deactivating Cu,S species. This could potentially be achieved by tuning the concentrations of O_2, CO or NH_3, but requires further investigations.

The results presented in this work strongly points to a certain influence of the coordination environment of Cu on the stability of the formed Cu,S species, and some Cu sites even appeared to be entirely inert to SO_2 exposure. Therefore, an increased understanding of how the zeolite structure, and the Al-distribution, affects the Cu,S interactions would be beneficial for developing and tailoring more SO_2 resistant Cu-zeolite catalysts. This may be realized either by controlling the locations of Al or by employing other zeolite structures.

Appendices

Appendix A

Supporting information to:

Reversible and irreversible deactivation of Cu-CHA NH_3-SCR catalysts by SO_2 and SO_3

Peter S. Hammershøi[a,b], Yasser Jangjou[c,d], William S. Epling[c,d], Anker D. Jensen[b], Ton V.W. Janssens[a,*]

[a]*Haldor Topsøe A/S, Haldor Topsøe's Allé 1, 2800 Kgs. Lyngby, Denmark*
[b]*Department of Chemical and Biochemical Engineering, Technical University of Denmark, Søltofts Plads B229, 2800 Kgs. Lyngby, Denmark*
[c]*Department of Chemical and Biomolecular Engineering, University of Houston, 4800 Calhoun Rd., Houston, TX 77204-4004, United States*
[d]*Department of Chemical Engineering, University of Virginia, 102 Engineers' Way, Charlottesville, VA 22904-4741*
**Corresponding author. Tel. +45 22 75 46 22, e-mail address: tvj@topsoe.com*

Appendix A

Monolith experiments - NO_x conversion data and Arrhenius plots of fresh, sulfated and regenerated catalysts

Steady state NO_x conversions were measured on 8 samples of the same Cu-CHA/cordierite monolith catalyst, which were exposed to 8 different SO_x treatments. The measured NO_x conversions of fresh, sulfated and regenerated states of the tested catalysts are shown as functions of temperature in Figure S1 and the corresponding data points are listed in Table S1 below.

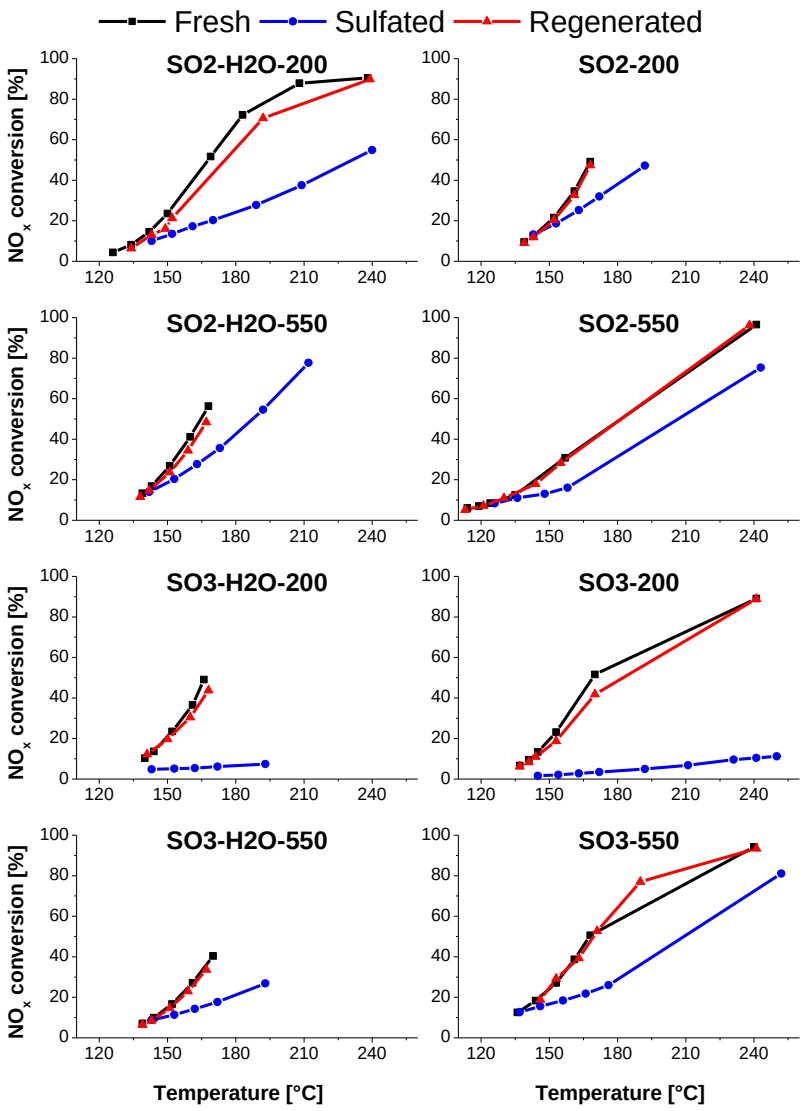

Figure S1 – Steady state NO_x conversions as functions of temperature for Cu-CHA catalysts in their fresh, sulfated and regenerated states. The SO_x treatment conditions are displayed in each plot. The regeneration conditions were the same for all catalysts, i.e. heating to 550 °C for 4 h in SCR gas.

Appendix A

Table S1 – Data for measured NO_x conversions of fresh, sulfated and regenerated states of the catalysts.

SO_x treatment	**Fresh**		**Sulfated**		**Regenerated**	
	Temperature [°C]	NO_x conversion	Temperature [°C]	NO_x conversion	Temperature [°C]	NO_x conversion
SO2-H2O-200	126	0.043	143	0.101	134	0.064
	134	0.082	152	0.135	143	0.132
	142	0.145	161	0.172	149	0.161
	150	0.236	170	0.203	152	0.213
	169	0.517	189	0.277	192	0.706
	183	0.722	209	0.375		
	208	0.879				
SO2-200	139	0.095	143	0.132	139	0.091
	143	0.125	153	0.187	143	0.119
	152	0.216	163	0.253	152	0.204
	161	0.346	172	0.320	161	0.326
	168	0.491	192	0.472	168	0.474
SO2-H2O-550	139	0.133	142	0.140	138	0.116
	143	0.169	153	0.204	142	0.147
	151	0.269	163	0.277	151	0.236
	160	0.411	173	0.356	159	0.344
	168	0.563	192	0.545	167	0.484
			212	0.777		
SO2-550	114	0.061	126	0.084	113	0.051
	119	0.070	136	0.110	121	0.072
	124	0.084	148	0.131	130	0.110
	135	0.124	158	0.161	144	0.179
	157	0.308	243	0.753	155	0.283
	241	0.966			238	0.962
SO3-H2O-200	140	0.103	143	0.048	141	0.122
	144	0.136	153	0.052	150	0.197
	152	0.235	162	0.054	160	0.305
	161	0.365	172	0.062	168	0.438
	166	0.490	193	0.074		
SO3-200	137	0.066	145	0.016	137	0.062
	141	0.095	154	0.021	141	0.084
	145	0.134	163	0.028	144	0.111
	153	0.232	172	0.035	153	0.188
	170	0.516	192	0.050	170	0.418
	241	0.890	211	0.068	241	0.889
			231	0.096		
			241	0.105		
			250	0.112		
SO3-H2O-550	139	0.071	143	0.088	139	0.065
	144	0.099	153	0.114	143	0.085
	152	0.167	162	0.143	151	0.147
	161	0.272	172	0.177	159	0.230
	170	0.404	193	0.269	167	0.337
SO3-550	136	0.125	137	0.127	146	0.189
	144	0.183	146	0.156	153	0.292
	153	0.271	156	0.184	163	0.393
	161	0.388	166	0.218	171	0.527
	168	0.506	176	0.260	190	0.770
	240	0.942	252	0.811	241	0.934

Appendix A

Based on the measured steady state NO_x conversions of the tested catalysts, rate constants were calculated in order to make Arrhenius plots. For the elaboration of the Arrhenius plots, the rate constants for NO_x conversions below 70 % for the fresh and regenerated states of each of the catalysts, were first combined to determine a common slope. Thereafter, the intersect was determined individually for the fresh and regenerated states of the catalysts with fixed slopes. The slopes and intersects of the sulfated states of the catalysts were determined simultaneously. The resulting Arrhenius plots for the fresh, sulfated and regenerated states of the tested catalysts are shown in Figure S2.

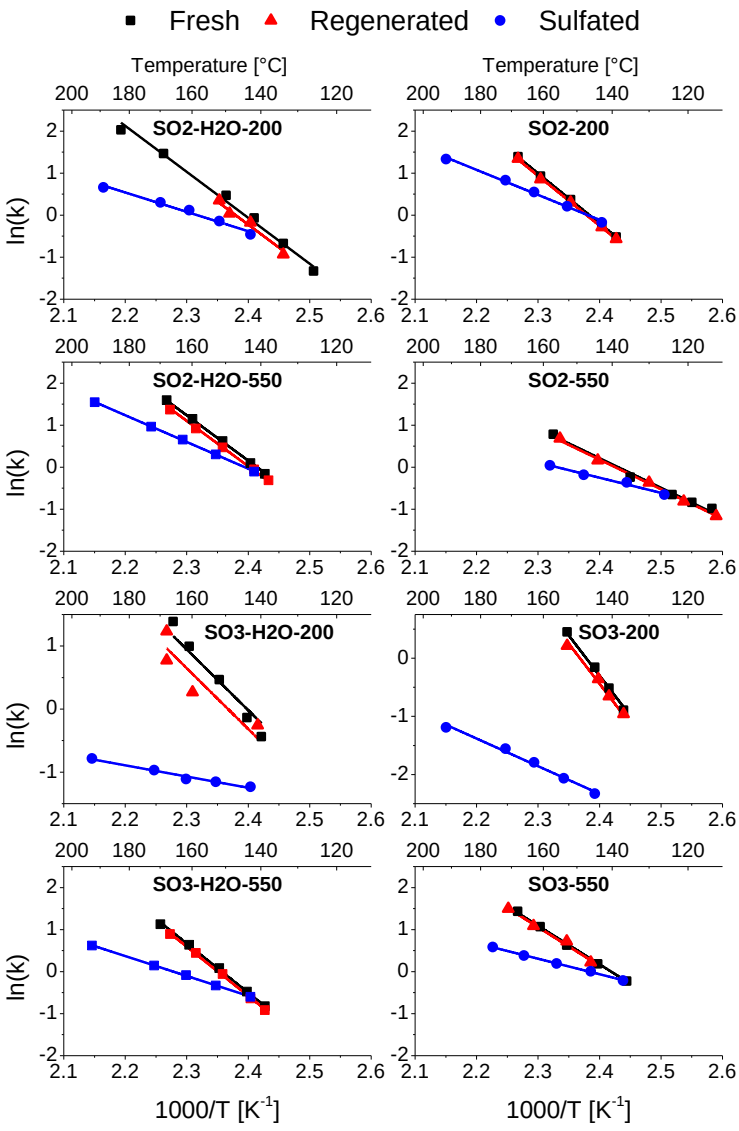

Figure S2 – Arrhenius plots of fresh, sulfated and regenerated states of al tested catalysts.

Desorption of SO_2 – detailed SO_2 desorption plots

During heating for regeneration at 550 °C in SCR gas and during heating to 900 °C in N_2, SO_2 desorbed from the catalysts, and the outlet concentration of SO_2 was measured, which is plotted in Figure S3 and Figure S4.

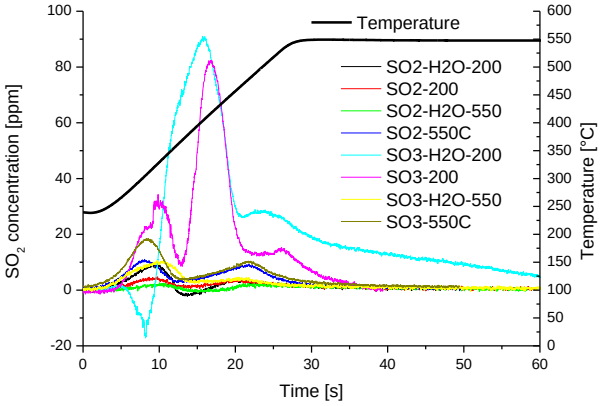

Figure S3 – SO_2 desorption from SO_x exposed catalysts during heating to 550 °C for regeneration in SCR gas.

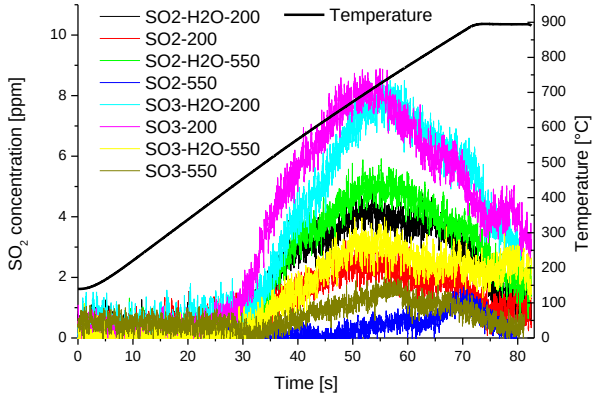

Figure S4 – SO_2 desorption from regenerated catalysts during heating to 900 °C in N_2.

Appendix A

Discussion – calculations for determination of the internal effectiveness factor

In order to assess if internal diffusion limitations can be responsible for the drop in activity that is observed after exposure to SO_2, the internal effectiveness factor, η, is calculated. For a first order reaction in a spherical crystal the internal effectiveness factor can be expressed as a function of the Thiele modulus, ϕ, as shown in Eq. (S1) [1].

$$\eta = \frac{3}{\phi^2}\left(\frac{\phi}{\tanh(\phi)} - 1\right) \tag{S1}$$

For a first order reaction, the Thiele modulus can be expressed by a relation between the crystal radius, R, the intrinsic volume based rate constant, k_V, and the effective diffusion coefficient, D_{eff}, which is shown in Eq. (S2) [1]. The volume based rate constant is obtained by multiplying the catalyst weight based rate constant by $22.4 \cdot 10^{-3}\,\mathrm{m^3/mol}$ and by the density of the catalyst, $\rho_{cat} = 1544 \cdot 10^3\,\mathrm{g/m^3}$, which has been calculated based on the CHA framework density and the Cu-loading of the catalyst.

$$\phi = R\sqrt{\frac{k_V}{D_{eff}}} = R\sqrt{\frac{k \cdot 22.4\frac{\mathrm{L}}{\mathrm{mol}} \cdot \rho_{cat}}{D_{eff}}} \tag{S2}$$

The crystal radius is approximately $0.5 \cdot 10^{-6}$ m, as verified with scanning electron microscopy. The rate constant at 183 °C for the fresh state of the catalyst before exposure to SO_2 at 200 °C with H_2O present is used in the calculations for the intrinsic rate constant, which is 390 s^{-1}. Effective diffusion coefficients of NH_3 in a Cu-CHA catalyst have been measured with quasielastic neutron scattering at 0, 50 and 100 °C [2]. Using the activation energy for the diffusion (4.4 kJ mol^{-1}) [2], extrapolation of the experimental diffusion coefficients to 180 °C has been done to obtain the value $1.2 \cdot 10^{-9}$ m^2 s^{-1}, for the effective diffusion coefficient used here to calculate the effectiveness factor for the fresh Cu-CHA catalyst.

References

[1] H.S. Fogler, Elements of Chemical Reaction Engineering, 4th ed., Pearson Education, Massachusetts, USA, 2010.

[2] A.J. O'Malley, I. Hitchcock, M. Sarwar, I.P. Silverwood, S. Hindocha, C.R.A. Catlow, et al., Ammonia mobility in chabazite: insight into the diffusion component of the NH3-SCR process, Phys. Chem. Chem. Phys. 18 (2016) 17159–17168. doi:10.1039/C6CP01160H.

Appendix A

Appendix B

Supporting information to:

Impact of SO_2-poisoning over the lifetime of a Cu-CHA catalyst for NH_3-SCR

Peter S. Hammershøi[a,b], Anker D. Jensen[b], Ton V.W. Janssens[a,*]

[a]*Umicore Denmark ApS, Nøjsomhedsvej 20, 2800 Kgs. Lyngby, Denmark*
[b]*Department of Chemical and Biochemical Engineering, Technical University of Denmark, Søltofts Plads B229, 2800 Kgs. Lyngby, Denmark*
**Corresponding author. Phone: +45 22 75 46 22, e-mail address: tonv.w.janssens@eu.umicore.com*

Measured NO conversions of SO_2 exposed and regenerated catalysts

Steady state NO conversions in the temperature range 160-550 °C were measured on the fresh Cu-CHA catalyst, and on each of the SO_1 exposed and regenerated catalyst samples. The NO conversions of catalysts exposed to SO2 at 200, 300, 400, and 500 °C are plotted as function of temperature in Figure 1, and similarly, the NO conversions of the regenerated catalysts are plotted in Figure 2.

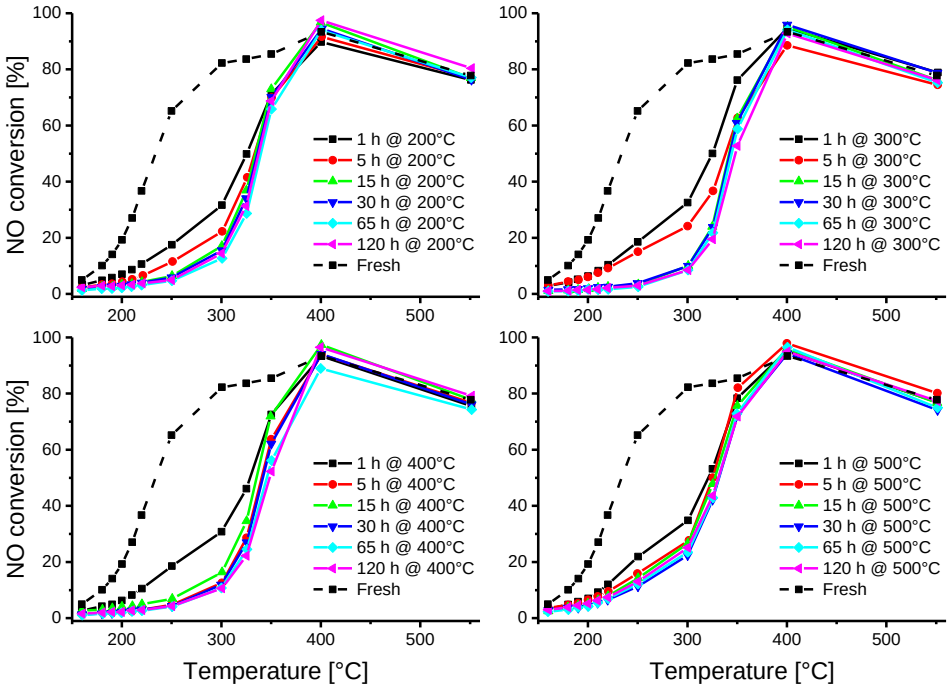

Figure 1 – Steady state NO conversions as function of temperature for the catalysts exposed to SO_2 at 200, 300, 400, and 500 °C.

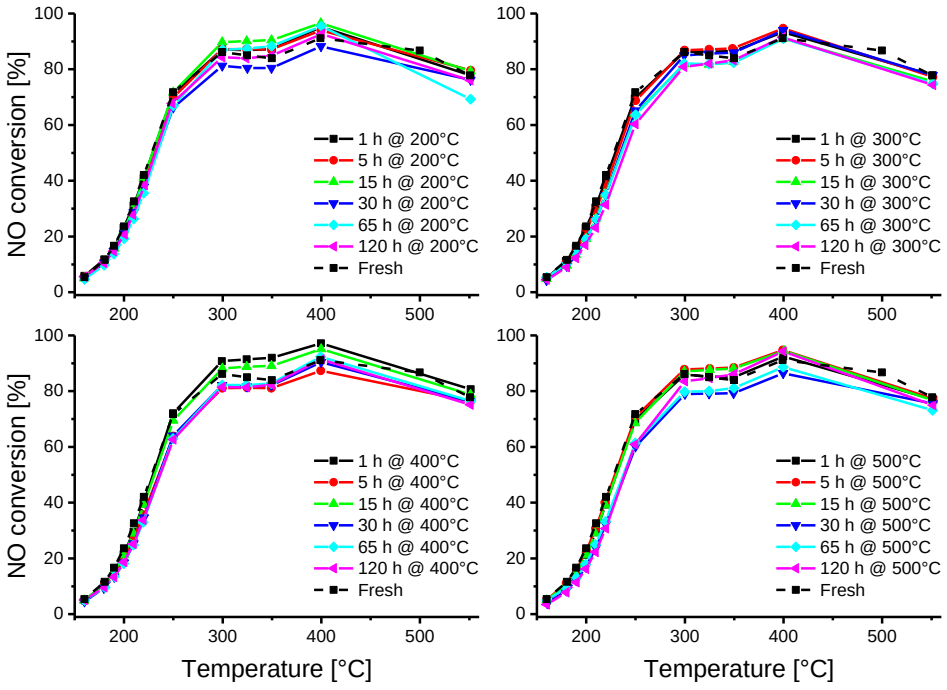

Figure 2 - Steady state NO conversions as function of temperature for the regenerated catalysts after exposure to SO_2 at 200, 300, 400, and 500 °C.

The NO conversions of the SO_2 exposed catalysts (Figure 1) are significantly lower in the temperature range 160-350 °C compared to those of the fresh catalyst, regardless of the SO_2 exposure temperature. Furthermore, the NO conversions of the regenerated catalysts (Figure 2) are all close to those of the fresh, which is also independent on the SO_2 exposure temperature. Thus, the same trend of significant low-temperature deactivation that can be partially regenerated at 550 °C, is observed for all the tested SO_2 exposure temperatures.

Appendix C

List of publications

1. P. S. Hammershøi, Y. Jangjou, W. S. Epling, A. D. Jensen, T. V. W. Janssens, *Reversible and irreversible deactivation of Cu-CHA NH_3-SCR catalysts by SO_2 and SO_3*, Appl. Catal. B 226 (**2018**) 38-45, https://doi.org/10.1016/j.apcatb.2017.12.018

2. P. S. Hammershøi, P. N. R. Vennestrøm, H. Falsig, A. D. Jensen, T. V. W. Janssens, *Importance of the Cu oxidation state for the SO_2-poisoning of a Cu-SAPO-34 catalyst in the NH_3-SCR reaction*, Appl. Catal. B 236 (**2018**) 377-383, https://doi.org/10.1016/j.apcatb.2018.05.038

3. P. S. Hammershøi, A. D. Jensen, T. V. W. Janssens, *Impact of SO_2-poisoning over the lifetime of a Cu-CHA catalyst for NH_3-SCR*, Appl. Catal. B 238 (**2018**) 104-110, https://doi.org/10.1016/j.apcatb.2018.06.039

4. C. Negri, P. S. Hammershøi, T. V. W. Janssens, P. Beato, G. Berlier, S. Bordiga, *Investigating the low temperature formation of Cu^{II}-(N,O) species on Cu-CHA zeolites for the selective catalytic reduction of NO_x*, Chem. Eur. J. 24 (**2018**) 12044-12053, https://doi.org/10.1002/chem.201802769

5. P. S. Hammershøi, A. D. Jensen, T. V. W. Janssens, *Cu-zeolit katalysatorer til effektiv NO_x-fjernelse fra dieseludstødning – En forsvarlig vej til lavere CO_2-emissioner*, Dansk Kemi 7 (**2018**)

6. P. S. Hammershøi, A. L. Godiksen, S. Mossin, P. N. R. Vennestrøm, A. D. Jensen, T. V. W. Janssens, *Site selective adsorption and relocation of SO_x in deactivation of Cu-CHA catalysts for NH_3-SCR*, Reac. Chem. Eng. (submitted)

Department of Chemical and Biochemical Engineering - CHEC
Technical University of Denmark
Søltofts Plads, Building 229
2800 Kgs. Lyngby
Denmark
Phone: +45 45 25 28 00
Web: www.kt.dtu.dk